

TOPIC 2 : DIFFRACTIONPRIMARY READING ASSIGNMENT

"Diffraction of Radiation by Crystals", from *The Physics of Solids*, F.C. Brown.

SUPPLEMENTARY REFERENCE

"X-ray Crystal Analysis", from Solid State Semiconductor Physics, J.P. McKelvey

"Diffraction I: The Directions of Diffracted Beams",

"Diffraction II: The Intensities of Diffracted Beams", and

"The Reciprocal Lattice", from *Elements of X-ray Diffraction*, B.D. Cullity

LECTURE PROGRAM

1. *Physics of X-ray Diffraction
 - a. Electromagnetic radiation
 - b. Reflection
 - c. Refraction
 - d. Diffraction
 - e. X-rays
2. von Laue Equations
3. Bragg Law
4. Experimental Methods for X-ray Diffraction and Crystal Structure Analysis
 - a. Rotating crystal technique
 - b. Debye-Scherrer technique
 - c. von Laue technique
5. *Reciprocal Lattice
 - a. Mathematical definition
 - b. Relation to the space lattice
 - c. Examples of reciprocal lattice
 - d. von Laue equation
 - e. Ewald construction
 - f. Brillouin zones
6. *Atomic Scattering Factor
7. *Geometric Structure Factor
8. Neutron Diffraction
9. Electron Diffraction

*Indicates that you may have to refer to the supplementary reference.

CHAPTER 3

DIFFRACTION OF RADIATION BY CRYSTALS

3-1 INTRODUCTION

In 1912 the German physicist, Max von Laue, suggested that crystals might act as natural diffraction gratings for x rays thus providing information about the nature of x rays as well as about the regular arrangement of atoms in crystals. The experiment was successfully carried out shortly afterwards by Friedrich, Knipping, and von Laue. These workers were successful because x-ray wavelengths are about 10^{-8} cm which is comparable to the spacing between atoms in a crystal. Subsequently, the law of crystal diffraction was developed in Cambridge by the English physicist, W. H. Bragg, and his son, W. L. Bragg. The younger Bragg was interested in using x rays to test the theories of W. Barlow on the structure of KCl and NaCl which, even at that time, were thought to be face-centered cubic as one might closely pack spheres. These early x-ray experiments confirmed the ideas of Barlow and demonstrated that a powerful new tool had been developed for the determination of crystal structures.

X rays are not the only external probe which can be used to study the structure of crystals. According to the laws of quantum mechanics, particles have a wave-like aspect, consequently electrons and neutrons—even a beam of atoms or molecules [1]—can be used in a diffraction experiment on solids. It is simply required that the wavelength of the radiation be about one angstrom which is roughly the spacing between atoms in a crystal. In the case of x rays, the expression for quantum energy, $E = hc/\lambda$, shows that kilovolt x rays are required for angstrom wave-

lengths. On the other hand, the de Broglie relation, $p = h/\lambda$, together with the relation between momentum p and energy E , indicate that electrons need be only about 100 eV, and neutrons with energy less than 0.1 eV will suffice for diffraction from solids.

The geometrical conditions for diffraction by x rays, electrons, and neutrons are all very similar; these will be derived in the next section. On the other hand, the penetration and the intensity of the scattering of each type of radiation are quite different. Both x rays and neutrons penetrate well below the surface and, therefore, serve as a probe for the volume of the crystal. In contrast, the electron beams used for diffraction are of low energy and do not penetrate far from the surface. Electron diffraction is therefore well suited for the investigation of surface properties or of thin films. We turn our attention first to the conditions for the diffraction of radiation with emphasis on x-ray diffraction.

The scattering of x rays by a lattice is usually considered to be elastic scattering. This is an excellent first approximation, since the x-ray energies commonly used correspond to about 50 kV, whereas the quanta of vibrational energy which can be excited or absorbed from the crystal are of the order of 0.05 eV or less. Moreover, x rays are scattered by the atomic electrons, and we are interested in that part of the scattering by electrons which occurs without change in wavelength. This is the part which is due to each electron radiating coherently as it moves in phase with the incident electromagnetic wave. On the other hand, scattering that is due to Compton effect results in a change in wavelength between incident and scattered waves. This gives rise to an incoherent background. Our main interest is in coherent x-ray scattering, in order to make use of the interference which occurs between radiation scattered by different atoms. Such interference effects tell us about the actual crystal structure. First, we will derive the geometrical conditions for diffraction and then the intensity of scattered radiation. We will see that x rays are in a sense reflected from lattice planes as envisioned by W. L. Bragg and described by the law which bears his name.

3-2 THE VON LAUE EQUATIONS

We turn first to a derivation of the von Laue diffraction equations in one dimension: Figure 3-1 shows a row of identical atoms with lattice vector \mathbf{a} . The direction of the incident x-ray beam can be specified either by the angle η_0 or the unit vector \hat{s}_0 , whereas the scattered direction is given by η or the unit vector \hat{s} . An electromagnetic wave passing over the electrons on the atom at P_1 or P_2 , for example, causes these electrons to reradiate as centers of spherical wave fronts [2, 3]. Since the wave-

length of interest in this problem is comparable with atomic dimensions, the electrons on each atom will not vibrate exactly in phase. However, their net effect at each atom can be described in terms of some atomic scattering factor f , as discussed more fully in Sections 3-7.

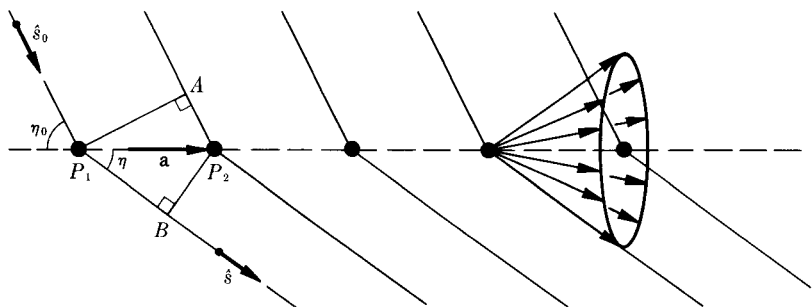


FIGURE 3-1. Scattering of an incident x-ray beam (incident direction \hat{s}_0) by a row of identical atoms of lattice spacing a . The direction of the scattered beam is specified by \hat{s} .

We inquire into the interference conditions for waves originating on different but identical atoms. Constructive interference will occur in a direction such that contributions from each lattice point differ in phase by 2π . This requires path differences of a whole wavelength or a multiple of one wavelength, i.e.,

$$P_1B - P_2A = e\lambda,$$

where

$$e = 0, 1, 2, 3, \dots$$

This condition can be restated in terms of angles or by using vector notation as follows:

$$\begin{aligned} a(\cos \eta - \cos \eta_0) &= e\lambda \\ \mathbf{a} \cdot (\hat{s} - \hat{s}_0) &= e\lambda. \end{aligned} \quad (3-1)$$

For a given incident direction λ_0 , lattice spacing a , wavelength λ , and integer value e , there is only one possible scattering angle η defining a cone of rays drawn about a line through the lattice points.

In the case of a two-dimensional lattice, a second equation similar to Eq. (3-1) must be satisfied. The allowed directions for interference lie along the intersection of two cones. In the case of three dimensions, a third condition must simultaneously be satisfied. Therefore, the von Laue conditions in three dimension are

$$\begin{aligned} \mathbf{a} \cdot (\hat{s} - \hat{s}_0) &= e\lambda \\ \mathbf{b} \cdot (\hat{s} - \hat{s}_0) &= f\lambda \\ \mathbf{c} \cdot (\hat{s} - \hat{s}_0) &= h\lambda, \end{aligned} \quad (3-2)$$

where \mathbf{a} , \mathbf{b} , and \mathbf{c} are primitive translation vectors. If one defines a vector $\mathbf{S} = \hat{s} - \hat{s}_0$, Eq. (3-2) becomes

$$\begin{aligned}\mathbf{a} \cdot \mathbf{S} &= e\lambda \\ \mathbf{b} \cdot \mathbf{S} &= f\lambda \\ \mathbf{c} \cdot \mathbf{S} &= g\lambda,\end{aligned}\quad (3-3)$$

which shows that the diffraction conditions involve the cosines of the angles between the vector \mathbf{S} and the crystallographic axes. It should be remarked that for a given λ and \hat{s}_0 , it is not always possible to find a solution to Eq. (3-2). Given a monochromatic incident beam, diffraction will be observed only for certain incident directions. Such a situation arises because of the restriction imposed by the third cone, and this is a crucial point in connection with the x-ray analysis of crystals. In practice, one meets the conditions for interference by using nonmonochromatic radiation and/or scanning through a number of incident angles.

3-3 BRAGG'S LAW

The definition of $\mathbf{S} = \hat{s} - \hat{s}_0$ leads to the idea of a *reflecting plane* drawn so as to bisect the angle between incident and reflected rays. The vector \mathbf{S} is normal to this plane, which bisects the angle 2θ between incident and diffracted directions as shown in Fig. 3-2. Notice that the magnitude of \mathbf{S} is given by

$$|\mathbf{S}| = 2 \sin \theta. \quad (3-4)$$

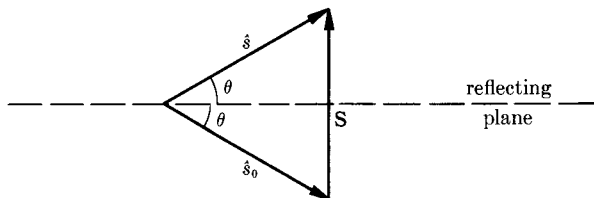


FIGURE 3-2. Showing the reflecting plane which bisects the angle between incident and diffracted beams.

The question naturally arises, what is the relation between the so-called reflecting plane, to which \mathbf{S} is normal, and the lattice planes? An answer to this question may be found as follows. Equations (3-3) tell us that the direction cosines of \mathbf{S} , with respect to the crystallographic axes, are proportional to $e/a, f/b, g/c$, that is,

$$a:\beta:\gamma = \frac{e}{a}:\frac{f}{b}:\frac{g}{c}. \quad (3-5)$$

Now a set of lattice planes are specified by the Miller indices (h, k, l) . By definition, these planes intersect the axes at the points a/h , b/k , and c/l .

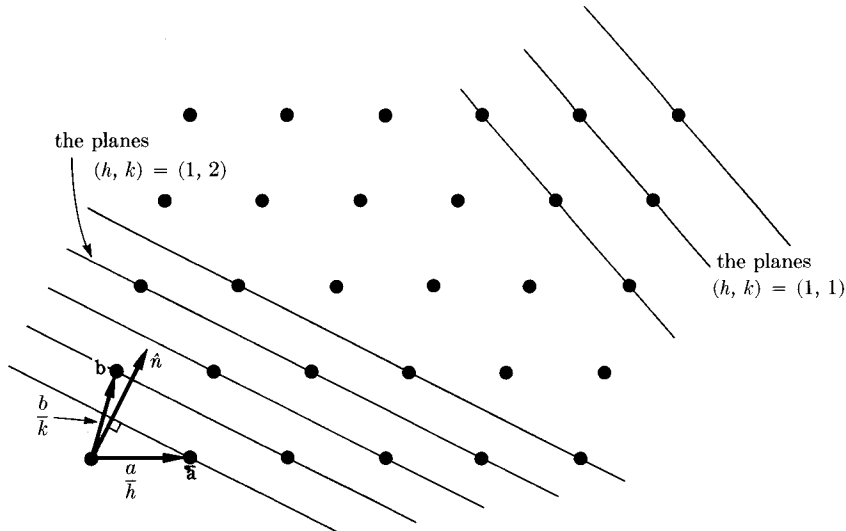


FIGURE 3-3. Illustrating the (h, k) planes for an oblique two-dimensional net. It is to be noted that the direction cosines of the normal \hat{n} are proportional to $1/a$ and to $2/b$, respectively.

Figure 3-3 shows that a unit vector \hat{n} , normal to the (h, k, l) plane, has direction cosines proportional to

$$\frac{h}{a} : \frac{k}{b} : \frac{l}{c} \quad (3-6)$$

Comparing the proportionality in Eq. (3-5) with that in Eq. (3-6), we see that the directions of \mathbf{S} and the unit normal \hat{n} are the same—all that is necessary is that $e = mh$, $f = mk$, and $g = ml$, where m is a common, constant factor. Reflection in the sense of the Laue equations can be interpreted as reflection from the h, k, l planes. The quantity m is just the largest common factor of the integers e, f , and g and is itself an integer. Now the spacing between the (h, k, l) planes is readily seen to be

$$d_{hkl} = \frac{\hat{n} \cdot \mathbf{a}}{h} = \frac{\hat{n} \cdot \mathbf{b}}{k} = \frac{\hat{n} \cdot \mathbf{c}}{l}. \quad (3-7)$$

Since \mathbf{S} is in the direction of the normal \hat{n} , and is given in magnitude by Eq. (3-4), the von Laue equations reduce to Bragg's law.

$$\mathbf{a} \cdot \mathbf{S} = \mathbf{a} \cdot \hat{n} 2 \sin \theta = e\lambda$$

or

$$2d_{hkl} \sin \theta = m\lambda. \quad (3-8)$$

Incidentally, the Eqs. (3-7) can be simplified to give the distance between planes in the case of a cubic crystal as

$$d_{hkl} = \frac{a}{(h^2 + k^2 + l^2)^{1/2}}. \quad (3-9)$$

3-4 EXPERIMENTAL METHODS FOR X-RAY DIFFRACTION

We have seen that given monochromatic x rays incident upon the lattice planes at a fixed angle, the diffraction relations Eq. (3-2) are not necessarily satisfied. Some parameter, such as angle of incidence or x-ray wavelength, must be varied in order to meet the conditions for constructive interference. There are three widely used experimental methods for achieving a diffraction pattern:

1. *The rotating crystal technique.* A monochromatic beam is utilized, while the crystal is rotated or oscillated about an axis which is usually perpendicular to the x-ray beam. As the angle changes, the conditions for diffraction will be met point by point. The record consists of a series of spots on a cylindrical film arranged around the sample. This technique is widely applied to the determination of crystal structures [4].

2. *Debye-Scherrer powdered sample arrangement.* Here a collimated monochromatic x-ray beam is incident upon a powder or fine grained polycrystalline sample with crystallites having various orientations. The x-ray film is arranged on the inside of a cylinder concentric with the sample. The diffracted rays which satisfy the Bragg condition proceed out from the sample parallel to the generators of cones concentric with the direction of the incident beam. Consequently the pattern or film is a set of concentric circles [5, 6].

3. *The von Laue technique.* This method uses a fixed, single crystal but requires a continuous or white spectrum of x rays. We discuss this method in some detail by way of illustration.

The von Laue method can be used either in transmission (usually at small angles) or in reflection (von Laue back-reflection method) as shown in Fig. 3-4. After a suitable exposure, spots are observed on the film in directions and for certain wavelengths corresponding to the conditions

for diffraction, Eqs. (3-2). High-energy, short-wavelength x rays are normally involved for transmission patterns, whereas longer wavelength and lower voltages can be used in reflection. Von Laue diagrams are used for: (a) determining the symmetry and structure of materials; (b) orienting single crystals; and (c) investigating distortion or polycrystallinity of samples. The back-reflection method permits the use of thick samples and has the advantage of higher resolution than the transmission method.

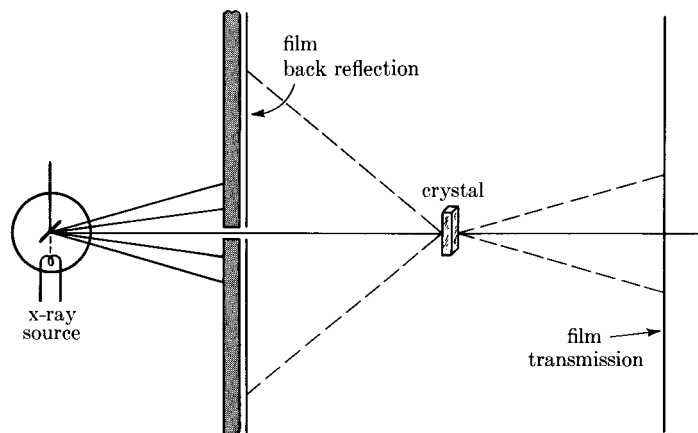


FIGURE 3-4. The arrangement of x-ray source ("white" radiation), crystal, and film for the von Laue method. Both back-reflection and transmission geometries are shown.

The impact on this field of new methods of instrumentation is currently being felt. For example, a very fast diffusion-transfer film and luminescent screen have been introduced which greatly shorten the exposure time necessary for von Laue photographs. There is also an increasing tendency to employ Geiger- or scintillation-counter techniques coupled with data processing equipment in place of film. In principle, the intensity of the diffracted x rays can be more accurately determined by counter methods than by the use of film.

Figure 3-5 shows three back-reflection patterns made in the laboratory in order to orient a single crystal of AgBr. The silver halides have the same crystal structure as NaCl, but they are soft and do not readily cleave along $\{100\}$ planes like the alkali halides. (Actually, AgCl can be cleaved while immersed in liquid helium, but this is a slightly troublesome procedure.) The crystal-to-film distance for the photographs of Fig. 3-5 was the customary 3.0 cm. Notice that the spots, which are reflections of the incident x-ray beams from different crystallographic planes, lie along hyperbola. The spots along a hyperbola are reflections

from planes of a particular *zone*. In Section 2-6 we showed that the planes of a zone are all planes parallel to a given direction, the zone axis. Figure 3-6 shows how the hyperbolas are formed from the intersection of a cone of rays reflected from the planes of a zone and the plane of the film.

Two angles in Fig. 3-6 are important, the angle of inclination of the zone axis φ and the angle α in the plane of the projection (plane of the film). When a zone axis lies in a plane parallel to the plane of the film ($\varphi = 0$), then the hyperbolas degenerate into straight lines passing through the origin and, moreover, these lines reveal the rotational symmetry of the crystal about the direction of the incident x-ray beam. Figure 3-5b clearly shows the 4-fold symmetry for the beam perpendicular to a (100) plane of the crystal. The 2-fold symmetry of a (110) face is evident in Fig. 3-5c. Three-fold symmetry would occur for a (111) direction.

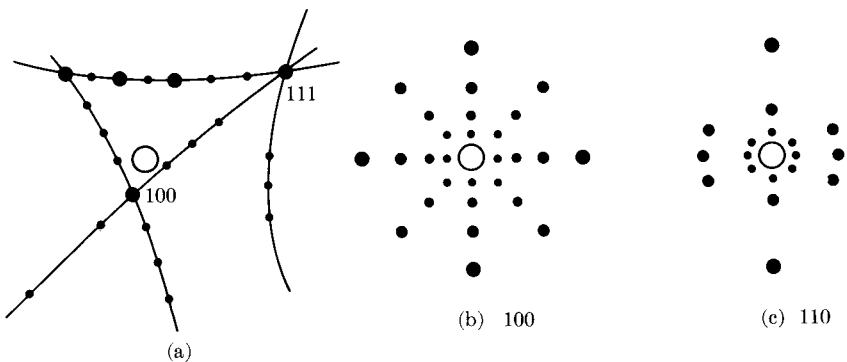


FIGURE 3-5. Sketches of von Laue back-reflection patterns obtained for a single crystal of AgCl oriented in: (a) nonprincipal direction, (b) (100) direction, and (c) (110) direction. The open circle is the hole in the center of the film.

The problem of determining the orientation of the crystal for Fig. 3-5a is somewhat complicated but can be done in a few minutes with standard techniques. Since the normals to each reflecting plane bisect the incident and reflected beam, a construction might be carried out to locate these normals on a stereogram, i.e., make a pole diagram. The problem then becomes one of comparing this diagram with a standard pole figure of the crystal (Barrett [5] gives such a pole diagram for cubic and for hexagonal crystals), and assigning indices to the spots. A simpler, although sometimes less accurate, procedure is to determine the angles between spots on a hyperbola using a Greninger chart such as given in the book by Barrett [5]. These angles can then be compared with a table which gives the angles between crystallographic planes in order to

assign indices to particular spots. This procedure allows the zone to be determined, and the angles φ and α can then be read directly from the Greninger chart.

In analyzing a diagram such as Fig. 3-11a, it helps to concentrate on the more intense and widely spaced spots, particularly those which are at the intersection of hyperbolas. These are the reflections from planes with lower indices. They are more intense because of the wider spacing between, and the higher density of atoms in such planes. Experience helps a good deal. For example, the widely spaced (45°) pair (001) and (011) can sometimes be quickly spotted along a hyperbola separated by three spots (013), (012), and (023). Dark spots from less prominent planes due to the intense K_α -emission line (superimposed on the x-ray continuum) often have to be overlooked. Of course, the symmetry of spots around a pole is helpful, even when the x-ray beam is not exactly along one of the rotation axes.

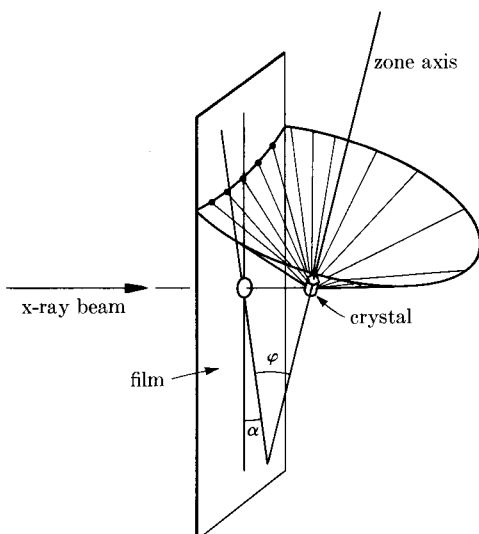


FIGURE 3-6. Showing how a hyperbola of spots is obtained in von Laue back reflection from a cone of rays reflected by the planes of a zone. (After C. S. Barrett [5].)

Finally, it should be mentioned that the sharpness of the spots of an x-ray photograph relates to the perfection of the crystal, particularly the state of perfection near the surface. An elongation of the spots known as asterism results when strain has been introduced. Polycrystallinity and small angle grain boundaries can be revealed when multiple spots occur.

3-5 THE RECIPROCAL LATTICE

Let us now express the conditions for x-ray diffraction in terms of the reciprocal lattice. For this purpose, we write the incoming wave as a plane wave and express the von Laue conditions in terms of the wave vectors of incident and diffracted waves. A plane wave traveling in the x direction can be written in complex notation as

$$\Psi = A e^{2\pi i((x/\lambda) - \nu t)}, \quad (3-10)$$

where A is the wave amplitude, λ the wavelength, and ν the frequency. Distance can be expressed in vector notation if a unit vector \hat{s}_0 in the direction of propagation is defined. The incident wave is then

$$\Psi_0 = A e^{2\pi i((\mathbf{r} \cdot \hat{s}_0/\lambda) - \nu t)}. \quad (3-11)$$

Alternatively, one can define a wave vector for the incident radiation as

$$\mathbf{k}_0 = \frac{2\pi}{\lambda} \hat{s}_0, \quad (3-12)$$

so that the phase factor becomes $\mathbf{k}_0 \cdot \mathbf{r}$, and the incident wave takes the form

$$\Psi_0 = A e^{i(\mathbf{k}_0 \cdot \mathbf{r} - \omega t)}. \quad (3-13)$$

A similar expression with a different propagation vector \mathbf{k} applies for the diffracted wave.

Equations (3-2) can now be rewritten in terms of wave vectors. The result is

$$\begin{aligned} \frac{1}{2\pi} \left(\mathbf{k} \cdot \frac{\mathbf{a}}{a} - \mathbf{k}_0 \cdot \frac{\mathbf{a}}{a} \right) &= \frac{e}{a} \\ \frac{1}{2\pi} \left(\mathbf{k} \cdot \frac{\mathbf{b}}{b} - \mathbf{k}_0 \cdot \frac{\mathbf{b}}{b} \right) &= \frac{f}{b} \end{aligned} \quad (3-14)$$

and

$$\frac{1}{2\pi} \left(\mathbf{k} \cdot \frac{\mathbf{c}}{c} - \mathbf{k}_0 \cdot \frac{\mathbf{c}}{c} \right) = \frac{g}{c}.$$

Note that terms of the form,

$$\mathbf{k} \cdot \frac{\mathbf{a}}{a} = k \cos \eta, \quad (3-15)$$

are the projection of the wave vectors on the different crystallographic axes.

The right-hand side of the von Laue equations, Eq. (3-14) involve reciprocals of the lattice spacings a , b , and c . This is reasonable since

the left side involves wave vectors. At this point, let us define a vector \mathbf{a}^* so that

$$\mathbf{a}^* \cdot \frac{\mathbf{a}}{a} = \frac{1}{a}; \quad \mathbf{a}^* \cdot \frac{\mathbf{b}}{b} = \mathbf{a}^* \cdot \frac{\mathbf{c}}{c} = 0; \quad (3-16)$$

or

$$\mathbf{a}^* \cdot \mathbf{a} = 1; \quad \mathbf{a}^* \cdot \mathbf{b} = \mathbf{a}^* \cdot \mathbf{c} = 0. \quad (3-17)$$

We can now write the first of Eqs. (3-14) in terms of these starred vectors:

$$\frac{1}{2\pi} \left(\mathbf{k} \cdot \frac{\mathbf{a}}{a} - \mathbf{k}_0 \cdot \frac{\mathbf{a}}{a} \right) = mha^* \cdot \frac{\mathbf{a}}{a}, \quad (3-18)$$

where we use $e = mh$ as before. The same procedure is adopted to define \mathbf{b}^* and \mathbf{c}^*

$$\mathbf{b}^* \cdot \mathbf{b} = 1; \quad \mathbf{b}^* \cdot \mathbf{a} = \mathbf{b}^* \cdot \mathbf{c} = 0; \quad (3-19)$$

$$\mathbf{c}^* \cdot \mathbf{c} = 1; \quad \mathbf{c}^* \cdot \mathbf{a} = \mathbf{c}^* \cdot \mathbf{b} = 0. \quad (3-20)$$

Finally, the three von Laue equations can be written more compactly as follows:

$$\begin{aligned} \frac{1}{2\pi} (\mathbf{k} - \mathbf{k}_0) &= mha^* + mkb^* + mlc^*, \\ &= \mathbf{r}_{hkl}^* \end{aligned} \quad (3-21)$$

where

$$\mathbf{r}_{hkl}^* = m(ha^* + kb^* + lc^*). \quad (3-22)$$

The quantities \mathbf{a}^* , \mathbf{b}^* , and \mathbf{c}^* are the basis vectors of a reciprocal *lattice*, and \mathbf{r}_{hkl}^* is a lattice vector in reciprocal or wave vector space. As before, e , f , and g are integers and m is just a common integer.

Because of the way \mathbf{a}^* was defined, it is perpendicular to the plane of the direct lattice vectors \mathbf{b} and \mathbf{c} . A similar remark can be made for \mathbf{b}^* and \mathbf{c}^* . In fact, it can be shown that

$$\mathbf{a}^* = \frac{\mathbf{b} \times \mathbf{c}}{\mathbf{a}(\mathbf{b} \times \mathbf{c})}; \quad \mathbf{b}^* = \frac{\mathbf{c} \times \mathbf{a}}{\mathbf{b}(\mathbf{c} \times \mathbf{a})}; \quad \mathbf{c}^* = \frac{\mathbf{a} \times \mathbf{b}}{\mathbf{c}(\mathbf{a} \times \mathbf{b})}. \quad (3-23)$$

Notice that the denominator of each of the Eqs. (3-23) is the unit cell volume. A part of a direct lattice is shown in Fig. 3-7, where two of the basis vectors of the reciprocal lattice are drawn in. It can be seen that the reciprocal lattice bears a definite orientation with respect to the direct lattice.

The reciprocal lattice vector \mathbf{r}_{hkl}^* , as given by Eq. (3-21), can be shown to be normal to the hkl plane of the direct lattice. To see this, take the dot product between \mathbf{r}_{hkl}^* and a vector lying in the hkl plane such as $((\mathbf{a}/h) - (\mathbf{b}/k))$ (remember that the hkl plane intersects the axes at a/h ,

b/k , and c/l). The result can be shown to be zero by using Eqs. (3-17) and (3-19) as follows:

$$\mathbf{r}_{hkl}^* \cdot \left(\frac{\mathbf{a}}{h} - \frac{\mathbf{b}}{k} \right) = 0. \quad (3-24)$$

It can also be seen that the magnitude of

$$|\mathbf{r}_{hkl}^*| = \frac{m}{d_{hkl}}, \quad (3-25)$$

where d_{hkl} is the spacing between the (hkl) planes given by:

$$d_{hkl} = \hat{n} \cdot \frac{\mathbf{a}}{h}. \quad (3-26)$$

In this last equation, the unit normal is given by $\hat{n} = \mathbf{r}^*/|\mathbf{r}^*|$, therefore

$$d_{hkl} = \frac{(\mathbf{r}^* \cdot \mathbf{a})}{h|\mathbf{r}^*|} = \frac{m}{|\mathbf{r}^*|}, \quad (3-27)$$

which proves the above statement, Eq. (3-25), about the magnitude of \mathbf{r}^* . The reciprocal lattice might be said to substitute points for planes of the direct lattice.

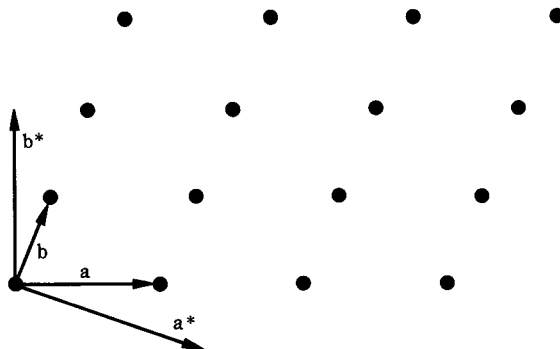


FIGURE 3-7. The reciprocal lattice vectors \mathbf{a}^* and \mathbf{b}^* can be compared with the direct lattice vectors \mathbf{a} and \mathbf{b} .

Let us now rearrange the von Laue condition for diffraction, Eq. (3-21), as follows

$$\mathbf{k} = \mathbf{k}_0 + 2\pi\mathbf{r}_{hkl}^*. \quad (3-28)$$

At this point, it is convenient to define a vector which is 2π times a reciprocal lattice vector:

$$\mathbf{K}_n = 2\pi\mathbf{r}_{hkl}^*, \quad (3-29)$$

where the subscript n stands for the indices h, k, l . In terms of this vector, Eq. (3-28) becomes

$$\mathbf{k} = \mathbf{k}_0 + \mathbf{K}_n. . \quad (3-30)$$

If we multiply this last equation by \hbar , we see that the von Laue equation amounts to a condition which resembles momentum conservation in scattering, i.e.,

$$\hbar\mathbf{k} = \hbar\mathbf{k}_0 + \hbar\mathbf{K}_n \quad (3-31)$$

Equation (3-31) shows that the incident photon, which in a particle-picture of light carries momentum $\hbar\mathbf{k}_0$, can be Bragg reflected by the lattice so as to come off with momentum $\hbar\mathbf{k}$. In the process an amount of momentum $\hbar\mathbf{K}_n$ is transferred to the lattice as a whole. The momentum transfer is not arbitrary but is restricted to the discrete values which \mathbf{K}_n can take on. This is a direct consequence of lattice periodicity.

We have not yet taken into account the fact that the scattering of x rays is closely elastic. Thus the wavelength of the scattered electromagnetic wave is very nearly the same as the wavelength of the incident wave; the scattered and incident vectors therefore have the same magnitude:

$$|\mathbf{k}| = |\mathbf{k}_0|. \quad (3-32)$$

With this condition Eq. (3-30) becomes

$$(\mathbf{k}_0 + \mathbf{K}_n)^2 = k_0^2 \quad (3-33)$$

or stated another way,

$$2\mathbf{k}_0 \cdot \mathbf{K}_n + K_n^2 = 0. \quad (3-34)$$

The conditions for diffraction can best be seen by a construction in the space of the reciprocal lattice known as the *Ewald sphere*. In order to illustrate this method for determining allowed k vectors, let us construct a kind of expanded reciprocal lattice by multiplying all reciprocal lattice vectors \mathbf{r}^* by 2π (some authors introduce this factor of 2π directly into the definition of the reciprocal lattice vectors Eq. (3-23)). We now plot wave vectors in this space as shown in Fig. 3-8. First draw the vector AO in the direction of the incident wave, of length k_0 and ending at the origin O of the reciprocal lattice. Next construct a sphere centered on A and of radius $k_0 = 2\pi/\lambda$. The intersections of this sphere with other reciprocal lattice points such as B give the directions \mathbf{k} of possible reflections. Since the vectors \mathbf{k} and \mathbf{k}_0 are of equal, or nearly equal, magnitude an isosceles triangle AOB is formed. The dotted line passing through A in Fig. 3-8 represents the reflecting plane to which \mathbf{K}_n is normal and which bisects this expanded reciprocal lattice vector.

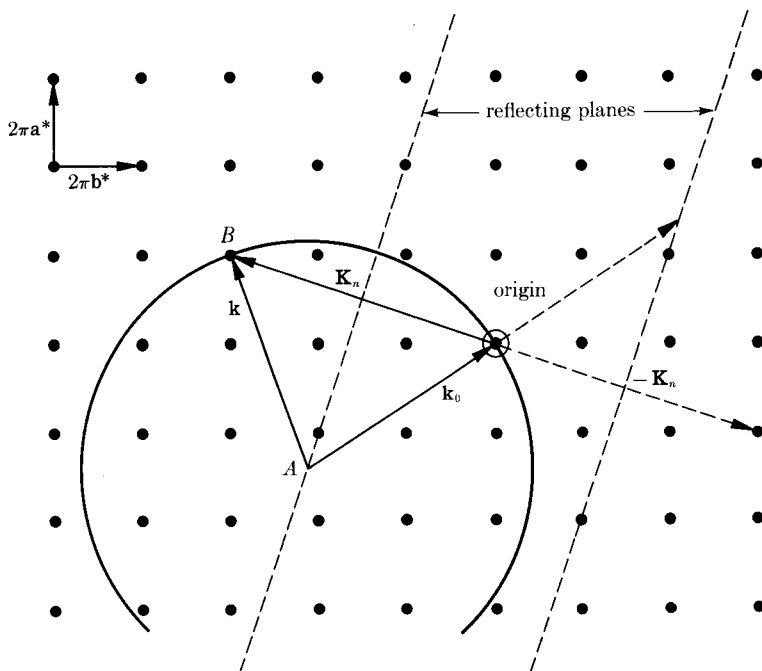


FIGURE 3-8. The Ewald construction in reciprocal space. The vector \mathbf{k} is positioned so that its tip is at the origin O of the expanded reciprocal lattice. A sphere of radius $|\mathbf{k}_0| = |\mathbf{k}|$ is then drawn about point A . In this particular case diffraction occurs in direction AB . The diffraction conditions are also met for the vector \mathbf{k}_0 drawn from the origin and terminating on the reflecting plane as shown by the dotted line.

3-6 BRILLOUIN ZONES

A somewhat different construction can be used in Fig. 3-8 which introduces the important concept of a *Brillouin zone*. Notice that both $\mathbf{K}_n = 2\pi\mathbf{r}^*$ and $-\mathbf{K}_n = -2\pi\mathbf{r}^*$ are vectors of the expanded reciprocal lattice. Also, it can be seen that another reflecting plane bisects the vector $-\mathbf{K}_n$ at $-\mathbf{K}_n/2$. Now if the incident wave vector \mathbf{k}_0 is drawn starting from the origin O , it must terminate on the $-\mathbf{K}_n/2$ reflecting plane in order for diffraction to occur. This fact suggests the use of the reciprocal lattice to construct Brillouin zones, the boundaries of which satisfy the von Laue conditions for diffraction.

As an example of a simple Brillouin zone, consider the two-dimensional square lattice of side a shown in Fig. 3-9. The expanded reciprocal lattice is shown in the second half of Fig. 3-9 where the unit vectors \hat{i} and

\hat{j} are drawn in the direction of $2\pi a^*$ and $2\pi b^*$, respectively. A general reciprocal lattice vector \mathbf{K}_n can be written as follows:

$$\mathbf{K}_n = 2\pi r_{hk}^* = mh \frac{2\pi}{a} \hat{i} + mk \frac{2\pi}{a} \hat{j}. \quad (3-35)$$

Since m is just an integer, and h or k can be either positive or negative, Eq. (3-35) can equally well be written as

$$\mathbf{K}_n = - \left(\frac{2\pi n_1}{a} \hat{i} + \frac{2\pi n_2}{a} \hat{j} \right), \quad (3-36)$$

where n_1 and n_2 are integers or zero. The diffraction conditions are met when \mathbf{k}_0 , drawn from the origin, terminates on the dotted lines (reflecting planes) which pass through $-\mathbf{K}_n/2$. For example, this occurs in the i direction when $n_1 = 1$, $n_2 = 0$, and $|\mathbf{k}_0| = \pi/a$. The boundaries of the zones specify the conditions for diffraction. These are given by Eq. (3-34), which can be rewritten with the aid of Eq. (3-36) as

$$k_x n_1 + k_y n_2 = -(n_1^2 + n_2^2) \frac{\pi}{a}. \quad (3-37)$$

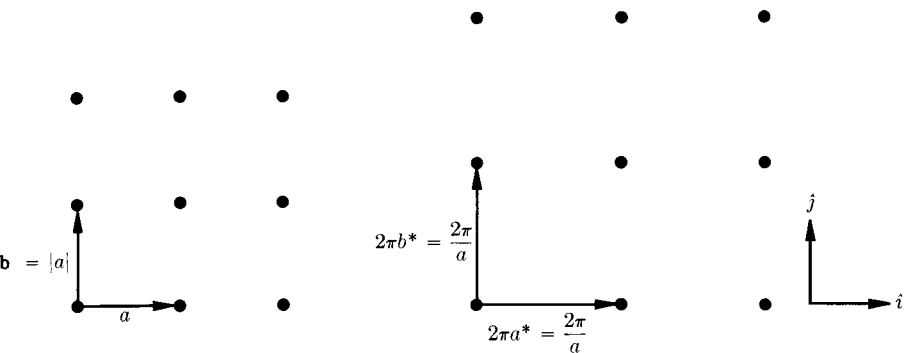


FIGURE 3-9. Showing the direct and reciprocal lattices for a square lattice of spacing a .

The boundaries of the first Brillouin zone intersect the k_x and the k_y axes at the points $k_x = \pm\pi/a$, as can be seen from Eq. (3-37) by setting $n_1 = \pm 1$, $n_2 = 0$ and $n_1 = 0$, $n_2 = \pm 1$, respectively. The outer boundary of the second Brillouin zone is obtained by setting $n_1 = 1$, $n_2 = 1$ and is given by $k_x + k_y = 2\pi/a$. Figure 3-10 shows the first, second, and third Brillouin zones of the simple square lattice. It should be noticed that each zone has the same total area. If the incident wave vector \mathbf{k}_0 drawn from the origin lies within a zone, no diffraction occurs; if \mathbf{k}_0 terminates on a boundary, then the conditions for diffraction are

met. It should also be noted that each zone repeats in k space. For example, the diffraction conditions which outline the first zone are satisfied when k_0 terminates on planes passing through $\pm\pi/a$ and also on the equivalent planes which intersect perpendicular to the k_x axis at $\pm 3\pi/a$, $\pm 5\pi/a$, etc.

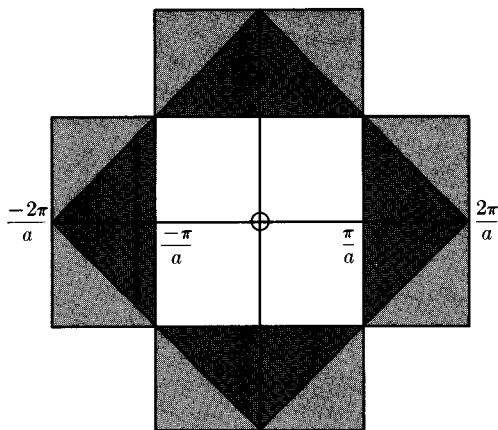


FIGURE 3-10. The first, second, and third Brillouin zones for a square lattice.

The Brillouin zones for three-dimensional structures are more interesting. For example, it can be shown that the reciprocal lattice for a body-centered cubic lattice is face-centered cubic. The boundaries of the first Brillouin zone for the bcc lattice are obtained by constructing the bisecting planes of the fcc reciprocal lattice vectors. The result is the dodecahedron shown in the lower part of Fig. 2-5a. It should be noticed that {110} reflecting planes are present in this case but that {100} and {111} planes are absent.

It is not hard to show that the reciprocal of a face-centered cubic lattice is body centered. The faces of the first Brillouin zone therefore form the polygon shown in the lower part of Fig. 2-5b. In this case {110} planes are absent, but reflections from {100} and {111} planes do occur. For further discussion, see the books by Brillouin [7] and Jones [8].

3-7 GENERAL FORMULAS FOR INTENSITY OF SCATTERED X RAYS

Up to now we have been considering the scattering of x rays by a point lattice. No account has been taken of the fact that the z electrons of an atom do not scatter, as if they were all concentrated at the nucleus. Let

us also look a little more carefully at the problem of the scattered x-ray intensity.

Consider first a single electron and an incident unpolarized x-ray beam of intensity I_0 . The electron is accelerated by the electric field of the electromagnetic wave and it radiates or scatters [3]. Classical theory shows that the intensity of the scattered radiation falls off inversely as the square of distance from the electron and depends upon the angle 2θ between primary and scattered beams as follows:

$$I(\theta) = \left[\left(\frac{e^2}{mc^2 R} \right)^2 \frac{1 + \cos^2 2\theta}{2} \right] I_0. \quad (3-38)$$

Suppose that we wish to compare the intensity of scattered radiation for an electron at point \mathbf{r} with an electron at the origin (center of the atom) as shown in Fig. 3-11. In general, we must sum over some charge density $\rho(\mathbf{r})$ for the atom, with proper regard to phase. The phase factors will just be of the form

$$\begin{aligned} e^{i\Phi} &= e^{i(2\pi/\lambda)\mathbf{r} \cdot (\hat{s} - \hat{s}_0)} \\ &= e^{i\mathbf{r} \cdot (\mathbf{k} - \mathbf{k}_0)} \end{aligned} \quad (3-39)$$

and these can be used to calculate the electric field amplitude for scattered waves of the form of Eq. (3-13). The intensity of scattered radiation will be proportional to the square of the electric field.

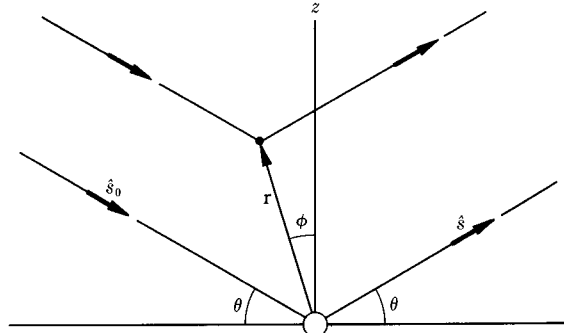


FIGURE 3-11. Referring a point \mathbf{r} to the center of an atom located at the origin O .

Integrating over the charge distribution and then taking the square of the field (in order to obtain intensity) $I \propto |E(\theta)|^2$, we have

$$I = I_0 C^2 \iiint \rho e^{i\mathbf{r} \cdot (\mathbf{k} - \mathbf{k}_0)} d\tau_r|^2. \quad (3-40)$$

The constant C^2 can simply be identified with the bracket in Eq. (3-38), which leaves the integral as the important quantity. This integral is

just the Fourier transform of the charge distribution [2] and, in fact, can be defined for quite a general distribution of charge, including the charge around the atom and the atoms in space.

The theory of Fourier transforms says that the transform of a convolution of two functions is just the product of the transforms of the individual functions. It is therefore convenient to construct the electron density for a crystal of point atoms, as we have done before, and then convolute or spread out these point atoms according to the electron distribution for the individual atoms. This will result in a product of transformations [9]. The transform for the individual electron distribution is known as the atomic scattering factor f . This quantity just relates the amplitude of the radiation scattered by the electron distribution of the atom to that which would be scattered by an electron located at the center of the atom.

The atomic scattering factor can be quite readily evaluated for a spherical electron distribution where the probability of finding an electron within a volume element $d\tau_r$ depends only upon the radial distance. The quantity f is just the triple integral which appears in Eq. 3-40, and this integral can be written as follows:

$$\begin{aligned} f &= \iiint \rho(r) e^{i\Phi} d\tau_r \\ &= \iiint \rho(r) e^{i(2\pi/\lambda)(\mathbf{r} \cdot \mathbf{S})} d\tau_r. \end{aligned} \quad (3-41)$$

The magnitude of \mathbf{S} which enters Eq. (3-41) is given in terms of the scattering angle by Eq. (3-4). Our axes are chosen as in Fig. 3-11 so that the angle between \mathbf{r} and \mathbf{S} is just the spherical coordinate φ . Integrating over the other angular coordinate introduces a factor 2π , so that Eq. (3-41) becomes

$$\begin{aligned} f &= \iint \rho(r) e^{i\mu r \cos \varphi} 2\pi r^2 \sin \varphi dr d\varphi \\ &= \int_0^\infty 4\pi r^2 \rho(r) \frac{\sin \mu r}{\mu r} dr, \end{aligned} \quad (3-42)$$

where $\mu = 4\pi \sin \theta / \lambda$. If the scattering angle θ is very small, f is simply given by

$$f = \int_0^\infty 4\pi r^2 \rho(r) dr,$$

which is the total charge of the atom (including all z electrons). Heavy, high- z elements produce a larger scattered intensity. In general, the scattered intensity will be less for large scattering angle θ than for small, according to Eq. (3-42). These atomic scattering factors, or form factors as they are sometimes called, are tabulated for the elements as a function of $\sin \theta / \lambda$ [10].

3-8 STRUCTURE FACTOR

The general scattering formula, Eq. (3-40) above, is now applied to a crystal. It is essential that the crystal is periodic. The Fourier transform of the charge density can therefore be broken down into the product of a transform for the point lattice—which for an infinite crystal is zero, except when the von Laue conditions Eq. (3-28) are met—and a transform $F(hkl)$ which is integrated over the volume of a *unit cell*. This integral $F(hkl)$ is called the structure factor and is given as follows:

$$F(hkl) = \iiint_{\substack{\text{unit} \\ \text{cell}}} \rho(\mathbf{r}) e^{i\mathbf{r} \cdot (\mathbf{k} - \mathbf{k}_0)} d\tau_r. \quad (3-43)$$

The atomic factors previously described can be incorporated into this last equation as well as interference effects due to cancellation of reflections from the various planes within the unit cell. It is convenient to construct the charge density for a crystal of point atoms and then to apply the above mentioned atomic scattering factors (which are very often taken to be spherical). Again, such a convolution results in the product of transformations. It also allows one to replace the integral in Eq. (3-43) by a sum over the atoms of a unit cell. The result is:

$$F(hkl) = \sum_{\substack{i \\ \text{unit} \\ \text{cell}}} f_i e^{i\mathbf{r}_i \cdot (\mathbf{k} - \mathbf{k}_0)}. \quad (3-44)$$

Here f_i is the atomic scattering factor and \mathbf{r}_i the position of the i th atom of the unit cell. If \mathbf{a} , \mathbf{b} , and \mathbf{c} are the edges of the unit cell, place the origin at the corner of the cell so that the various atomic positions can be specified as fractions, u_i , v_i , w_i , of these lattice displacements, i.e.,

$$\mathbf{r}_i = u_i \mathbf{a} + v_i \mathbf{b} + w_i \mathbf{c}. \quad (3-45)$$

By way of illustration let us evaluate the structure factor for a simple case, that of the body-centered cubic unit cell. In order for diffraction to occur, the von Laue condition states that

$$\mathbf{k} - \mathbf{k}_0 = 2\pi m(h\mathbf{a}^* + k\mathbf{b}^* + l\mathbf{c}^*).$$

We set the common factor m equal to one, as in first-order reflection, and the structure factor Eq. (3-44) becomes

$$\begin{aligned} F(hkl) &= \sum_{\substack{i \\ \text{unit} \\ \text{cell}}} f_i e^{2\pi i(\mathbf{r}_i \cdot \mathbf{r}_{hkl}^*)} \\ &= \sum_{\substack{i \\ \text{unit} \\ \text{cell}}} f_i e^{i2\pi(hu_i + kv_i + lw_i)}. \end{aligned} \quad (3-46)$$

For the case of a bcc structure with two *identical* atoms per unit cell at the fractional positions 0, 0, 0, and $\frac{1}{2}, \frac{1}{2}, \frac{1}{2}$, Eq. (3-46) readily gives

$$F = f[1 + e^{i\pi(h+k+l)}]. \quad (3-47)$$

The structure factor $F = 0$ when $(h + k + l)$ is odd, which means that reflections from {100}, {300}, {111}, and {221} planes are absent. In this case, reflections from {100} and {200} planes do occur, however. This was also the result obtained by inspection of the faces of the Brillouin zone for the bcc structure. It is left as an exercise to work out the structure for the fcc lattice.

When the structure factor is known, the scattered x-ray intensities give enough information to construct a map of electron density in the crystal. This can be shown as follows: The density of electrons in the crystal is a periodic function, i.e.,

$$\rho(\mathbf{r} + \mathbf{T}) = \rho(\mathbf{r}), \quad (3-48)$$

and can therefore be expanded in terms of a triple Fourier series [7]. Using the reciprocal lattice vectors $-\mathbf{K}_n$ (or \mathbf{K}_n) (where the components of these vectors involve the integers h, k, l) it follows that:

$$\rho(\mathbf{r}) = \sum_{hkl} \rho_{hkl} e^{-i\mathbf{K}_n \cdot \mathbf{r}}. \quad (3-49)$$

The coefficients ρ_{hkl} are evaluated by integrating over the unit cell volume V as follows:

$$\rho_{hkl} = \frac{1}{V} \iiint_{\text{unit cell}} \rho(\mathbf{r}) e^{i\mathbf{K}_n \cdot \mathbf{r}} d\tau_r. \quad (3-50)$$

The charge density Eq. (3-49) is therefore,

$$\rho(\mathbf{r}) = \frac{1}{V} \sum_{hkl} \left[\iiint \rho(\mathbf{r}') e^{i\mathbf{K}_n \cdot \mathbf{r}'} d\tau_{r'} \right] e^{-i\mathbf{K}_n \cdot \mathbf{r}}, \quad (3-51)$$

and it can be seen from Eq. (3-43), along with the diffraction conditions Eq. (3-30), that the factor in brackets is just the structure factor $F(hkl)$. The important relation results:

$$\rho(\mathbf{r}) = \frac{1}{V} \sum_{hkl} F(hkl) e^{-i\mathbf{K}_n \cdot \mathbf{r}} \quad (3-52)$$

or, in terms of xyz

$$\rho(xyz) = \frac{1}{V} \sum_{hkl} F(hkl) e^{-2\pi i(hx+ky+lz)}. \quad (3-53)$$

This equation shows that if the complex quantities $F(hkl)$ are known, the charge density can be evaluated. Unfortunately, the observed scattered x-ray intensities give only the magnitude $|F(hkl)|$ as follows:

$$I(hkl) = \text{const } F(hkl)F^*(hkl) = \text{const } |F(hkl)|^2, \quad (3-54)$$

where $F^*(hkl)$ is a complex conjugate. Thus enters the famous phase problem of crystallography. Various procedures have been worked out for solving this problem, but they usually involve assuming a model and performing successively refined Fourier summations Eqs. (3-44) and (3-53). It is thus possible from x-ray data to construct a map of electron density throughout the crystal. Such a charge density plot is shown in Fig. 4-1 for NaCl.

It is apparent that the determination of $F(hkl)$ and the solving of the phase problem for unknown structures is a difficult task. Nevertheless, careful work and great insight have permitted the description of the really complicated molecular structures of certain proteins and biologically active molecules such as vitamin B₁₂ [11, 12]. Modern instrumentation and computational methods have greatly reduced the time involved in unraveling the phase and determining the density of scattering centers for simple structures. These same methods are promising for the more complex situations.

Up to now we have made no mention of the effects of thermal energy and lattice vibrations on x-ray scattering. The conditions for Bragg reflection were derived assuming the atoms of the crystal fixed in position, although it must be realized that they are always in vibratory motion due to thermal energy. This causes the diffraction pattern to become fuzzy; a temperature-dependent, diffuse x-ray background occurs around each Bragg spot. Consequently, the atomic structure factors f_i in Eq. (3-44) must be multiplied by modifying factors which depend upon temperature. To a first approximation the magnitude of the diffuse x-ray scattering depends upon the mean-square amplitude of vibration of the atoms, which in turn can be related to the frequency of vibration of the lattice by the principle of equipartition of energy. There is, in effect, a transfer of scattering intensity from processes which give rise to the main Bragg spots, as governed by Eq. (3-30), to processes involving an additional term due to momentum transfer from a lattice vibration. By measuring the diffuse x-ray scattering intensity for different points in the region of each Bragg spot, it is possible to determine the frequency versus momentum dependence of the lattice vibrational spectrum. The procedure for doing this, however, is difficult and not very accurate due to the small size of the energy transfers involved compared to the energy of the x rays. Nevertheless, meaningful lattice dispersion curves have been obtained in this way for a number of substances including the ionic crystal

AgCl [13]. Inelastic neutron scattering has turned out to be a more powerful tool for probing the nature of lattice vibrations and this method will be discussed in both the next section and Section 6-9.

3-9 CRYSTAL DYNAMICS AND NEUTRON SCATTERING

Toward the end of the preceding section we have in effect been discussing crystal dynamics. How can the diffraction of radiation be utilized to reveal the nature of lattice vibrations as well as crystal structure? It turns out that this can best be answered for neutrons.

Inelastic neutron scattering has developed into a powerful tool for the study of crystal dynamics. The experimental techniques for this work have evolved especially rapidly since World War II with the availability of relatively high-intensity beams of thermal neutrons from nuclear reactors. The elastic scattering of neutrons by solids is also important because of certain features which distinguish neutron from x-ray diffraction. We will discuss these differences here and in the next section. A detailed description of inelastic neutron scattering will be postponed until Chapter 6.

Neutron scattering can therefore be either elastic or inelastic, and the conditions of an experiment can usually be adjusted to favor one process over another. For example, elastic scattering would be favored for a beam of very slow or cold neutrons incident on a crystal which is at low temperature. In this case few lattice vibrational quanta are present in the lattice and the neutron beam is of insufficient energy to excite many such quanta.

Neutron scattering comes about because of interactions with the nuclei of the atoms of the crystal. The total neutron-scattering cross section for an element can be written as a sum of coherent and incoherent contributions as follows

$$\sigma_{\text{tot}} = \sigma_{\text{coh}} + \sigma_{\text{inc.}} \quad (3-55)$$

both σ_{coh} and $\sigma_{\text{inc.}}$ vary widely from element to element in the periodic system [14]. The more-or-less important incoherent contribution arises because of spin and other considerations. For example, neutrons have a spin 1, so they interact with nuclei having either parallel or antiparallel alignment resulting in widely different scattering amplitudes. This gives rise to an incoherent background. Furthermore, any given element may consist of more than one isotope, each with different nuclear properties and randomly distributed in the crystal. Vanadium is an example of an element with an unusually large incoherent scattering cross section [15]. One is usually interested in coherent scattering which is governed by

diffraction conditions similar to Eq. (3-30). However, incoherent processes are sometimes of special interest. For example, Placzek and Van Hove [16] have pointed out that incoherent scattering involving one lattice vibrational quanta is important in connection with crystal dynamics since these processes depend upon the overall lattice frequency distribution. Another example has to do with the use of neutron scattering to study disordered alloys the constituents of which have different nuclear properties.

Elastic neutron scattering is especially important for certain kinds of crystal structure determinations. This is the case for crystals which contain hydrogen where, because of the small z value, x-ray diffraction would be of little help in determining the location of the hydrogen atoms. The structure of ice, for example, has been elucidated with the help of neutron diffraction [14]. Another application has to do with determination of the magnetic structure of certain materials. In this case interaction of the magnetic moment of the neutron with the orbital and spin moments of the atoms of magnetic materials is of special importance. To summarize, we list the special features of neutron scattering which distinguish this technique from x-ray scattering: (1) sensitivity to the presence of light elements such as hydrogen in crystal structure analysis; (2) determination of magnetic structure through spin interaction; (3) important incoherent scattering which depends upon the distribution of isotopes or which can be used to study disorder in alloys; (4) inelastic neutron scattering and the precise determination of lattice vibrational frequencies.

Item (4) will be discussed more completely in Section 6-9. Let us now consider a quantum mechanical derivation of the elastic neutron scattering cross section.

3-10 ELASTIC NEUTRON SCATTERING

Neutrons are scattered by the atoms of a solid because they interact at close range with the atomic nuclei. In the case of fast neutrons, whose energy is higher than the binding energy of the atoms of the solid, the collisions can be classified as hard-sphere or billiard-ball type. The interaction lengths then are simply of the order of nuclear dimensions, $\sim 10^{-12}$ cm, and tend to increase as $A^{1/3}$, where A is the atomic mass number. Here we are more interested in thermal neutrons whose de Broglie wavelengths are of the order of 10^{-8} cm, which is much larger than the range of the neutron-nucleus force. Collisions between these neutrons and the atoms of a solid must be treated quantum mechanically.

Fortunately, the interaction between neutron and nucleus is relatively

weak, so that we can calculate the scattering in the Born approximation. The problem is handled by the method of localized impacts through the use of a pseudo-potential [17]. The essential point is that the range of the force during interaction is very small compared to the wavelength of the neutron. Consequently, the nucleus appears as a point scatterer, and the scattering is isotropic. In this case, the interaction potential for the i th ion can be written in terms of a delta function as follows:

$$V(\mathbf{r} - \mathbf{r}_i) = \frac{2\pi\hbar^2}{m_n} a_i \delta(\mathbf{r} - \mathbf{r}_i), \quad (3-56)$$

where m_n is the mass of the neutron and a_i is the scattering length for the bound i th atom. The scattering potential of the crystal is a sum of these spherically symmetric potentials,

$$V = \sum_i V(\mathbf{r} - \mathbf{r}_i). \quad (3-57)$$

A cross section for scattering by one nucleus can be obtained from the asymptotic solution to Schrödinger's equation, assuming the scattering potential drops to zero at large distances. This approximate solution can be written as the sum of an incident plane wave and a spherical outgoing wave; i.e.,

$$\psi = \psi_0 + \psi_s = e^{i\mathbf{k}_0 \cdot \mathbf{r}} + f(\theta, \varphi) (e^{i\mathbf{k} \cdot \mathbf{r}} / r), \quad (3-58)$$

where, in general, the scattering amplitude $f(\theta, \varphi)$ depends upon two scattering angles. Now the differential scattering cross section is just equal to the probability that a particle within a beam of unit area will be deflected into the element of solid angle, $d\Omega$. In other words, it is just the ratio of the current scattered into $d\Omega$ to incident current, where the incident current is given by probability ($\psi\psi^* = 1$) times velocity (or $\hbar\mathbf{k}_0/m_n$). The current of deflected particles per unit area (passing through unit area on a sphere of radius r) is

$$\frac{\hbar k}{m_n} \psi\psi^* = \frac{\hbar k}{m_n r^2} |f(\theta, \varphi)|^2, \quad (3-59)$$

and this must be multiplied by $r^2 d\Omega$ to obtain the flux scattered into solid angle $d\Omega$. Taking the ratio of currents and setting $|k| = |k_0|$ for elastic scattering, we have

$$d\sigma = |f(\theta, \varphi)|^2 d\Omega. \quad (3-60)$$

The total cross section is obtained by integrating over solid angle.

The scattering is therefore evaluated by determining ψ_s or the amplitude f of the outgoing spherical wave. It will be satisfactory for our purposes here, to use the stationary state wave equation corresponding

to steady incoming and outgoing waves. The integral-equation form of the scattered wave amplitude in the Born approximation at large distances is [18]:

$$f(\theta, \varphi) \simeq -\frac{m_n}{2\pi\hbar^2} \iiint e^{i(\mathbf{k}-\mathbf{k}_0)\cdot\mathbf{r}'} V(r') d\tau_{r'}. \quad (3-61)$$

(Of course we could equally well have used time-dependent perturbation theory to estimate the rate of scattering from states $\Psi(\mathbf{k}_0)$ to $\Psi(\mathbf{k})$ and from this obtain the differential cross section.)

Let us now substitute our crystal potential Eq. (3-57) into Eq. (3-61), multiply and divide by $e^{i(\mathbf{k}-\mathbf{k}_0)\cdot\mathbf{r}_i}$, and take the sum over the i nuclei outside of the integral sign. The result is

$$f(\theta, \varphi) = \frac{-m_n}{2\pi\hbar^2} \sum_i e^{i(\mathbf{k}-\mathbf{k}_0)\cdot\mathbf{r}_i} \iiint V(\mathbf{r}' - \mathbf{r}_i) e^{i(\mathbf{k}-\mathbf{k}_0)\cdot(\mathbf{r}' - \mathbf{r}_i)} d\tau_{r'}. \quad (3-62)$$

The integral is just the Fourier transform $F(\mathbf{k} - \mathbf{k}_0)$ of the scattering potential of one of the nuclei. It is quite analogous to Eq. (3-43) where $\rho(\mathbf{r})$ is replaced by $V(\mathbf{r}' - \mathbf{r}_i)$. Finally, the scattering amplitude is given by

$$f(\theta, \varphi) = -\frac{m_n}{2\pi\hbar^2} F(\mathbf{k} - \mathbf{k}_0) \sum_i e^{i(\mathbf{k}-\mathbf{k}_0)\cdot\mathbf{r}_i}. \quad (3-63)$$

By writing the direct lattice vectors $\mathbf{r}_i = l\mathbf{a} + m\mathbf{b} + n\mathbf{c}$ where l , m , and n are integers and the reciprocal lattice vectors \mathbf{K}_n are defined as before, it is easy to show that the \sum_i vanishes unless

$$\mathbf{k} - \mathbf{k}_0 = \mathbf{K}_n. \quad (3-64)$$

We thus recover our earlier condition for Bragg reflection. Finally, by substituting the delta function potential, Eq. (3-56), we can calculate the differential cross section per atom in the crystal using Eqs. (3-60) and (3-62). The result is

$$d\sigma = f^* d\Omega = a_i^2 d\Omega. \quad (3-65)$$

Thus integrating over all angles the coherent cross section per atom is just

$$\sigma_{coh} = 4\pi a_i^2, \quad (3-66)$$

as it should be if the scattering length, a_i , is properly defined. The quantities a_i vary substantially from element to element due to resonance contributions which depend upon the behavior of the neutron within

the nucleus. In the simple case above, we have evaluated a coherent cross section and assumed all the scattering centers the same. Usually the differential cross section for a crystal will have both coherent and incoherent parts and must be an average, or sum over all nuclei, with proper regard to the a_i and a random distribution of isotopes. The reader is referred to the literature [14, 19, 20] for further discussion.

3-11 ELECTRON DIFFRACTION

The energy of electrons of suitable wavelength for diffraction is quite low, and the interaction of electrons with matter is high. Such low-energy electrons will penetrate only a small distance into a solid so that electron diffraction is better suited for the investigation of thin films or of the surface of crystals. Whereas most of our knowledge of solid state physics ignores the surface and has to do with the bulk, there is increasing realization of the importance of surface structure. Thermionic emission, photo-emission, corrosion, and catalysis are some of the phenomena strongly dependent upon the structure of the surface.

A freshly prepared surface, cleaved or electropolished, rapidly becomes contaminated with foreign atoms; therefore experiments on the structure of the surface are necessarily carried out in ultrahigh vacuum at pressures of 10^{-10} to 10^{-9} Torr. The techniques for electron diffraction at a surface have been available for 40 years, but the routine achievement of ultrahigh vacuum is a rather recent development. Consequently, renewed interest in electron diffraction has appeared and rapid progress is being made on understanding the surfaces of some crystalline materials. It is found, for example, that clean surfaces of nickel, which has a fcc structure, can be prepared with just the atomic arrangement expected for {111}, {100}, or {110} surface planes. With care, an ideal surface can likewise be prepared on the bcc metal tungsten. On the other hand, when clean surfaces of Ge or Si are prepared, it is found that the structure is drastically modified by the dangling bonds at the surface. An interesting introduction to this subject has been given recently by one of the discoverers of electron diffraction, L. H. Germer [21].

Thus we conclude our discussion of the diffraction of radiation by crystals. We found many similarities and some differences between the behavior of electromagnetic and particle radiation of appropriate wavelength. Very similar diffraction conditions apply in each case. Again, the periodicity of the lattice is a central feature, and important concepts such as Brillouin zones were introduced. Certain topics such as lattice dynamics were touched upon, but these will be discussed at greater length in later chapters.

CHAPTER 2

axis of rotation

(111) plane in
in a cubic crystal?
bic crystal?
sic crystal? Again (hkl) plane.
and c -axes in a
n of the methoden atoms or mol
oms or molecules
external electric
e waves that for
stant) we should

don (1928).

955).

(1956).

isco (1959).

Green & Co,

(1940).

York (1951).

atalog Co., Inc,

X-RAY CRYSTAL ANALYSIS

2.1

INTRODUCTION

The use of X-ray diffraction as a technique for crystal structure analysis dates from von Laue's discovery of the X-ray diffraction effect for single crystal samples in 1912. Laue predicted that the atoms of a single crystal specimen would diffract a parallel, monochromatic X-ray beam, giving a series of diffracted beams whose directions and intensities would be dependent upon the lattice structure and chemical composition of the crystal. These predictions were soon verified by the experimental work of Friedrich and Knipping. A schematic diagram of the experimental arrangement is shown in Figure 2.1(a). The location of the diffraction maxima was explained by W. L.

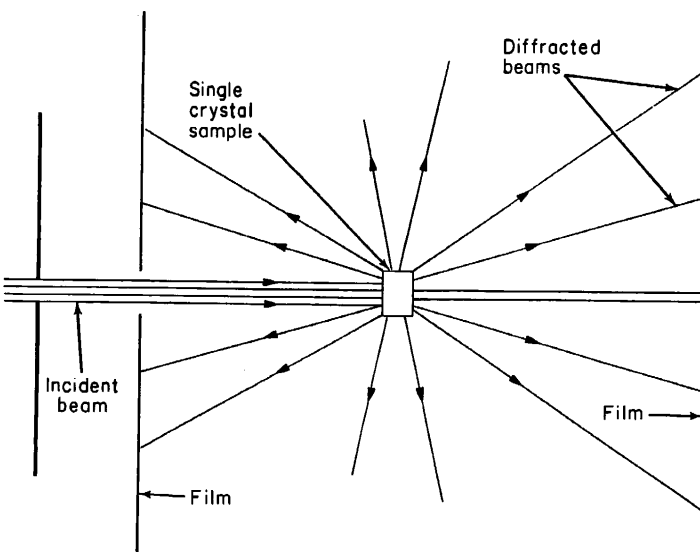


FIGURE 2.1. (a) Schematic diagram of X-ray diffraction by the Laue technique.

Bragg¹ on the basis of a very simple model in which it is assumed that the X-radiation is reflected specularly from successive planes of various (hkl) families in the crystal, the diffraction maxima being found for directions of incidence and reflection such that the reflections from adjacent planes of a family interfere constructively, differing in phase by $2\pi n$ radians, where n is an integer.

According to this idea, the path difference for successive reflections must equal an integral number of X-ray wavelengths. But this path difference, from Figure 2.2, is $2d \sin \theta$, where d is the spacing between adjacent atomic planes, as given by (1.5-2) or (1.5-5), and θ is the glancing angle between the atomic plane and the incident beam.

¹ W. L. Bragg, *Proc. Cambridge Phil. Soc.* 17, 43 (1912).

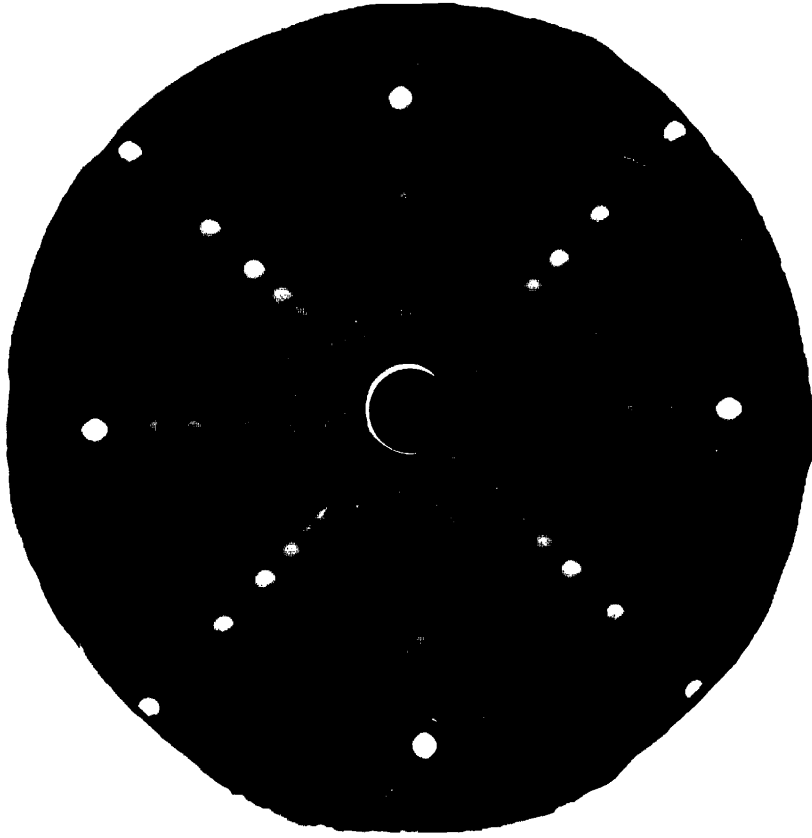


FIGURE 2.1 (Cont'd). (b) A Laue diffraction pattern of a lithium fluoride crystal, incident X-ray beam along a {100} direction. [Photo courtesy of H. A. McKinstry, Materials Research Laboratory, Pennsylvania State University.]

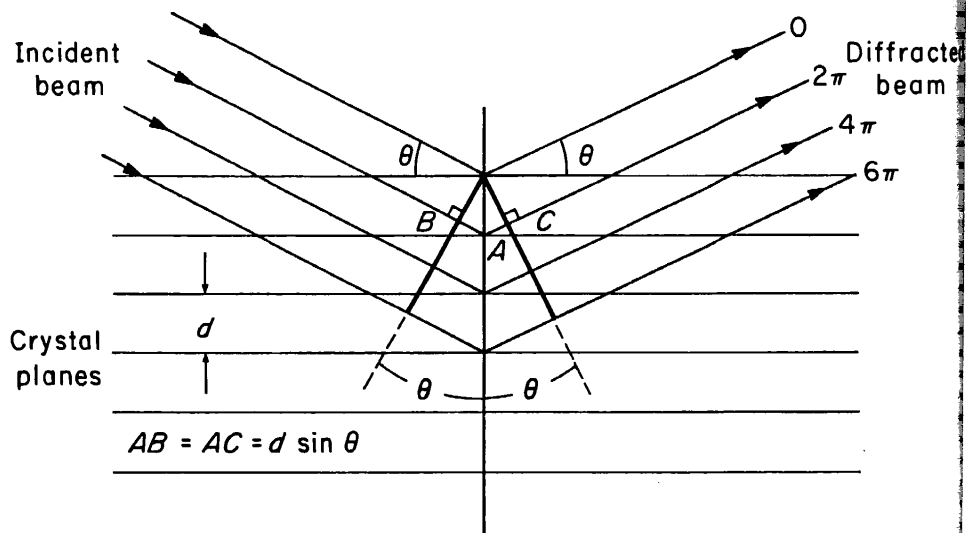


FIGURE 2.2. The Bragg picture of X-ray diffraction in terms of in-phase reflections from successive planes of a particular (hkl) family.

The strongly diffracted beams, then, must propagate out from the crystal in directions for which the Bragg equation

$$n\lambda = 2d \sin \theta \quad (2.1-1)$$

is satisfied.

The experimental observation of X-ray diffraction patterns was greatly simplified by the introduction of the powder method by Debye and Scherrer² in 1916. In this method, as illustrated in Figure 2.3(a), a parallel, monochromatic beam of X-rays is

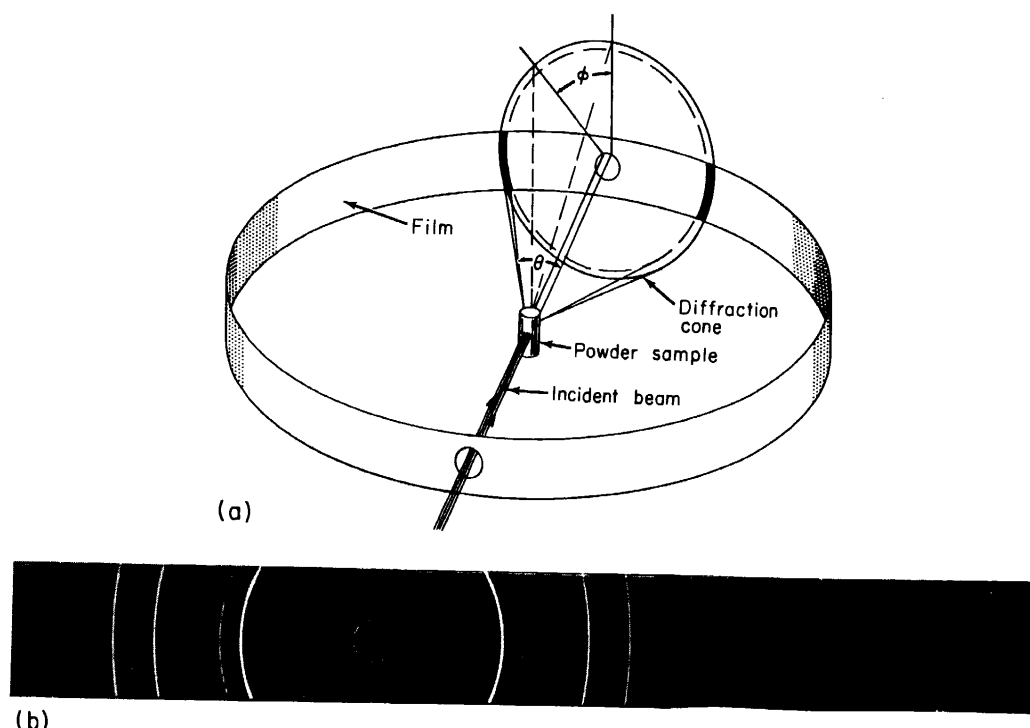


FIGURE 2.3. (a) Schematic diagram of X-ray diffraction by the Debye-Scherrer powder technique. (b) A Debye-Scherrer powder diffraction pattern from a sample of a complex scandium-zirconium oxide. [Photo courtesy of H. A. McKinstry, Materials Research Laboratory, Pennsylvania State University.]

allowed to pass through a very finely powdered specimen. Just by chance, some of the microcrystals of the powdered specimen will be oriented at the correct diffraction angle for a particular set of planes (hkl), as given by (2.1-1), and a diffracted beam will result. Since the diffraction condition can be satisfied for any possible angular orientation ϕ of the normal to the scattering planes around the incident beam axis, and since there will always be microcrystals oriented such as to produce the (hkl) diffraction for any value of ϕ , the diffracted beam will have the form of a cone whose apex angle is θ , rather than just a pencil of rays. It is customary to wrap a film strip around the inside of a cylindrical chamber, concentric with the sample, so as to intercept a certain portion of these diffraction cones, a series of arcs being produced on the film. A powder pattern made in this way is shown in Figure 2.3(b).

² P. Debye and P. Scherrer, *Physikal. Zeitschr.* **17**, 277 (1916).

2.2 PHYSICS OF X-RAY DIFFRACTION: THE VON LAUE EQUATIONS

X-rays can easily be produced by allowing high-energy electrons to strike a metal target anode. The X-rays so produced possess, in addition to a continuous background spectrum, a few very intense, nearly monochromatic spectrum lines, whose frequency is characteristic of the target material. These lines arise from the excitation of inner-shell atomic electrons to more highly excited states, from which they decay to the original ground state with the emission of X-ray quanta. The production of X-rays by the interaction of high-energy electrons with matter is discussed in some detail by Leighton.³

If a potential V_0 exists between the cathode and anode of the X-ray tube, the electrons acquire energy eV_0 , where e is the magnitude of the electronic charge, from the accelerating potential as they reach the anode. The most energetic X-ray quantum which can be produced by such electrons is that for which the quantum energy $h\nu$ equals eV_0 . Thus, for such a quantum,

$$eV_0 = h\nu = hc/\lambda, \quad (2.2-1)$$

where $h (= 6.62 \times 10^{-27} \text{ erg-sec})$ is Planck's constant. The shortest X-ray wavelength which can be produced is thus

$$\lambda = \frac{hc}{eV_0}. \quad (2.2-2)$$

For a voltage of 10 kilovolts, this shows that the minimum X-ray wavelength which can be excited is $1.24 \times 10^{-8} \text{ cm.}$, or 1.24 \AA ngström units. This is just of the order of interatomic distances in actual crystals, and is, according to the Bragg equation (2.1-1), just right for producing observable diffraction effects with reasonable values of d and θ . An X-ray tube in which electrons are accelerated by a potential of a few tens of kilovolts may thus be regarded as satisfactory for producing X-rays which are suitable for crystal diffraction work.

When the atoms of a crystal are exposed to electromagnetic radiation, such as X-rays, they experience electrical forces due to the interaction of the charged particles of the atoms with the electric field vector of the electromagnetic wave. The atomic electrons are therefore vibrated harmonically at the frequency of the incident radiation, thus undergoing acceleration. These accelerated charges, according to electromagnetic theory, reradiate electromagnetic energy at the frequency of vibration, that is, at the incident wave frequency. At visible light frequencies, where the incident wavelength is much larger than the interatomic distances, the superposition of the waves thus reradiated or *scattered* by the individual atoms of the crystal simply gives rise to the well-known effects of optical refraction and reflection. At X-ray frequencies, however, the incident wavelength is comparable to the interatomic spacing, and diffraction of the radiation by the atoms of the crystal can be observed.

Bragg assumed that systems of crystal planes could act to reflect X-rays specularly, provided that the condition for constructive interference between reflections from successive atomic planes is satisfied. We wish now to examine in detail the way in

³ R. B. Leighton, *Principles of Modern Physics*, McGraw-Hill Book Co., Inc., New York (1959), pp. 405-421.

THE VON LAUE

by electrons to strike a metal to a continuous background spectrum lines, whose frequency from the excitation of inner atom which they decay to the a. The production of X-ray is discussed in some detail

node of the X-ray tube, the of the electronic charge, from lost energetic X-ray quantum which the quantum energy $h\nu$

(2.2-1)

the shortest X-ray wavelength

(2.2-2)

a X-ray wavelength which This is just of the order according to the Bragg equation with reasonable values produced by a potential of a few producing X-rays which are

magnetic radiation, such as of the charged particles magnetic wave. The atomic of the incident radiation, owing to electromagnetic radiation, that is, at the incident wavelength of the waves thus gives rise to the frequencies, however, and diffraction of

X-rays specularly, reflections from detail the way in

New York (1959),

which X-rays scattered from different individual atoms can recombine, proving the validity of the Bragg picture, and establishing methods which can be used to extend the Bragg result in a number of ways. Let us examine the radiation scattered by two identical scattering centers separated by a distance \mathbf{r} . The vector \mathbf{n}_0 is defined to be a unit vector in the direction of the incident beam, and the vector \mathbf{n}_1 is taken to be a unit vector in an arbitrary scattering direction, as shown in Figure 2.4. The incident radiation is assumed to be a parallel beam, and the scattered beam is assumed to be detected at a very distant observation point. The path difference between the radiation scattered at P and that scattered at O is then

$$PA - OB = \mathbf{r} \cdot \mathbf{n}_0 - \mathbf{r} \cdot \mathbf{n}_1 = \mathbf{r} \cdot (\mathbf{n}_0 - \mathbf{n}_1). \quad (2.2-3)$$

The vector $\mathbf{n}_0 - \mathbf{n}_1 = \mathbf{N}$ is the normal to what would in the Bragg picture be called the reflecting plane, if \mathbf{n}_1 were a diffraction direction, as shown in Figure 2.5. It is clear from this figure, also, that the magnitude of this vector is

$$N = 2 \sin \theta. \quad (2.2-4)$$

The phase difference ϕ_r between the radiation scattered at the two points is

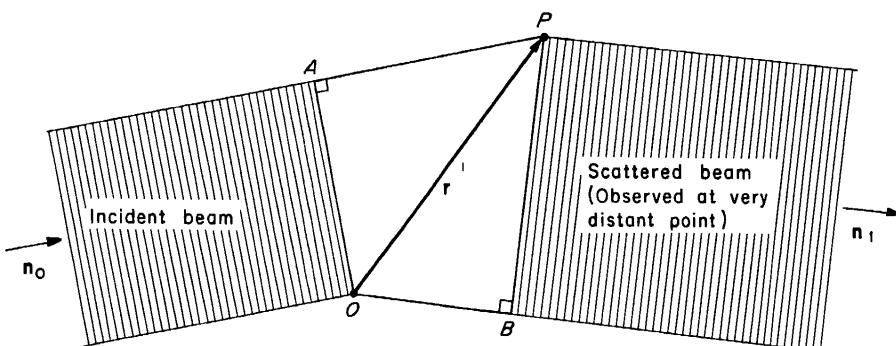


FIGURE 2.4. Geometry of the X-ray scattering situation discussed in Section 2.2.

simply $2\pi/\lambda$ times the path difference, whereby

$$\phi_r = \frac{2\pi}{\lambda} (\mathbf{r} \cdot \mathbf{N}). \quad (2.2-5)$$

Now, in order that the direction \mathbf{n} be a diffraction maximum, the scattering contribution from *every atom in the crystal* in that direction must differ in phase by an integral multiple of 2π radians. In order for this to be true, it is only necessary for the radiation from atoms separated by the *primitive* lattice vectors \mathbf{a} , \mathbf{b} , and \mathbf{c} to add in phase, for then the contribution from other atoms, separated from the origin by integral combinations of these vectors will certainly add in phase. If scattering contributions from neighboring atoms were to differ in phase in any other manner, it would then always be possible to find an atom somewhere in the crystal which would contribute radiation just π radians out of phase with the contribution from a given atom; these contributions would then cancel, atom by atom, giving no diffracted beam. A consideration of an example where neighboring atoms along the \mathbf{a} -direction contribute radiation components in a given direction which are out of phase by π radians (or $\pi/2$, $\pi/4$, $\pi/6$, etc.,) will quickly serve to verify this assertion.

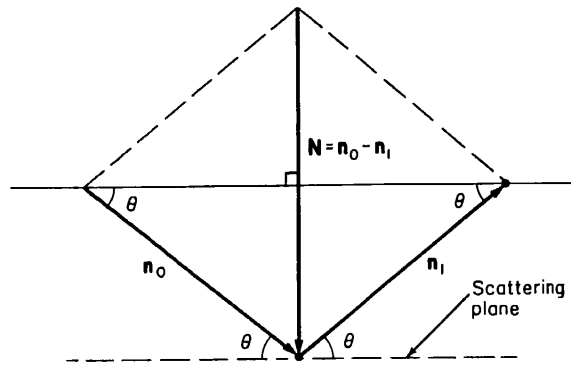


FIGURE 2.5. Geometrical relation of the incident and diffracted beams, the scattering normal, and the "scattering plane."

We need thus only require that an integral multiple of 2π be obtained in (2.2-5) when \mathbf{r} equals \mathbf{a} , \mathbf{b} , or \mathbf{c} , that is, we must require simultaneously that

$$\begin{aligned} \frac{2\pi}{\lambda} (\mathbf{a} \cdot \mathbf{N}) &= 2\pi h' = 2\pi nh \\ \frac{2\pi}{\lambda} (\mathbf{b} \cdot \mathbf{N}) &= 2\pi k' = 2\pi nk \\ \frac{2\pi}{\lambda} (\mathbf{c} \cdot \mathbf{N}) &= 2\pi l' = 2\pi nl. \end{aligned} \quad (2.2-6)$$

Here h' , k' , l' can be *any* three integers; in general, these three integers *may* contain a largest integer common factor n greater than unity, in which case we can write $h' = nh$, $k' = nk$ and $l' = nl$, where now h , k , and l are three integers in the same ratio as h' , k' and l' , but having no common factor greater than unity. If h' , k' , and l' do not have a common factor greater than unity, then n is simply taken to be unity. If α , β , and γ are the angles between the scattering normal N and the \mathbf{a} -, \mathbf{b} -, and \mathbf{c} -axes of the crystal, respectively, then, according to (2.2-4), $\mathbf{a} \cdot \mathbf{N} = aN \cos \alpha = 2a \sin \theta \cos \alpha$, etc., where by (2.2-6) can be written

$$\begin{aligned} 2a \sin \theta \cos \alpha &= h'\lambda = nh\lambda, \\ 2b \sin \theta \cos \beta &= k'\lambda = nk\lambda, \\ 2c \sin \theta \cos \gamma &= l'\lambda = nl\lambda. \end{aligned} \quad (2.2-7)$$

These equations are called the Laue equations. For a given incident wavelength λ and given values of the integers h , k , l , and n , the equations determine a certain value of θ and two of the three quantities ($\cos \alpha$, $\cos \beta$, $\cos \gamma$). However, only two of the three quantities (α, β, γ) are independent, because once the angles between a vector and two of the three coordinate axes are fixed, the direction of the vector is fixed and the third angle can be determined trigonometrically. For example, in an orthogonal

coordinate system, an elementary result of analytic geometry is that $\cos^2 \alpha + \cos^2 \beta + \cos^2 \gamma = 1$. The three equations (2.2-7) thus serve to determine a unique value for θ and N , thus defining a scattering direction. The direction cosines of the scattering normal N are seen from (2.2-7) to be proportional to h/a , k/b , and l/c . However, neighboring planes whose *Miller indices* are (hkl) intersect the a -, b -, and c -axes at intervals a/h , b/k , and c/l ; the direction cosines of the normal to the (hkl) family of planes are therefore, according to (1.5-1), also proportional to h/a , k/b and l/c . The scattering normal N is thus identical to the normal to the (hkl) planes, and hence the (hkl) planes may be regarded as the reflecting planes of the Bragg picture.

The Bragg equation can be shown to follow from the Laue equations by setting $h = a \cos \alpha/d$, $k = b \cos \beta/d$, $l = c \cos \gamma/d$, in Equation (1.5-1), whereby each of the three Laue equations reduces to

$$n\lambda = 2d \sin \theta,$$

where d is the distance between adjacent planes of the (hkl) system, and where the order n of the diffraction is the greatest common factor between the orders of interference h' , k' , and l' . It is customary to refer to an observed X-ray reflection by the numbers $(h'k'l')$ which give the order of interference between neighboring atoms along the crystal axes; thus the first order diffraction maximum for the (111) planes is referred to as the (111) reflection, the second order diffraction maximum for the same set of planes ($n = 2$, $h' = 2h$, $k' = 2k$, $l' = 2l$) as the (222) reflection, the third order as the (333) reflection, etc.

(2.2-6)

2.3 THE ATOMIC SCATTERING FACTOR

The calculations of the previous section were based on the assumption of point scattering centers at the lattice points. We now wish to take into account that the scattering, which is the result of an interaction between the atomic electrons and an X-ray beam, may take place anywhere the electrons may happen to be. More precisely, we wish to modify our calculations by considering that the X-radiation is scattered by a continuous distribution of "electron density" associated with each lattice point. This concept, as we shall see later, is in full accord with a wave-mechanical view of the process. It should be noted, however, that we are neglecting the scattering effect of the atomic nuclei, which interact much less strongly with the X-rays. We shall find that the effect of the finite extent of the electron density distribution is that the amplitude of the diffracted radiation is multiplied by a factor involving the X-ray wavelength, the glancing angle and the electron density distribution associated with the atoms.

We begin by inquiring into the ratio between the X-ray diffraction amplitude, at the Bragg angle, scattered by an element of charge $p(\mathbf{r})dv$, located in a volume element dv about the point \mathbf{r} , and that scattered by a single point electron at the lattice point, as illustrated in Figure 2.6. Here $p(\mathbf{r})$ is the electron density; $Z^{-1}p(\mathbf{r})dv$ is the probability that an electron will be found in the volume element dv . It must be required, of course, that

$$\int_v p(\mathbf{r}) dv = Z, \quad (2.3-1)$$

wavelength
in value
o of the
a vector
is fixed
agonal

(2.2-7)

contain a
ite $h' = nh$,
as h' , k' ,
not have
 α , β , and γ
the crystal,
ic., where-

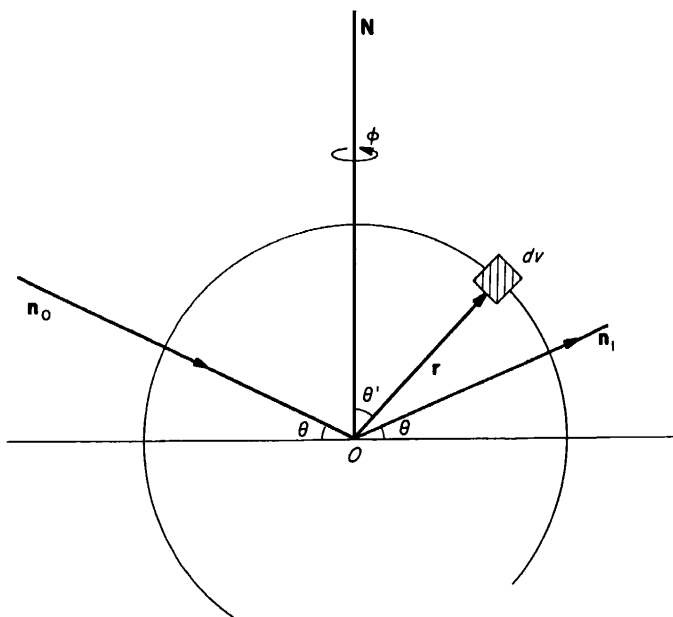


FIGURE 2.6. Geometry of the X-ray scattering situation discussed in Section 2.3. Radiation scattered at the Bragg angle by an electron density contained within the volume element dv at \mathbf{r} is compared with that which would be scattered by a point electron at O .

where Z is the number of atomic electrons per atom, that is, the atomic number of the atoms of which the crystal is composed. The above integral is taken over all space, although in making actual calculations it is usually assumed that the "electron clouds" associated with different atoms in the crystal do not overlap appreciably, hence that the electron cloud of a single atom is confined to the volume of a unit cell.

The difference in phase ϕ_r , between the radiation scattered at the origin and that scattered in the element dv at \mathbf{r} is, from (2.2-5)

$$\phi_r = \frac{2\pi}{\lambda} (\mathbf{r} \cdot \mathbf{N}). \quad (2.3-2)$$

If the scattering amplitude from the point electron along the direction \mathbf{n}_1 is represented as $Ae^{i(k_s - \omega t)}$, where $k = 2\pi/\lambda$ and s is a distance coordinate along the scattering direction \mathbf{n}_1 , then the scattering amplitude along that direction from the element dv will be $\rho(\mathbf{r})dv$ times as strong (since it will be proportional to the amount of charge in that element) and out of phase by an amount given by (2.3-2). The ratio of the amplitude of the radiation scattered by the element dv to that scattered by a point electron at the origin, which we shall call df , will then be

$$df = \frac{Ae^{i(k_s - \omega t) + i\phi_r} \rho(\mathbf{r}) dv}{Ae^{i(k_s - \omega t)}} = \rho(\mathbf{r}) e^{(2\pi i/\lambda)(\mathbf{r} \cdot \mathbf{N})} dv. \quad (2.3-3)$$

If we integrate over all space, we shall find the ratio f of the scattered amplitude from

the whole atom to that for a point electron at the lattice point. Thus,

$$f = \int_v \rho(\mathbf{r}) e^{(2\pi i/\lambda)(\mathbf{r} \cdot \mathbf{N})} dv. \quad (2.3-4)$$

However, according to (2.2-4)

$$\frac{2\pi}{\lambda} (\mathbf{r} \cdot \mathbf{N}) = \frac{2\pi}{\lambda} Nr \cos \theta' = \frac{4\pi}{\lambda} r \sin \theta \cos \theta' = \mu r \cos \theta', \quad (2.3-5)$$

where

$$\mu = \frac{4\pi}{\lambda} \sin \theta. \quad (2.3-6)$$

If the charge density of the atom is spherically symmetric, and thus a function of r only, $\rho(\mathbf{r}) = \rho(r)$ and

$$f = \int_0^\infty \int_0^\pi \int_0^{2\pi} \rho(r) e^{i\mu r \cos \theta'} r^2 \sin \theta' dr d\theta' d\phi. \quad (2.3-7)$$

It is possible to evaluate the angular parts of this integral, integrating first over ϕ , then over θ' (letting $x = \cos \theta'$, $dx = -\sin \theta' d\theta'$), finally expressing the exponential factors as trigonometric functions, obtaining

$$f(\mu) = \int_0^\infty 4\pi r^2 \rho(r) \frac{\sin \mu r}{\mu r} dr. \quad (2.3-8)$$

This quantity, the ratio of the amplitude scattered by the actual atom to that scattered by a point electron on the lattice point, is called the atomic scattering factor. As $\theta \rightarrow 0$, $\mu \rightarrow 0$, and $\sin \mu r / \mu r \rightarrow 1$, whereby

$$\lim_{\mu \rightarrow 0} f(\mu) = \int_0^\infty 4\pi r^2 \rho(r) dr = \int_v \rho dv = Z. \quad (2.3-9)$$

The values of $\rho(r)$ must be obtained by evaluating, quantum mechanically, the "wave functions" of the atoms in the crystal. We shall see in a later chapter precisely what is involved in this process. In practice, the wave functions for free atoms are often used in scattering factor calculations to obtain approximate results for expected intensities, rather than the actual modified wave functions which are appropriate for the atoms when present in a crystal lattice.

2.4 THE GEOMETRICAL STRUCTURE FACTOR

Up to this point we have assumed that we are dealing with unit cells having atoms only at the corners (that is, primitive unit cells). If we wish to predict the characteristics of radiation diffracted from crystals having complex unit cells containing more than

one atom, such as the cubic cells for the b.c.c. and f.c.c. structures, we must account for the interaction of beams which are diffracted by the various atoms within the unit cell. If, for the $(h'k'l')$ reflection, we denote the ratio of the amplitude of the radiation scattered by the entire unit cell to that scattered by a point electron at the origin by $F(h'k'l')$, then

$$F(h'k'l') = \sum_i f_i e^{i\phi_i}. \quad (2.4-1)$$

Here f_i is the atomic scattering factor for the i th atom of the unit cell and ϕ_i refers to the phase difference between radiation scattered at the origin and radiation scattered from the i th atom of the unit cell. The sum is taken over all atoms belonging to a unit cell. The phase difference ϕ_i is given by (2.3-2), whereby (2.4-1) may be written

$$F(h'k'l') = \sum_i f_i e^{(2\pi i/\lambda)(\mathbf{r}_i \cdot \mathbf{N})}, \quad (2.4-2)$$

where \mathbf{r}_i is a vector from the origin to the i th atom of the unit cell. If the fractional positional coordinates of the i th atom, as defined in Section 1.4, are (x_i, y_i, z_i) , then \mathbf{r}_i can be written

$$\mathbf{r}_i = x_i \mathbf{a} + y_i \mathbf{b} + z_i \mathbf{c}. \quad (2.4-3)$$

However, according to Equation (2.2-6), $\mathbf{a} \cdot \mathbf{N} = h'\lambda$, etc.; substituting (2.4-3) into (2.4-2) and using this result, we find

$$\mathbf{r}_i \cdot \mathbf{N} = \lambda(h'x_i + k'y_i + l'z_i), \quad (2.4-4)$$

whereby

$$F(h'k'l') = \sum_i f_i e^{2\pi i(h'x_i + k'y_i + l'z_i)}. \quad (2.4-5)$$

When all atoms of the crystal are *identical*, this can be written in a particularly simple form, for then all the f_i have the same value f . Equation (2.4-5) then becomes

$$F(h'k'l') = f S \quad (2.4-6)$$

where

$$S = \sum_i e^{2\pi i(h'x_i + k'y_i + l'z_i)}. \quad (2.4-7)$$

The total scattered amplitude is thus given by the product of the atomic scattering factor and a factor S which is governed by the geometrical arrangement of atoms within the unit cell and which is called the *geometrical structure factor*. For crystals where all atoms are not identical, no such separation is possible, and the more general form (2.4-5) must be used.

The *intensity* of the diffracted beam is proportional to the square of the amplitude F , or, more accurately, since F is complex, to the square of the absolute value of F , which is F^*F , where F^* is the complex conjugate of F . If $F(h'k'l')$ as given by (2.4-5) is written as the complex number $\alpha + i\beta$, then $F^* = \alpha - i\beta$ and

$$|F|^2 = F^*F = \alpha^2 + \beta^2, \quad (2.4-8)$$

uctures, we must account for all atoms within the unit cell. The amplitude of the radiation scattered by an electron at the origin by (2.4-1) may be written

(2.4-1)

he unit cell and ϕ_i refers to the angle of radiation scattered by all atoms belonging to a given atom. This by (2.4-1) may be written

(2.4-2)

unit cell. If the fractional coordinates of the atoms, given in 1.4, are (x_i, y_i, z_i) , then

(2.4-3)

substituting (2.4-3) into (2.4-1) we get

(2.4-4)

(2.4-5)

in a particularly simple case, the expression (2.4-4) then becomes

(2.4-6)

(2.4-7)

product of the atomic scattering factor and the arrangement of atoms within the unit cell. For crystals where the atoms are arranged in a regular lattice, the more general expression for the amplitude of the scattered radiation is given by (2.4-5)

(2.4-8)

where

$$\alpha = \operatorname{Re}(F) = \sum_i [f_i \cos 2\pi(h'x_i + k'y_i + l'z_i)], \quad (2.4-9)$$

and

$$\beta = \operatorname{Im}(F) = \sum_i [f_i \sin 2\pi(h'x_i + k'y_i + l'z_i)]. \quad (2.4-10)$$

As an example, let us discuss the case of a b.c.c. crystal in which all atoms are identical. There are two atoms in the cubic unit cell in this structure, one corner atom and one body-center atom, and we may proceed by arbitrarily assigning the corner atom whose coordinates (x_i, y_i, z_i) are $(0,0,0)$ to the unit cell and excluding the other corner atoms from consideration; the other atom in the cell is the body-center atom which belongs exclusively to the unit cell and whose cell coordinates are $(\frac{1}{2}, \frac{1}{2}, \frac{1}{2})$. According to this scheme, then, the diffraction amplitude according to (2.4-6) and (2.4-7) is, for the $(h'k'l')$ diffraction direction,

$$F(h'k'l') = f \sum_i e^{2\pi i(h'x_i + k'y_i + l'z_i)} = f[1 + e^{i\pi(h' + k' + l')}] \quad (2.4-11)$$

The way in which *one* corner atom was assigned to the cell and the others left out may be thought to be rather arbitrary; a more reasonable way might be proposed, in which $\frac{1}{8}$ of each corner atom is assigned to the cell, each at its respective cell coordinate location. This alternative way of proceeding can be shown to lead to exactly the same expression as that obtained in (2.4-11) for the geometrical structure factor. The verification of this statement is assigned as an exercise. In general, the assignment of the atoms belonging in the unit cell can be made in an arbitrary fashion, as above, as long as the correct number of atoms of each category (face, corner, edge, interior) is assigned to the unit cell.

According to (2.4-11) the geometrical structure factor $1 + \exp[i\pi(h' + k' + l')]$ vanishes for any $(h'k'l')$ reflection for which $h' + k' + l'$ is an odd number, since $\exp(n\pi i) = -1$ when n is odd. Therefore, in the b.c.c. structure, certain $(h'k'l')$ reflections which would be present for a simple cubic structure of the same cube edge dimension, are missing. There is, for example, no (100) reflection, although the (200) is present; there is likewise no (111) reflection, although (222) is present. This effect can be understood physically, at least for the case of the (100) reflection, by noting first that for a simple cubic structure the beams reflected from the top and bottom cube faces of the unit cell differ in phase by 2π for the (100) diffraction direction. In the b.c.c. structure having the same cube edge dimension, however, there is another plane of atoms (body centers) located parallel to and halfway between the top and bottom cube face planes of the unit cells, as shown in Figure 2.7. The density of atoms in these intermediate planes is the same as that of the top and bottom cube face planes, and they therefore give rise to diffracted beams of intensity equal to those produced by the top and bottom planes of the unit cell, but out of phase with these beams by π radians. The diffracted beams from the top planes and body-center planes thus interfere destructively in pairs, giving no net diffracted beam for this set of conditions. The (200) reflection is present, however, because for this case the top and bottom planes give rise to beams which are out of phase by 4π . The planes of body centers then contribute beams which differ by 2π in phase from the reflections from top and bottom planes, hence reinforcing them rather than cancelling. The other missing reflections for the b.c.c. structure may be accounted for physically using similar lines of reasoning.

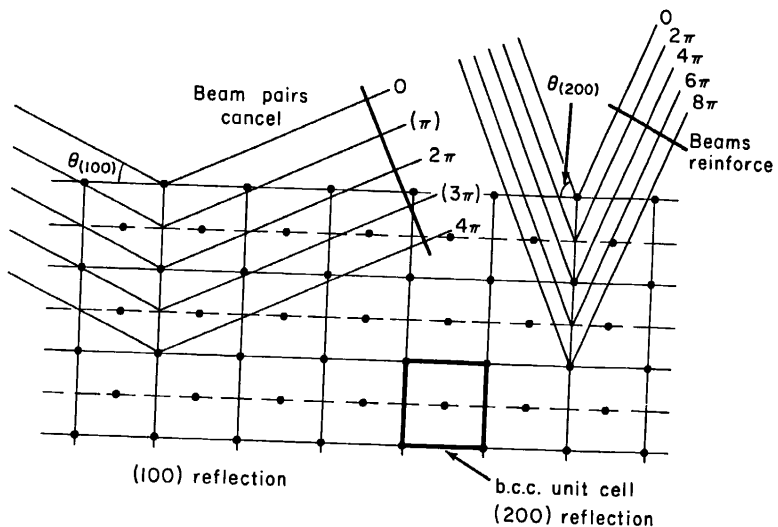


FIGURE 2.7. Phase relations for the (100) and (200) diffraction angles in a body-centered cubic structure.

2.5 THE RECIPROCAL LATTICE

It is convenient at this point to introduce the concept of the reciprocal lattice. The reciprocal lattice is a lattice of points which is related in a certain way to the direct space lattice. The Bragg condition for X-ray diffraction can be expressed in a very simple way with the aid of the reciprocal lattice, and we shall find in a later chapter that the wave-mechanical behavior of electrons in periodic crystal lattices is also most readily understood in terms of the reciprocal lattice of the crystal.

If \mathbf{a} , \mathbf{b} , and \mathbf{c} are the *primitive* translation vectors of a direct space lattice, the primitive translation vectors of the *reciprocal* lattice, \mathbf{a}^* , \mathbf{b}^* , and \mathbf{c}^* are defined by the relations

$$\mathbf{a}^* \cdot \mathbf{a} = \mathbf{b}^* \cdot \mathbf{b} = \mathbf{c}^* \cdot \mathbf{c} = 1 \quad (2.5-1)$$

and $\mathbf{a}^* \cdot \mathbf{b} = \mathbf{a}^* \cdot \mathbf{c} = \mathbf{b}^* \cdot \mathbf{c} = \mathbf{b}^* \cdot \mathbf{a} = \mathbf{c}^* \cdot \mathbf{a} = \mathbf{c}^* \cdot \mathbf{b} = 0. \quad (2.5-2)$

Since from (2.5-2) $\mathbf{a}^* \cdot \mathbf{b} = \mathbf{a}^* \cdot \mathbf{c} = 0$, the vector \mathbf{a}^* is perpendicular to the plane determined by \mathbf{b} and \mathbf{c} . It is therefore parallel to the vector $\mathbf{b} \times \mathbf{c}$, and can be expressed as a multiple of that vector, that is,

$$\mathbf{a}^* = A(\mathbf{b} \times \mathbf{c}), \quad (2.5-3)$$

where A is a scalar constant. However, from (2.5-1),

$$\mathbf{a}^* \cdot \mathbf{a} = A(\mathbf{b} \times \mathbf{c}) \cdot \mathbf{a} = 1, \quad (2.5-4)$$

whereby, solving for A and substituting the value so obtained into (2.5-3),

$$\mathbf{a}^* = \frac{\mathbf{b} \times \mathbf{c}}{\mathbf{a} \cdot \mathbf{b} \times \mathbf{c}}. \quad (2.5-5)$$

In a similar fashion, one can show that

$$\mathbf{b}^* = \frac{\mathbf{c} \times \mathbf{a}}{\mathbf{a} \cdot \mathbf{b} \times \mathbf{c}}$$

$$\mathbf{c}^* = \frac{\mathbf{a} \times \mathbf{b}}{\mathbf{a} \cdot \mathbf{b} \times \mathbf{c}}$$

Using the same general approach, the reverse transformations

$$\mathbf{a} = \frac{\mathbf{b}^* \times \mathbf{c}^*}{\mathbf{a}^* \cdot \mathbf{b}^* \times \mathbf{c}^*}, \quad (2.5-6)$$

etc., can be obtained.

Suppose, as an example, we wish to determine the reciprocal lattice for a f.c.c. structure. We must start with the primitive unit cell of Figure 1.5(a) for which the primitive basis vectors \mathbf{a} , \mathbf{b} , and \mathbf{c} can be written

$$\mathbf{a} = \frac{a}{2} (\mathbf{i}_x + \mathbf{i}_y)$$

$$\mathbf{b} = \frac{a}{2} (\mathbf{i}_x + \mathbf{i}_z) \quad (2.5-7)$$

$$\mathbf{c} = \frac{a}{2} (\mathbf{i}_y + \mathbf{i}_z),$$

where a is the edge of the cubic cell, and where the x -coordinate axis is taken to be along \mathbf{a} , the y -axis along \mathbf{b} and the z -axis along \mathbf{c} . Then

$$\mathbf{a}^* = \frac{\mathbf{b} \times \mathbf{c}}{\mathbf{a} \cdot \mathbf{b} \times \mathbf{c}} = \frac{\frac{a^2}{4} (\mathbf{i}_x + \mathbf{i}_z) \times (\mathbf{i}_y + \mathbf{i}_z)}{\frac{a^3}{8} (\mathbf{i}_x + \mathbf{i}_y) \cdot [(\mathbf{i}_x + \mathbf{i}_z) \times (\mathbf{i}_y + \mathbf{i}_z)]} = \frac{1}{a} (\mathbf{i}_x + \mathbf{i}_y - \mathbf{i}_z);$$

$$\text{similarly, } \mathbf{b}^* = \frac{1}{a} (\mathbf{i}_x - \mathbf{i}_y + \mathbf{i}_z), \quad \mathbf{c}^* = \frac{1}{a} (-\mathbf{i}_x + \mathbf{i}_y + \mathbf{i}_z). \quad (2.5-8)$$

It is clear that these vectors have the cube diagonal directions, as do the primitive vectors of the b.c.c. structure, as shown in Figure 1.5(b). In addition, it should be noted that the lattice spacing of the reciprocal lattice is proportional to $1/a$. More explicitly, it is evident that any vector \mathbf{r}^* connecting two lattice points of the reciprocal lattice must have the form

$$\mathbf{r}^* = l\mathbf{a}^* + m\mathbf{b}^* + n\mathbf{c}^*, \quad (2.5-9)$$

TABLE 2.1.
Lattice Points for the f.c.c. Reciprocal Lattice
(All points are of the form $[(l+m-n), (l-m+n), (-l+m+n)]$)

	$l = -2$	$l = -1$	$l = 0$	$l = 1$	$l = 2$
$m = -2$	$(-n-4, n, n)$ -2, -2, -2	$(-n-3, n+1, n-1)$ -2, 0, -2	$(-n-2, n+2, n-2)$ -2, 2, -2		
				$(-n-1, n+1, n-1)$ -1, 1, -1	$(-n, n+2, n-2)$ -1, 1, -1
$m = -1$	$(-n-3, n-1, n+1)$ -2, -2, 0	$(-n-2, n, n)$ -1, -1, -1	$(-n-1, n+1, n-1)$ -2, 2, 0	$(-n, n+2, n-2)$ 0, 2, -2	
				$(-n-2, n-2, n+2)$ 0, -2, -2	$(-n, n, n)$ 0, 0, -2
				$(-n-1, n-1, n+1)$ -1, -1, 1	$(1-n, n+1, n-1)$ 0, 0, 0
$m = 0$	$(-n-2, n-2, n+2)$ -2, -2, 2	$(-n-1, n-1, n+1)$ -2, 0, 2	$(1-n, n-1, n+1)$ 0, -2, 0	$(2-n, n+2, n-2)$ -2, 2, 2	
				$(-n, n-1, n+1)$ 1, -1, 1	$(2-n, n, n)$ 2, 0, 0
				$(1-n, n-1, n+1)$ 0, 0, 2	$(3-n, n+1, n-1)$ 1, 1, 1
$m = 1$	$(2-n, n-2, n+2)$ 0, -2, 2	$(1-n, n-1, n+1)$ 2, -2, 0	$(2-n, n, n)$ 2, -2, 0	$(4-n, n, n)$ 2, 2, 2	
					$(3-n, n+1, n-1)$ 0, 2, 2

		(1 - n, n - 1, n + 1)	(2 - n, n, n)	(3 - n, n + 1, n - 1)
		1, -1, 1	2, 0, 0	
		0, 0, 2	1, 1, 1	
		2, -2, 0	0, 2, 2	
		(2 - n, n - 2, n + 2)	(3 - n, n - 1, n + 1)	(4 - n, n, n)
		2, -2, 2	2, 0, 2	2, 2, 2

m = 2

where l , m , and n are integers; substituting the expressions for \mathbf{a}^* , \mathbf{b}^* , and \mathbf{c}^* from (2.5-8) into (2.5-9), it is obvious that the points of the reciprocal lattice must have (x, y, z) coordinates of the form

$$(x, y, z) = \frac{1}{a} [(l + m - n), \quad (l - m + n), \quad (-l + m + n)], \quad (2.5-10)$$

where l , m , and n may take on integer values. Table 2.1 shows a tabulation of these possible lattice points; the various boxes of the table correspond to specific values of l and m ; this restricts the form of coordinates listed in each box to vary with n only according to (2.5-10) with the pertinent values of l and m inserted. In the tabulation given here any point whose x , y , or z coordinate exceeds 2 (apart from the constant factor $1/a$, which is dropped in listing the entries in the table) is discarded; the points which are retained are then sufficient to depict 8 unit cells of the reciprocal lattice. When these points are plotted, inserting the constant factor $1/a$, it is clear, as it should be from the form of the reciprocal lattice primitive vectors, that the resulting reciprocal lattice is a b.c.c. structure whose cube edge dimension is $2/a$. In a similar fashion it may be shown that the reciprocal lattice for a b.c.c. direct lattice is a f.c.c. structure.

It is a property of the reciprocal lattice that a vector $\mathbf{r}^* = h'\mathbf{a}^* + k'\mathbf{b}^* + l'\mathbf{c}^*$ from the origin to any lattice point of the reciprocal lattice is normal to the (hkl) plane of the direct lattice. Here the triad (hkl) is simply the triad $(h'k'l')$ divided through by the largest common factor n among $(h'k'l')$, just as in Section 2.2. In other words, $h'/h = k'/k = l'/l = n$. To prove this result, one first notes from Figure 2.8 that vector AC , equal to $-(\mathbf{a}/h) + (\mathbf{c}/l)$, lies in the (hkl) plane, as does vector AB , which is equal to $-(\mathbf{a}/h) + (\mathbf{b}/k)$. But, using (2.5-1) and (2.5-2),

$$\mathbf{r}^* \cdot [-(\mathbf{a}/h) + (\mathbf{c}/l)] = (h'\mathbf{a}^* + k'\mathbf{b}^* + l'\mathbf{c}^*) \cdot [-(\mathbf{a}/h) + (\mathbf{c}/l)] = -\frac{h'}{h} + \frac{l'}{l} = 0, \quad (2.5-11)$$

recalling that $h'/h = l'/l = n$, according to (2.2-6). In like fashion,

$$\mathbf{r}^* \cdot [-(\mathbf{a}/h) + (\mathbf{b}/k)] = (h'\mathbf{a}^* + k'\mathbf{b}^* + l'\mathbf{c}^*) \cdot [-(\mathbf{a}/h) + (\mathbf{b}/k)] = -\frac{h'}{h} + \frac{k'}{k} = 0. \quad (2.5-12)$$

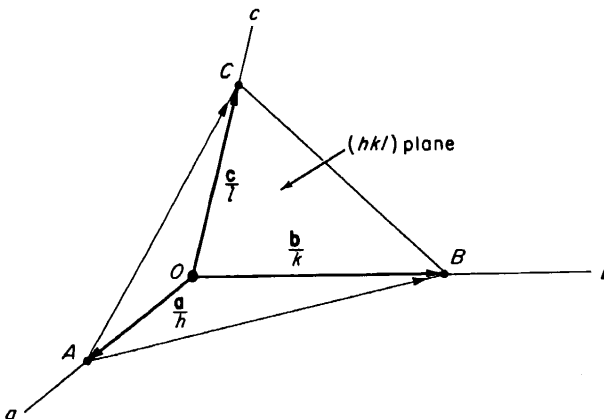


FIGURE 2.8. Vector geometry in the direct lattice for the calculations of Section 2.5.

The vector \mathbf{r}^* is thus perpendicular to two linearly independent vectors, \mathbf{AC} and \mathbf{AB} , both of which lie in the (hkl) plane. It must thus be perpendicular to the plane itself.

Also, if \mathbf{n} is a unit normal vector to the (hkl) plane of the direct lattice, we may write $\mathbf{n} = \mathbf{r}^*/r^*$, since \mathbf{r}^* is known to be a vector normal to (hkl) . However, if d is the distance between adjacent (hkl) planes, from (1.5-2) it must be true that

$$d = \frac{\mathbf{a} \cdot \mathbf{n}}{h} = \frac{\mathbf{a} \cdot \mathbf{r}^*}{hr^*} = \frac{\mathbf{a} \cdot (h'\mathbf{a}^* + k'\mathbf{b}^* + l'\mathbf{c}^*)}{hr^*} = \frac{n}{r^*}, \quad (2.5-13)$$

whereby the magnitude of \mathbf{r}^* is simply given by

$$r^* = n/d, \quad (2.5-14)$$

where n is an integer defined as in equation (2.2-6).

2.6 THE BRAGG CONDITION IN TERMS OF THE RECIPROCAL LATTICE

The Bragg condition may be expressed as a relation between vectors in the reciprocal lattice. Referring to Figure 2.9, the vector AO is a vector whose length is $1/\lambda$, drawn in the direction of the incident X-ray beam, and ending at the origin of the reciprocal lattice. Note that the tail of the vector AO does not necessarily have to rest on a

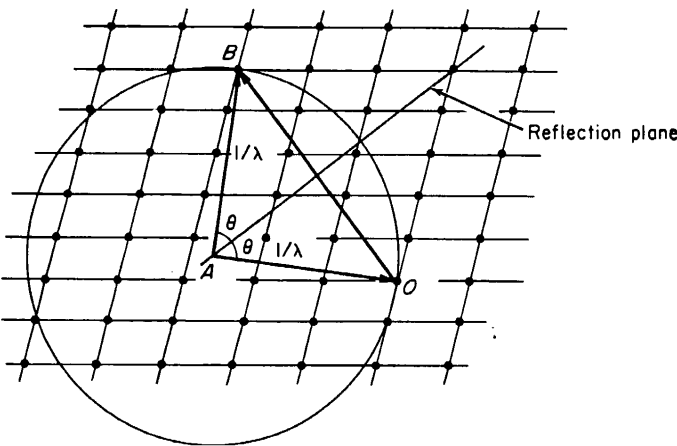


FIGURE 2.9. Vector geometry of Bragg reflection in the *reciprocal lattice*.

lattice point of the reciprocal lattice. A sphere of radius $1/\lambda$ is constructed about point A as center. Suppose now that this sphere intersects some point (h',k',l') of the reciprocal lattice at B . The vector OB then represents a vector connecting the origin of the reciprocal lattice and a point (h',k',l') of that lattice; as such it must be

vectors, AC and AB ,
ilar to the plane itself.
direct lattice, we may
. However, if d is the
true that

$$\frac{n}{r^*}, \quad (2.5-13)$$

$$(2.5-14)$$

THE

ors in the reciprocal
length is $1/\lambda$, drawn
gin of the reciprocal
y have to rest on a

n plane

constructed about
e point (h', k', l') of
or connecting the
s such it must be

normal to the (hkl) plane of the direct lattice, and it must also be of length n/d , where n is the largest integral factor common to the three numbers (h', k', l') . But from the trigonometrical relations in Figure 2.9, the length of OB can also be readily expressed as $2 \sin \theta/\lambda$. Equating these two expressions for the length of vector OB , we find

$$n\lambda = 2d \sin \theta,$$

and the Bragg condition is satisfied. Referring again to Figure 2.9, it is clear that vector OB represents a normal to the reflecting planes (hkl) , and that vector AB is a vector in the direction of the diffracted beam. The latter statement can be understood more easily by translating vector AB parallel with itself until its tail rests upon point O , when it will be seen that AO , OB , and AB are in the familiar relation of incident beam direction, scattering normal and diffracted beam direction. It is evident from this geometrical construction that the Bragg condition will be satisfied for a given wavelength *for each intersection of the surface of a sphere of radius $1/\lambda$ drawn about A with a point of the reciprocal lattice*. The appropriate Bragg angle will be given in each case by the angle between the vector AO and a plane normal to OB . When the Bragg condition is thus satisfied, the vectors AO and AB form an isosceles triangle with a lattice vector OB of the reciprocal lattice. From this disposition of the vectors, as illustrated in Figure 2.9, it can be seen that AB must be the vector sum of AO and OB , and the vector geometry of Figure 2.9 permits us to express the Bragg reflection condition in a particularly simple way.

To accomplish this, it is customary to imagine all the vectors of Figure 2.9 to be multiplied by a constant scale factor of 2π , as represented by Figure 2.10. In this figure, then, the vector G is simply 2π times the vector OB of Figure 2.9 and the vector k is 2π times the vector AO of Figure 2.9. Again the disposition of the vectors is such that vector $A'B'$ of Figure 2.10 must be the vector sum of k and G . Since the magnitude of this vector and the magnitude of the incident beam vector k must be equal whenever

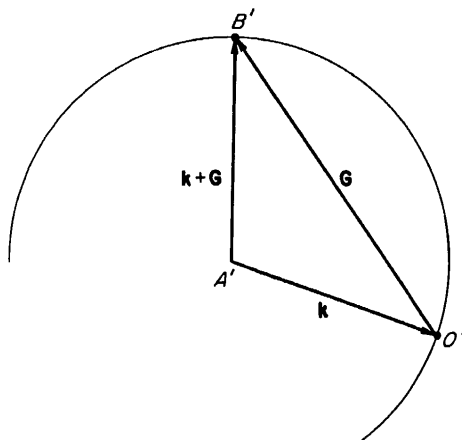


FIGURE 2.10. Vector diagram of Figure 2.9 expanded by a scale factor 2π and relabeled. [The notation follows that used by C. Kittel, *Introduction to Solid State Physics*, John Wiley & Sons, New York (1956).]

the Bragg condition is satisfied, the Bragg condition must imply that

$$(\mathbf{k} + \mathbf{G})^2 = (\mathbf{k} + \mathbf{G}) \cdot (\mathbf{k} + \mathbf{G}) = k^2, \quad (2.6-1)$$

or, expanding the dot product and simplifying,

$$2\mathbf{k} \cdot \mathbf{G} + G^2 = 0, \quad (2.6-2)$$

where \mathbf{G} is 2π times a vector from the origin to a lattice point of the reciprocal lattice, and where \mathbf{k} is a vector of magnitude $2\pi/\lambda$ along the direction of the incident X-ray beam. Equation (2.6-2) is the vector form of the Bragg equation.⁴

EXERCISES

1. In a cubic crystal, using X -radiation of wavelength 1.5 \AA , a first order (100) reflection is observed at a glancing angle of 18° . What is the distance between the (100) planes of the crystal?
2. For the hydrogen atom in its lowest energy state the wave function is given by

$$\psi_{1s} = \frac{e^{-r/a_0}}{a_0^{3/2} \sqrt{\pi}}$$

where a_0 is the radius of the first Bohr orbit, $h^2/4\pi^2me^2 = 0.53 \text{ \AA}$. The electron density for such an atom is given by $\psi_{1s}^* \psi_{1s}$, whereby

$$\rho(r) = \frac{e^{-2r/a_0}}{\pi a_0^3}.$$

Using this electron density distribution function, compute the atomic scattering factor for a hypothetical crystal made up of such atoms, and plot it as a function of $\mu (= 4\pi \sin \theta/\lambda)$.

3. Show that for the b.c.c. structure in which all atoms are identical, a scheme of assigning 1/8 of each corner atom at its respective cell coordinate location to the unit cell plus the body center atom in the central position leads to the same result for the geometrical structure factor for this lattice as that derived in Equation (2.4-11).
4. Find the diffraction amplitude $F(h'k'l')$ for the $(h'k'l')$ reflection of a crystal having the CsCl structure, as shown in Figure 1.7(b). Would you expect the (100) reflection to be present for this crystal? Explain.
5. Find the geometrical structure factor for the f.c.c. structure (all atoms identical). Which of the following X-ray reflections would be present, and which would be missing for such a crystal: (100), (110), (111), (200), (220), (222), (211), (221), (123)?
6. Find the geometrical structure factor for the diamond lattice. Express your result as the product of the geometrical structure factor for the f.c.c. structure times another factor. Which of the X-ray reflections mentioned in connection with Problem 5 would be present

⁴ This construction was originated by Ewald [P. P. Ewald, *Zeitschrift für Kristallographie* 56, 129 (1921)] and is sometimes referred to as the *Ewald Construction*.

hat

(2.6-1)

and which would be missing for this structure? Hint: Assign atoms to a cubic unit cell in accordance with the diagram of Figure 1.9.

7. Show that the reciprocal lattice for a simple cubic structure is another simple cubic, thus that the simple cubic structure is self-reciprocal.

8. Show that the reciprocal lattice for a b.c.c. lattice is a f.c.c. structure. Make a table of lattice points and plot them out to form a diagram of your results.

(2.6-2)

GENERAL REFERENCES

W. H. Bragg, *An Introduction to Crystal Analysis*, G. Bell & Sons, London (1928).

W. L. Bragg, *The Crystalline State*, Vol. I, G. Bell & Sons, London (1955).

R. B. Leighton, *Principles of Modern Physics*, McGraw-Hill Book Co., Inc., New York (1959).

A. Taylor, *X-Ray Metallography*, John Wiley & Sons, New York (1961).

the reciprocal lattice,
the incident X-ray

order (100) reflection
the (100) planes of the

on is given by

: electron density for

: scattering factor for a
 $\mu (= 4\pi \sin \theta / \lambda)$.
, a scheme of assign-
the unit cell plus the
geometrical structure

: of a crystal having
100) reflection to be

: all atoms identical).
would be missing for
?

: Express your result
times another factor.
5 would be present

Über Kristallographie 56,

CHAPTER 3

DIFFRACTION I: THE DIRECTIONS OF DIFFRACTED BEAMS

3-1 Introduction. After our preliminary survey of the physics of x-rays and the geometry of crystals, we can now proceed to fit the two together and discuss the phenomenon of x-ray diffraction, which is an interaction of the two. Historically, this is exactly the way this field of science developed. For many years, mineralogists and crystallographers had accumulated knowledge about crystals, chiefly by measurement of interfacial angles, chemical analysis, and determination of physical properties. There was little knowledge of interior structure, however, although some very shrewd guesses had been made, namely, that crystals were built up by periodic repetition of some unit, probably an atom or molecule, and that these units were situated some 1 or 2\AA apart. On the other hand, there were indications, but only indications, that x-rays might be electromagnetic waves about 1 or 2\AA in wavelength. In addition, the phenomenon of diffraction was well understood, and it was known that diffraction, as of visible light by a ruled grating, occurred whenever wave motion encountered a set of regularly spaced scattering objects, provided that the wavelength of the wave motion was of the same order of magnitude as the repeat distance between the scattering centers.

Such was the state of knowledge in 1912 when the German physicist von Laue took up the problem. He reasoned that, if crystals were composed of regularly spaced atoms which might act as scattering centers for x-rays, and if x-rays were electromagnetic waves of wavelength about equal to the interatomic distance in crystals, then it should be possible to diffract x-rays by means of crystals. Under his direction, experiments to test this hypothesis were carried out: a crystal of copper sulfate was set up in the path of a narrow beam of x-rays and a photographic plate was arranged to record the presence of diffracted beams, if any. The very first experiment was successful and showed without doubt that x-rays were diffracted by the crystal out of the primary beam to form a pattern of spots on the photographic plate. These experiments proved, at one and the same time, the wave nature of x-rays and the periodicity of the arrangement of atoms within a crystal. Hindsight is always easy and these ideas appear quite simple to us now, when viewed from the vantage point of more than forty years' development of the subject, but they were not at all obvious in 1912, and von Laue's hypothesis and its experimental verification must stand as a great intellectual achievement.

The account of these experiments was read with great interest by two English physicists, W. H. Bragg and his son W. L. Bragg. The latter although only a young student at the time—it was still the year 1912—successfully analyzed the Laue experiment and was able to express the necessary conditions for diffraction in a somewhat simpler mathematical form than that used by von Laue. He also attacked the problem of crystal structure with the new tool of x-ray diffraction and, in the following year solved the structures of NaCl, KCl, KBr, and KI, all of which have the NaCl structure; these were the first complete crystal-structure determinations ever made.

3-2 Diffraction. Diffraction is due essentially to the existence of certain phase relations between two or more waves, and it is advisable, at the start, to get a clear notion of what is meant by phase relations. Consider a beam of x-rays, such as beam 1 in Fig. 3-1, proceeding from left to right. For convenience only, this beam is assumed to be plane-polarized in order that we may draw the electric field vector \mathbf{E} always in one plane. We may imagine this beam to be composed of two equal parts, ray 2 and ray 3, each of half the amplitude of beam 1. These two rays, on the wave front AA' , are said to be completely *in phase* or *in step*; i.e., their electric-field vectors have the same magnitude and direction at the same instant at any point x measured along the direction of propagation of the wave. A *wave front* is a surface perpendicular to this direction of propagation.

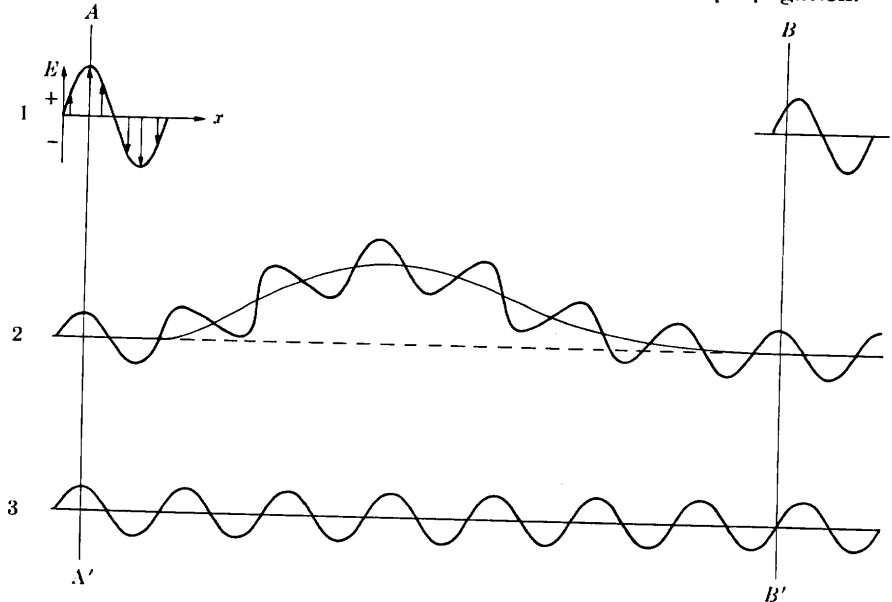


FIG. 3-1. Effect of path difference on relative phase.

Now consider an imaginary experiment, in which ray 3 is allowed to continue in a straight line but ray 2 is diverted by some means into a curved path before rejoining ray 3. What is the situation on the wave front BB' where both rays are proceeding in the original direction? On this front, the electric vector of ray 2 has its maximum value at the instant shown, but that of ray 3 is zero. The two rays are therefore *out of phase*. If we add these two imaginary components of the beam together, we find that beam 1 now has the form shown in the upper right of the drawing. If the amplitudes of rays 2 and 3 are each 1 unit, then the amplitude of beam 1 at the left is 2 units and that of beam 1 at the right is 1.4 units, if a sinusoidal variation of \mathbf{E} with x is assumed.

Two conclusions may be drawn from this illustration:

(1) Differences in the length of the path traveled lead to differences in phase.

(2) The introduction of phase differences produces a change in amplitude.

The greater the path difference, the greater the difference in phase, since the path difference, measured in wavelengths, exactly equals the phase difference, also measured in wavelengths. If the diverted path of ray 2 in Fig. 3-1 were a quarter wavelength longer than shown, the phase difference would be a half wavelength. The two rays would then be completely out of phase on the wave front BB' and beyond, and they would therefore annul each other, since at any point their electric vectors would be either both zero or of the same magnitude and opposite in direction. If the difference in path length were made three quarters of a wavelength greater than shown, the two rays would be one complete wavelength out of phase, a condition indistinguishable from being completely in phase since in both cases the two waves would combine to form a beam of amplitude 2 units, just like the original beam. We may conclude that two rays are completely in phase whenever their path lengths differ either by zero or by a whole number of wavelengths.

Differences in the path length of various rays arise quite naturally when we consider how a crystal diffracts x-rays. Figure 3-2 shows a section of a crystal, its atoms arranged on a set of parallel planes A, B, C, D, \dots , normal to the plane of the drawing and spaced a distance d' apart. Assume that a beam of perfectly parallel, perfectly monochromatic x-rays of wavelength λ is incident on this crystal at an angle θ , called the Bragg angle, where θ is measured between the incident beam and the particular crystal planes under consideration.

We wish to know whether this incident beam of x-rays will be diffracted by the crystal and, if so, under what conditions. A *diffracted beam* may be defined as a beam composed of a large number of scattered rays mutually reinforcing one another. Diffraction is, therefore, essentially a scattering phe-

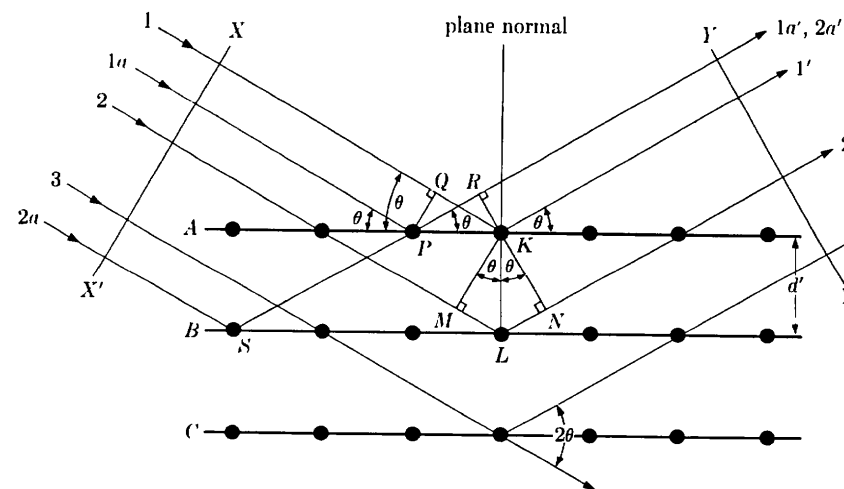


FIG. 3-2. Diffraction of x-rays by a crystal.

nomenon and not one involving any "new" kind of interaction between x-rays and atoms. We saw in Sec. 1-5 that atoms scatter incident x-rays in all directions, and we shall see presently that in some of these directions the scattered beams will be completely in phase and so reinforce each other to form diffracted beams.

For the particular conditions described by Fig. 3-2 the only diffracted beam formed is that shown, namely one making an angle θ of reflection* equal to the angle θ of incidence. We will show this, first, for one plane of atoms and, second, for all the atoms making up the crystal. Consider rays 1 and 1a in the incident beam; they strike atoms K and P in the first plane of atoms and are scattered in all directions. Only in the directions 1' and 1'a', however, are these scattered beams completely in phase and so capable of reinforcing one another; they do so because the difference in their length of path between the wave fronts XX' and YY' is equal to

$$QK - PR = PK \cos \theta - PK \cos \theta = 0.$$

Similarly, the rays scattered by all the atoms in the first plane in a direction parallel to 1' are in phase and add their contributions to the diffracted beam. This will be true of all the planes separately, and it remains to find the condition for reinforcement of rays scattered by atoms in different planes. Rays 1 and 2, for example, are scattered by atoms K and L, and

* Note that these angles are defined differently in x-ray diffraction and in general optics. In the latter, the angles of incidence and reflection are the angles which the incident and reflected beams make with the *normal* to the reflecting surface.

the path difference for rays $1K1'$ and $2L2'$ is

$$ML + LN = d' \sin \theta + d' \sin \theta.$$

This is also the path difference for the overlapping rays scattered by S and P in the direction shown, since in this direction there is no path difference between rays scattered by S and L or P and K . Scattered rays $1'$ and $2'$ will be completely in phase if this path difference is equal to a whole number n of wavelengths, or if

$$n\lambda = 2d' \sin \theta. \quad (3-1)$$

This relation was first formulated by W. L. Bragg and is known as the Bragg law. It states the essential condition which must be met if diffraction is to occur. n is called the order of reflection; it may take on any integral value consistent with $\sin \theta$ not exceeding unity and is equal to the number of wavelengths in the path difference between rays scattered by adjacent planes. Therefore, for fixed values of λ and d' , there may be several angles of incidence $\theta_1, \theta_2, \theta_3, \dots$ at which diffraction may occur, corresponding to $n = 1, 2, 3, \dots$. In a first-order reflection ($n = 1$), the scattered rays $1'$ and $2'$ of Fig. 3-2 would differ in length of path (and in phase) by one wavelength, rays $1'$ and $3'$ by two wavelengths, rays $1'$ and $4'$ by three wavelengths, and so on throughout the crystal. The rays scattered by all the atoms in all the planes are therefore completely in phase and reinforce one another (constructive interference) to form a diffracted beam in the direction shown. In all other directions of space the scattered beams are out of phase and annul one another (destructive interference). The diffracted beam is rather strong compared to the sum of all the rays scattered in the same direction, simply because of the reinforcement which occurs,* but extremely weak compared to the incident beam since the atoms of a crystal scatter only a small fraction of the energy incident on them.

* If the scattering atoms were not arranged in a regular, periodic fashion but in some independent manner, then the rays scattered by them would have a random phase relationship to one another. In other words, there would be an equal probability of the phase difference between any two scattered rays having any value between zero and one wavelength. Neither constructive nor destructive interference takes place under these conditions, and the intensity of the beam scattered in a particular direction is simply the sum of the intensities of all the rays scattered in that direction. If there are N scattered rays each of amplitude A and therefore of intensity A^2 in arbitrary units, then the intensity of the scattered beam is NA^2 . On the other hand, if the rays are scattered by the atoms of a crystal in a direction satisfying the Bragg law, then they are all in phase and the amplitude of the scattered beam is N times the amplitude A of each scattered ray, or NA . The intensity of the scattered beam is therefore N^2A^2 , or N times as large as if reinforcement had not occurred. Since N is very large for the scattering of x-rays from even a small bit of crystal, the role of reinforcement in producing a strong diffracted beam is considerable.

We have here regarded a diffracted beam as being built up of rays scattered by successive planes of atoms within the crystal. It would be a mistake to assume, however, that a single plane of atoms A would diffract x-rays just as the complete crystal does but less strongly. Actually, the single plane of atoms would produce, not only the beam in the direction $1'$ as the complete crystal does, but also additional beams in other directions, some of them not confined to the plane of the drawing. These additional beams do not exist in the diffraction from the complete crystal precisely because the atoms in the other planes scatter beams which destructively interfere with those scattered by the atoms in plane A , except in the direction $1'$.

At first glance, the diffraction of x-rays by crystals and the reflection of visible light by mirrors appear very similar, since in both phenomena the angle of incidence is equal to the angle of reflection. It seems that we might regard the planes of atoms as little mirrors which "reflect" the x-rays. Diffraction and reflection, however, differ fundamentally in at least three aspects:

- (1) The diffracted beam from a crystal is built up of rays scattered by all the atoms of the crystal which lie in the path of the incident beam. The reflection of visible light takes place in a thin surface layer only.
- (2) The diffraction of monochromatic x-rays takes place only at those particular angles of incidence which satisfy the Bragg law. The reflection of visible light takes place at any angle of incidence.
- (3) The reflection of visible light by a good mirror is almost 100 percent efficient. The intensity of a diffracted x-ray beam is extremely small compared to that of the incident beam.

Despite these differences, we often speak of "reflecting planes" and "reflected beams" when we really mean diffracting planes and diffracted beams. This is common usage and, from now on, we will frequently use these terms without quotation marks but with the tacit understanding that we really mean diffraction and not reflection.*

To sum up, diffraction is essentially a scattering phenomenon in which a large number of atoms cooperate. Since the atoms are arranged periodically on a lattice, the rays scattered by them have definite phase relations between them; these phase relations are such that destructive interference occurs in most directions of scattering, but in a few directions constructive interference takes place and diffracted beams are formed. The two essentials are a wave motion capable of interference (x-rays) and a set of periodically arranged scattering centers (the atoms of a crystal).

* For the sake of completeness, it should be mentioned that x-rays can be totally reflected by a solid surface, just like visible light by a mirror, but only at very small angles of incidence (below about one degree). This phenomenon is of little practical importance in x-ray metallography and need not concern us further.

3-3 The Bragg law. Two geometrical facts are worth remembering:

(1) The incident beam, the normal to the reflecting plane, and the diffracted beam are always coplanar.

(2) The angle between the diffracted beam and the transmitted beam is always 2θ . This is known as the diffraction angle, and it is this angle, rather than θ , which is usually measured experimentally.

As previously stated, diffraction in general occurs only when the wavelength of the wave motion is of the same order of magnitude as the repeat distance between scattering centers. This requirement follows from the Bragg law. Since $\sin \theta$ cannot exceed unity, we may write

$$\frac{n\lambda}{2d'} = \sin \theta < 1. \quad (3-2)$$

Therefore, $n\lambda$ must be less than $2d'$. For diffraction, the smallest value of n is 1. ($n = 0$ corresponds to the beam diffracted in the same direction as the transmitted beam. It cannot be observed.) Therefore the condition for diffraction at any observable angle 2θ is

$$\lambda < 2d'. \quad (3-3)$$

For most sets of crystal planes d' is of the order of 3A or less, which means that λ cannot exceed about 6A. A crystal could not possibly diffract ultraviolet radiation, for example, of wavelength about 500A. On the other hand, if λ is very small, the diffraction angles are too small to be conveniently measured.

The Bragg law may be written in the form

$$\lambda = 2 \frac{d'}{n} \sin \theta. \quad (3-4)$$

Since the coefficient of λ is now unity, we can consider a reflection of any order as a first-order reflection from planes, real or fictitious, spaced at a distance $1/n$ of the previous spacing. This turns out to be a real convenience, so we set $d = d'/n$ and write the Bragg law in the form

$$\boxed{\lambda = 2d \sin \theta}. \quad (3-5)$$

This form will be used throughout this book.

This usage is illustrated by Fig. 3-3. Consider the second-order 100 reflection* shown in (a). Since it is second-order, the path difference ABC between rays scattered by adjacent (100) planes must be two whole wave-

* This means the reflection from the (100) planes. Conventionally, the Miller indices of a reflecting plane hkl , written without parentheses, stand for the reflected beam from the plane (hkl) .

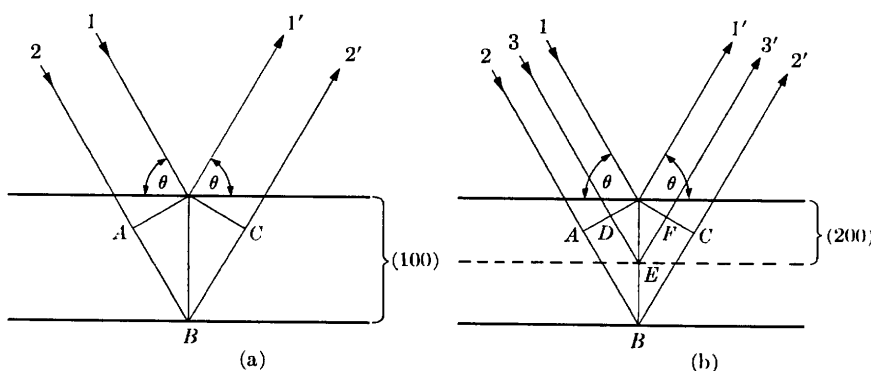


FIG. 3-3. Equivalence of (a) a second-order 100 reflection and (b) a first-order 200 reflection.

lengths. If there is no real plane of atoms between the (100) planes, we can always imagine one as in Fig. 3-3(b), where the dotted plane midway between the (100) planes forms part of the (200) set of planes. For the same reflection as in (a), the path difference DEF between rays scattered by adjacent (200) planes is now only one whole wavelength, so that this reflection can properly be called a first-order 200 reflection. Similarly, 300, 400, etc., reflections are equivalent to reflections of the third, fourth, etc., orders from the (100) planes. In general, an n th-order reflection from (hkl) planes of spacing d' may be considered as a first-order reflection from the $(nh nk nl)$ planes of spacing $d = d'/n$. Note that this convention is in accord with the definition of Miller indices since $(nh nk nl)$ are the Miller indices of planes parallel to the (hkl) planes but with $1/n$ the spacing of the latter.

3-4 X-ray spectroscopy. Experimentally, the Bragg law can be utilized in two ways. By using x-rays of known wavelength λ and measuring θ , we can determine the spacing d of various planes in a crystal: this is *structure analysis* and is the subject, in one way or another, of the greater part of this book. Alternatively, we can use a crystal with planes of known spacing d , measure θ , and thus determine the wavelength λ of the radiation used: this is *x-ray spectroscopy*.

The essential features of an x-ray spectrometer are shown in Fig. 3-4. X-rays from the tube T are incident on a crystal C which may be set at any desired angle to the incident

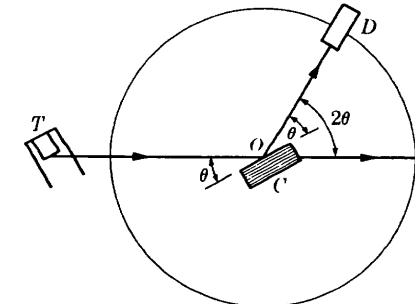


FIG. 3-4. The x-ray spectrometer.

beam by rotation about an axis through O , the center of the spectrometer circle. D is an ionization chamber or some form of counter which measures the intensity of the diffracted x-rays; it can also be rotated about O and set at any desired angular position. The crystal is usually cut or cleaved so that a particular set of reflecting planes of known spacing is parallel to its surface, as suggested by the drawing. In use, the crystal is positioned so that its reflecting planes make some particular angle θ with the incident beam, and D is set at the corresponding angle 2θ . The intensity of the diffracted beam is then measured and its wavelength calculated from the Bragg law, this procedure being repeated for various angles θ . It is in this way that curves such as Fig. 1-5 and the characteristic wavelengths tabulated in Appendix 3 were obtained. W. H. Bragg designed and used the first x-ray spectrometer, and the Swedish physicist Siegbahn developed it into an instrument of very high precision.

Except for one application, the subject of fluorescent analysis described in Chap. 15, we are here concerned with x-ray spectroscopy only in so far as it concerns certain units of wavelength. Wavelength measurements made in the way just described are obviously relative, and their accuracy is no greater than the accuracy with which the plane spacing of the crystal is known. For a cubic crystal this spacing can be obtained independently from a measurement of its density. For any crystal,

$$\text{Density} = \frac{\text{weight of atoms in unit cell}}{\text{volume of unit cell}},$$

$$\rho = \frac{\Sigma A}{NV}, \quad (3-6)$$

where ρ = density (gm/cm^3), ΣA = sum of the atomic weights of the atoms in the unit cell, N = Avogadro's number, and V = volume of unit cell (cm^3). NaCl, for example, contains four sodium atoms and four chlorine atoms per unit cell, so that

$$\Sigma A = 4(\text{at. wt Na}) + 4(\text{at. wt Cl}).$$

If this value is inserted into Eq. (3-6), together with Avogadro's number and the measured value of the density, the volume of the unit cell V can be found. Since NaCl is cubic, the lattice parameter a is given simply by the cube root of V . From this value of a and the cubic plane-spacing equation (Eq. 2-5), the spacing of any set of planes can be found.

In this way, Siegbahn obtained a value of 2.814A for the spacing of the (200) planes of rock salt, which he could use as a basis for wavelength measurements. However, he was able to measure wavelengths in terms of this spacing much more accurately than the spacing itself was known, in the sense that he could make relative wavelength measurements accurate

to six significant figures whereas the spacing in absolute units (angstroms) was known only to four. It was therefore decided to define arbitrarily the (200) spacing of rock salt as 2814.00 X units (XU), this new unit being chosen to be as nearly as possible equal to 0.001A .

Once a particular wavelength was determined in terms of this spacing, the spacing of a given set of planes in any other crystal could be measured. Siegbahn thus measured the (200) spacing of calcite, which he found more suitable as a standard crystal, and thereafter based all his wavelength measurements on this spacing. Its value is 3029.45 XU. Later on, the kilo X unit (kX) was introduced, a thousand times as large as the X unit and nearly equal to an angstrom. The kX unit is therefore *defined* by the relation

$$1 \text{ kX} = \frac{(200) \text{ plane spacing of calcite}}{3.02945}. \quad (3-7)$$

On this basis, Siegbahn and his associates made very accurate measurements of wavelength in relative (kX) units and these measurements form the basis of most published wavelength tables.

It was found later that x-rays could be diffracted by a ruled grating such as is used in the spectroscopy of visible light, provided that the angle of incidence (the angle between the incident beam and the plane of the grating) is kept below the critical angle for total reflection. Gratings thus offer a means of making absolute wavelength measurements, independent of any knowledge of crystal structure. By a comparison of values so obtained with those found by Siegbahn from crystal diffraction, it was possible to calculate the following relation between the relative and absolute units:

$$1 \text{ kX} = 1.00202\text{A}. \quad (3-8)$$

This conversion factor was decided on in 1946 by international agreement, and it was recommended that, in the future, x-ray wavelengths and the lattice parameters of crystals be expressed in angstroms. If V in Eq. (3-6) for the density of a crystal is expressed in A^3 (*not* in kX^3) and the currently accepted value of Avogadro's number inserted, then the equation becomes

$$\rho = \frac{1.66020\Sigma A}{V}. \quad (3-9)$$

The distinction between kX and A is unimportant if no more than about three significant figures are involved. In precise work, on the other hand, units must be correctly stated, and on this point there has been considerable confusion in the past. Some wavelength values published prior to about 1946 are stated to be in angstrom units but are actually in kX units. Some crystallographers have used such a value as the basis for a

precise measurement of the lattice parameter of a crystal and the result has been stated, again incorrectly, in angstrom units. Many published parameters are therefore in error, and it is unfortunately not always easy to determine which ones are and which ones are not. The only safe rule to follow, in stating a precise parameter, is to give the wavelength of the radiation used in its determination. Similarly, any published table of wavelengths can be tested for the correctness of its units by noting the wavelength given for a particular characteristic line, Cu $K\alpha_1$ for example. The wavelength of this line is 1.54051 Å or 1.53740 kX.

3-5 Diffraction directions. What determines the possible directions, i.e., the possible angles 2θ , in which a given crystal can diffract a beam of monochromatic x-rays? Referring to Fig. 3-3, we see that various diffraction angles $2\theta_1$, $2\theta_2$, $2\theta_3$, ... can be obtained from the (100) planes by using a beam incident at the correct angle θ_1 , θ_2 , θ_3 , ... and producing first-, second-, third-, ... order reflections. But diffraction can also be produced by the (110) planes, the (111) planes, the (213) planes, and so on. We obviously need a general relation which will predict the diffraction angle for *any* set of planes. This relation is obtained by combining the Bragg law and the plane-spacing equation (Appendix 1) applicable to the particular crystal involved.

For example, if the crystal is cubic, then

$$\lambda = 2d \sin \theta$$

and

$$\frac{1}{d^2} = \frac{(h^2 + k^2 + l^2)}{a^2}.$$

Combining these equations, we have

$$\sin^2 \theta = \frac{\lambda^2}{4a^2} (h^2 + k^2 + l^2). \quad (3-10)$$

This equation predicts, for a particular incident wavelength λ and a particular cubic crystal of unit cell size a , all the possible Bragg angles at which diffraction can occur from the planes (hkl) . For (110) planes, for example, Eq. (3-10) becomes

$$\sin^2 \theta_{110} = \frac{\lambda^2}{2a^2}.$$

If the crystal is tetragonal, with axes a and c , then the corresponding general equation is

$$\sin^2 \theta = \frac{\lambda^2}{4} \left(\frac{h^2 + k^2}{a^2} + \frac{l^2}{c^2} \right), \quad (3-11)$$

and similar equations can readily be obtained for the other crystal systems.

These examples show that the directions in which a beam of given wavelength is diffracted by a given set of lattice planes is determined by the crystal system to which the crystal belongs and its lattice parameters. In short, *diffraction directions are determined solely by the shape and size of the unit cell*. This is an important point and so is its converse: all we can possibly determine about an unknown crystal by measurements of the *directions* of diffracted beams are the shape and size of its unit cell. We will find, in the next chapter, that the *intensities* of diffracted beams are determined by the positions of the atoms within the unit cell, and it follows that we must measure intensities if we are to obtain any information at all about atom positions. We will find, for many crystals, that there are particular atomic arrangements which reduce the intensities of some diffracted beams to zero. In such a case, there is simply no diffracted beam at the angle predicted by an equation of the type of Eqs. (3-10) and (3-11). It is in this sense that equations of this kind predict all *possible* diffracted beams.

3-6 Diffraction methods. Diffraction can occur whenever the Bragg law, $\lambda = 2d \sin \theta$, is satisfied. This equation puts very stringent conditions on λ and θ for any given crystal. With monochromatic radiation, an arbitrary setting of a single crystal in a beam of x-rays will not in general produce *any* diffracted beams. Some way of satisfying the Bragg law must be devised, and this can be done by continuously varying either λ or θ during the experiment. The ways in which these quantities are varied distinguish the three main diffraction methods:

	λ	θ
Laue method	Variable	Fixed
Rotating-crystal method	Fixed	Variable (in part)
Powder method	Fixed	Variable

The **Laue method** was the first diffraction method ever used, and it reproduces von Laue's original experiment. A beam of white radiation, the continuous spectrum from an x-ray tube, is allowed to fall on a fixed single crystal. The Bragg angle θ is therefore fixed for every set of planes in the crystal, and each set picks out and diffracts that particular wavelength which satisfies the Bragg law for the particular values of d and θ involved. Each diffracted beam thus has a different wavelength.

There are two variations of the Laue method, depending on the relative positions of source, crystal, and film (Fig. 3-5). In each, the film is flat and placed perpendicular to the incident beam. The film in the *transmission Laue method* (the original Laue method) is placed behind the crystal so as to record the beams diffracted in the forward direction. This

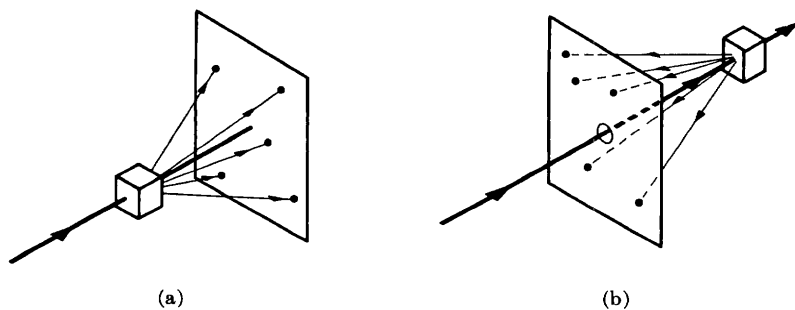


FIG. 3-5. (a) Transmission and (b) back-reflection Laue methods.

method is so called because the diffracted beams are partially transmitted through the crystal. In the *back-reflection Laue method* the film is placed between the crystal and the x-ray source, the incident beam passing through a hole in the film, and the beams diffracted in a backward direction are recorded.

In either method, the diffracted beams form an array of spots on the film as shown in Fig. 3-6. This array of spots is commonly called a pattern, but the term is not used in any strict sense and does not imply any periodic arrangement of the spots. On the contrary, the spots are seen to lie on certain curves, as shown by the lines drawn on the photographs.

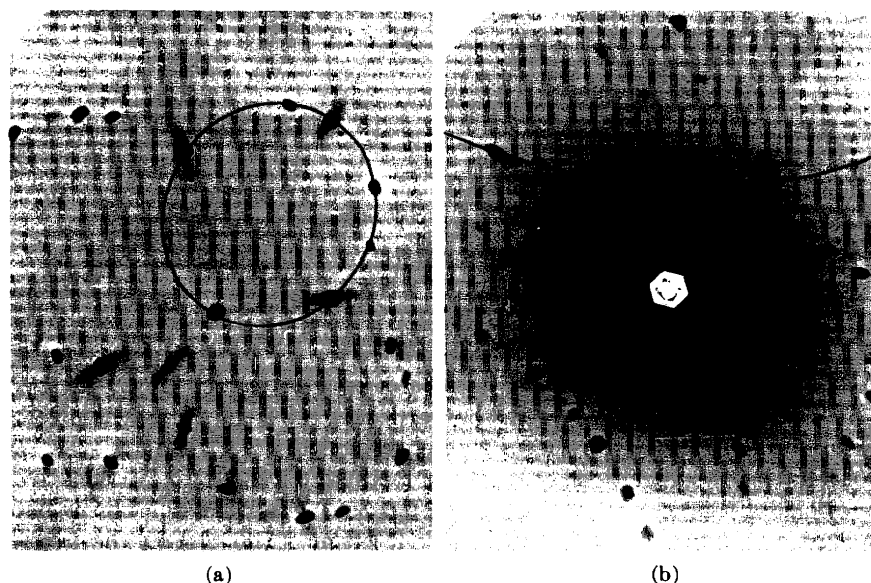


FIG. 3-6. (a) Transmission and (b) back-reflection Laue patterns of an aluminum crystal (cubic). Tungsten radiation, 30 kv, 19 ma.

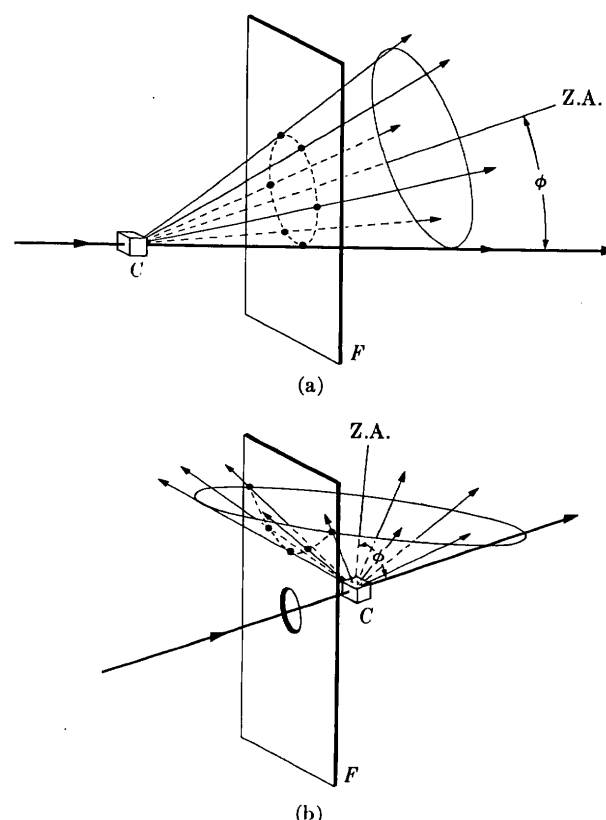


FIG. 3-7. Location of Laue spots (a) on ellipses in transmission method and (b) on hyperbolas in back-reflection method. (C = crystal, F = film, Z.A. = zone axis.)

These curves are generally ellipses or hyperbolas for transmission patterns [Fig. 3-7(a)] and hyperbolas for back-reflection patterns [Fig. 3-7(b)].

The spots lying on any one curve are reflections from planes belonging to one zone. This is due to the fact that the Laue reflections from planes of a zone all lie on the surface of an imaginary cone whose axis is the zone axis. As shown in Fig. 3-7(a), one side of the cone is tangent to the transmitted beam, and the angle of inclination ϕ of the zone axis (Z.A.) to the transmitted beam is equal to the semi-apex angle of the cone. A film placed as shown intersects the cone in an imaginary ellipse passing through the center of the film, the diffraction spots from planes of a zone being arranged on this ellipse. When the angle ϕ exceeds 45° , a film placed between the crystal and the x-ray source to record the back-reflection pattern will intersect the cone in a hyperbola, as shown in Fig. 3-7(b).

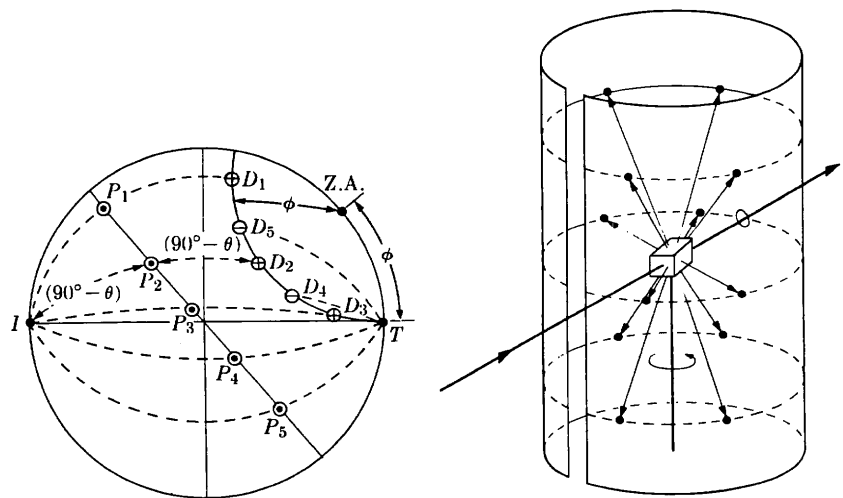


FIG. 3-8. Stereographic projection of transmission Laue method.

FIG. 3-9. Rotating-crystal method.

The fact that the Laue reflections from planes of a zone lie on the surface of a cone can be nicely demonstrated with the stereographic projection. In Fig. 3-8, the crystal is at the center of the reference sphere, the incident beam I enters at the left, and the transmitted beam T leaves at the right. The point representing the zone axis lies on the circumference of the basic circle and the poles of five planes belonging to this zone, P_1 to P_5 , lie on the great circle shown. The direction of the beam diffracted by any one of these planes, for example the plane P_2 , can be found as follows. I , P_2 , D_2 (the diffraction direction required), and T are all coplanar. Therefore D_2 lies on the great circle through I , P_2 , and T . The angle between I and P_2 is $(90^\circ - \theta)$, and D_2 must lie at an equal angular distance on the other side of P_2 , as shown. The diffracted beams so found, D_1 to D_5 , are seen to lie on a small circle, the intersection with the reference sphere of a cone whose axis is the zone axis.

The positions of the spots on the film, for both the transmission and the back-reflection method, depend on the orientation of the crystal relative to the incident beam, and the spots themselves become distorted and smeared out if the crystal has been bent or twisted in any way. These facts account for the two main uses of the Laue methods: the determination of crystal orientation and the assessment of crystal perfection.

In the **rotating-crystal method** a single crystal is mounted with one of its axes, or some important crystallographic direction, normal to a monochromatic x-ray beam. A cylindrical film is placed around it and the crystal is rotated about the chosen direction, the axis of the film coinciding with the axis of rotation of the crystal (Fig. 3-9). As the crystal rotates,

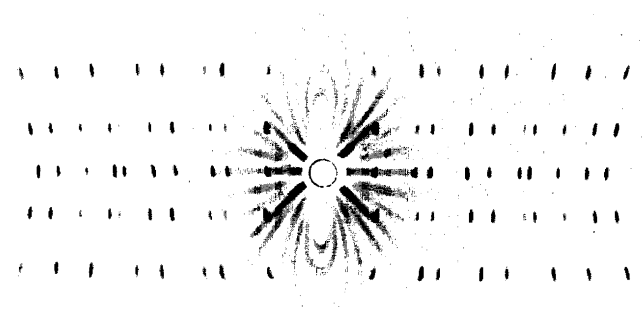


FIG. 3-10. Rotating-crystal pattern of a quartz crystal (hexagonal) rotated about its c axis. Filtered copper radiation. (The streaks are due to the white radiation not removed by the filter.) (Courtesy of B. E. Warren.)

a particular set of lattice planes will, for an instant, make the correct Bragg angle for reflection of the monochromatic incident beam, and at that instant a reflected beam will be formed. The reflected beams are again located on imaginary cones but now the cone axes coincide with the rotation axis. The result is that the spots on the film, when the film is laid out flat, lie on imaginary horizontal lines, as shown in Fig. 3-10. Since the crystal is rotated about only one axis, the Bragg angle does not take on all possible values between 0° and 90° for every set of planes. Not every set, therefore, is able to produce a diffracted beam; sets perpendicular or almost perpendicular to the rotation axis are obvious examples.

The chief use of the rotating-crystal method and its variations is in the determination of unknown crystal structures, and for this purpose it is the most powerful tool the x-ray crystallographer has at his disposal. However, the complete determination of complex crystal structures is a subject beyond the scope of this book and outside the province of the average metallurgist who uses x-ray diffraction as a laboratory tool. For this reason the rotating-crystal method will not be described in any further detail, except for a brief discussion in Appendix 15.

In the **powder method**, the crystal to be examined is reduced to a very fine powder and placed in a beam of monochromatic x-rays. Each particle of the powder is a tiny crystal oriented at random with respect to the incident beam. Just by chance, some of the particles will be correctly oriented so that their (100) planes, for example, can reflect the incident beam. Other particles will be correctly oriented for (110) reflections, and so on. The result is that every set of lattice planes will be capable of reflection. The mass of powder is equivalent, in fact, to a single crystal rotated, not about one axis, but about all possible axes.

Consider one particular hkl reflection. One or more particles of powder will, by chance, be so oriented that their (hkl) planes make the correct

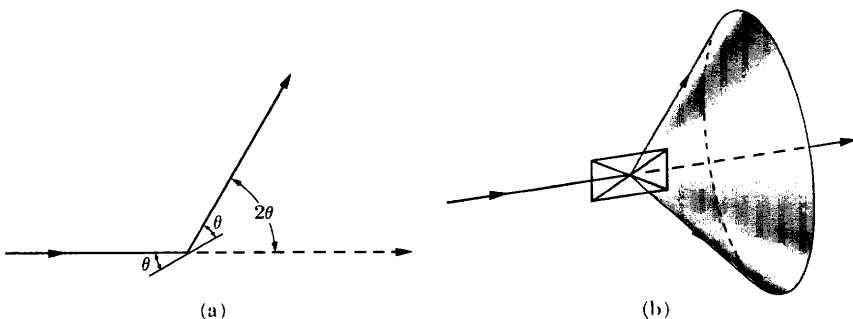


FIG. 3-11. Formation of a diffracted cone of radiation in the powder method.

Bragg angle for reflection; Fig. 3-11(a) shows one plane in this set and the diffracted beam formed. If this plane is now rotated about the incident beam as axis in such a way that θ is kept constant, then the reflected beam will travel over the surface of a cone as shown in Fig. 3-11(b), the axis of the cone coinciding with the transmitted beam. This rotation does not actually occur in the powder method, but the presence of a large number of crystal particles having all possible orientations is equivalent to this rotation, since among these particles there will be a certain fraction whose (hkl) planes make the right Bragg angle with the incident beam and which at the same time lie in all possible rotational positions about the axis of the incident beam. The hkl reflection from a stationary mass of powder thus has the form of a cone of diffracted radiation, and a separate cone is formed for each set of differently spaced lattice planes.

Figure 3-12 shows four such cones and also illustrates the most common powder-diffraction method. In this, the Debye-Scherrer method, a narrow strip of film is curved into a short cylinder with the specimen placed on its axis and the incident beam directed at right angles to this axis. The cones of diffracted radiation intersect the cylindrical strip of film in lines and, when the strip is unrolled and laid out flat, the resulting pattern has the appearance of the one illustrated in Fig. 3-12(b). Actual patterns, produced by various metal powders, are shown in Fig. 3-13. Each diffraction line is made up of a large number of small spots, each from a separate crystal particle, the spots lying so close together that they appear as a continuous line. The lines are generally curved, unless they occur exactly at $2\theta = 90^\circ$ when they will be straight. From the measured position of a given diffraction line on the film, θ can be determined, and, knowing λ , we can calculate the spacing d of the reflecting lattice planes which produced the line.

Conversely, if the shape and size of the unit cell of the crystal are known, we can predict the position of all possible diffraction lines on the film. The line of lowest 2θ value is produced by reflection from planes of the greatest

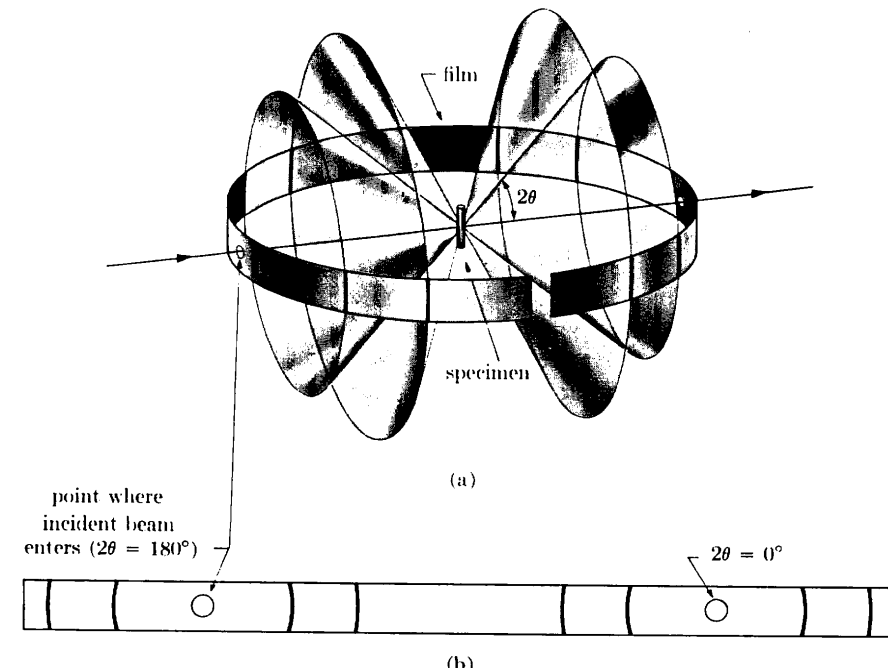


FIG. 3-12. Debye-Scherrer powder method: (a) relation of film to specimen and incident beam; (b) appearance of film when laid out flat.

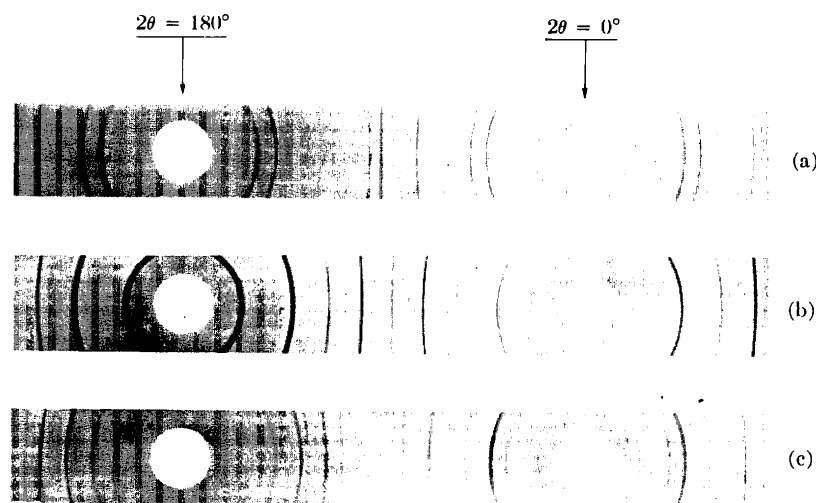


FIG. 3-13. Debye-Scherrer powder patterns of (a) copper (FCC), (b) tungsten (BCC), and (c) zinc (HCP). Filtered copper radiation, camera diameter = 5.73 cm.

spacing. In the cubic system, for example, d is a maximum when $(h^2 + k^2 + l^2)$ is a minimum, and the minimum value of this term is 1, corresponding to (hkl) equal to (100). The 100 reflection is accordingly the one of lowest 2θ value. The next reflection will have indices hkl corresponding to the next highest value of $(h^2 + k^2 + l^2)$, namely 2, in which case (hkl) equals (110), and so on.

The Debye-Scherrer and other variations of the powder method are very widely used, especially in metallurgy. The powder method is, of course, the only method that can be employed when a single crystal specimen is not available, and this is the case more often than not in metallurgical work. The method is especially suited for determining lattice parameters with high precision and for the identification of phases, whether they occur alone or in mixtures such as polyphase alloys, corrosion products, refractories, and rocks. These and other uses of the powder method will be fully described in later chapters.

Finally, the x-ray spectrometer can be used as a tool in diffraction analysis. This instrument is known as a **diffractometer** when it is used with x-rays of *known* wavelength to determine the *unknown* spacing of crystal planes, and as a spectrometer in the reverse case, when crystal planes of known spacing are used to determine unknown wavelengths. The diffractometer is always used with monochromatic radiation and measurements may be made on either single crystals or polycrystalline specimens; in the latter case, it functions much like a Debye-Scherrer camera in that the counter intercepts and measures only a short arc of any one cone of diffracted rays.

3-7 Diffraction under nonideal conditions. Before going any further, it is important to stop and consider with some care the derivation of the Bragg law given in Sec. 3-2 in order to understand precisely under what conditions it is strictly valid. In our derivation we assumed certain ideal conditions, namely a perfect crystal and an incident beam composed of perfectly parallel and strictly monochromatic radiation. These conditions never actually exist, so we must determine the effect on diffraction of various kinds of departure from the ideal.

In particular, the way in which destructive interference is produced in all directions except those of the diffracted beams is worth considering in some detail, both because it is fundamental to the theory of diffraction and because it will lead us to a method for estimating the size of very small crystals. We will find that only the infinite crystal is really perfect and that small size alone, of an otherwise perfect crystal, can be considered a crystal imperfection.

The condition for reinforcement used in Sec. 3-2 is that the waves involved must differ in path length, that is, in phase, by exactly an integral

number of wavelengths. But suppose that the angle θ in Fig. 3-2 is such that the path difference for rays scattered by the first and second planes is only a quarter wavelength. These rays do not annul one another but, as we saw in Fig. 3-1, simply unite to form a beam of smaller amplitude than that formed by two rays which are completely in phase. How then does destructive interference take place? The answer lies in the contributions from planes deeper in the crystal. Under the assumed conditions, the rays scattered by the second and third planes would also be a quarter wavelength out of phase. But this means that the rays scattered by the first and third planes are exactly half a wavelength out of phase and would completely cancel one another. Similarly, the rays from the second and fourth planes, third and fifth planes, etc., throughout the crystal, are completely out of phase; the result is destructive interference and no diffracted beam. Destructive interference is therefore just as much a consequence of the periodicity of atom arrangement as is constructive interference.

This is an extreme example. If the path difference between rays scattered by the first two planes differs only slightly from an integral number of wavelengths, then the plane scattering a ray exactly out of phase with the ray from the first plane will lie deep within the crystal. If the crystal is so small that this plane does not exist, then complete cancellation of all the scattered rays will not result. It follows that there is a connection between the amount of "out-of-phasesness" that can be tolerated and the size of the crystal.

Suppose, for example, that the crystal has a thickness t measured in a direction perpendicular to a particular set of reflecting planes (Fig. 3-14). Let there be $(m + 1)$ planes in this set. We will regard the Bragg angle θ as a variable and call θ_B the angle which exactly satisfies the Bragg law for the particular values of λ and d involved, or

$$\lambda = 2d \sin \theta_B.$$

In Fig. 3-14, rays A, D, \dots, M make exactly this angle θ_B with the reflecting planes. Ray D' , scattered by the first plane below the surface, is therefore one wavelength out of phase with A' ; and ray M' , scattered by the m th plane below the surface, is m wavelengths out of phase with A' . Therefore, at a diffraction angle $2\theta_B$, rays A', D', \dots, M' are completely in phase and unite to form a diffracted

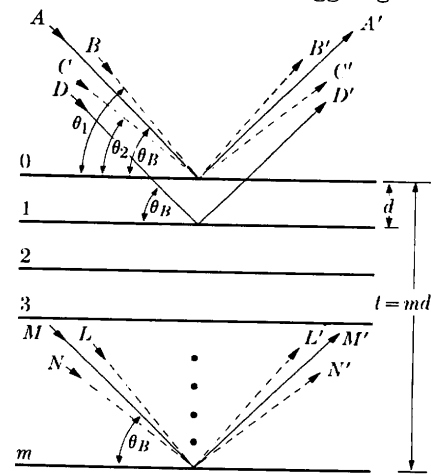


FIG. 3-14. Effect of crystal size on diffraction.

beam of maximum amplitude, i.e., a beam of maximum intensity, since the intensity is proportional to the square of the amplitude.

When we consider incident rays that make Bragg angles only slightly different from θ_B , we find that destructive interference is not complete. Ray B, for example, makes a slightly larger angle θ_1 , such that ray L' from the m th plane below the surface is $(m + 1)$ wavelengths out of phase with B', the ray from the surface plane. This means that midway in the crystal there is a plane scattering a ray which is one-half (actually, an integer plus one-half) wavelength out of phase with ray B' from the surface plane. These rays cancel one another, and so do the other rays from similar pairs of planes throughout the crystal, the net effect being that rays scattered by the top half of the crystal annul those scattered by the bottom half. The intensity of the beam diffracted at an angle $2\theta_1$ is therefore zero. It is also zero at an angle $2\theta_2$ where θ_2 is such that ray N' from the m th plane below the surface is $(m - 1)$ wavelengths out of phase with ray C' from the surface plane. It follows that the diffracted intensity at angles near $2\theta_B$, but not greater than $2\theta_1$ or less than $2\theta_2$, is *not zero* but has a value intermediate between zero and the maximum intensity of the beam diffracted at an angle $2\theta_B$. The curve of diffracted intensity *vs.* 2θ will thus have the form of Fig. 3-15(a) in contrast to Fig. 3-15(b), which illustrates the hypothetical case of diffraction occurring only at the exact Bragg angle.

The width of the diffraction curve of Fig. 3-15(a) increases as the thickness of the crystal decreases. The width B is usually measured, in radians, at an intensity equal to half the maximum intensity. As a rough measure

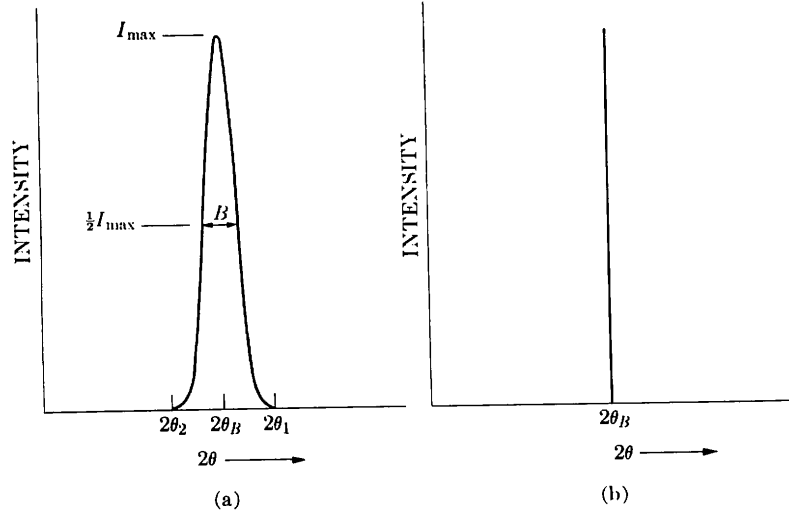


FIG. 3-15. Effect of fine particle size on diffraction curves (schematic).

of B , we can take half the difference between the two extreme angles at which the intensity is zero, or

$$B = \frac{1}{2}(2\theta_1 - 2\theta_2) = \theta_1 - \theta_2.$$

The path-difference equations for these two angles are

$$2t \sin \theta_1 = (m + 1)\lambda,$$

$$2t \sin \theta_2 = (m - 1)\lambda.$$

By subtraction we find

$$t(\sin \theta_1 - \sin \theta_2) = \lambda,$$

$$2t \cos \left(\frac{\theta_1 + \theta_2}{2} \right) \sin \left(\frac{\theta_1 - \theta_2}{2} \right) = \lambda.$$

But θ_1 and θ_2 are both very nearly equal to θ_B , so that

$$\theta_1 + \theta_2 = 2\theta_B \quad (\text{approx.})$$

and

$$\sin \left(\frac{\theta_1 - \theta_2}{2} \right) = \left(\frac{\theta_1 - \theta_2}{2} \right) \quad (\text{approx.}).$$

Therefore

$$2t \left(\frac{\theta_1 - \theta_2}{2} \right) \cos \theta_B = \lambda,$$

$$t = \frac{\lambda}{B \cos \theta_B}. \quad (3-12)$$

A more exact treatment of the problem gives

$$t = \frac{0.9\lambda}{B \cos \theta_B}, \quad (3-13)$$

which is known as the Scherrer formula. It is used to estimate the *particle size* of very small crystals from the measured width of their diffraction curves. What is the order of magnitude of this effect? Suppose $\lambda = 1.5\text{\AA}$, $d = 1.0\text{\AA}$, and $\theta = 49^\circ$. Then for a crystal 1 mm in diameter the breadth B , due to the small crystal effect alone, would be about 2×10^{-7} radian (0.04 sec), or too small to be observable. Such a crystal would contain some 10^7 parallel lattice planes of the spacing assumed above. However, if the crystal were only 500\text{\AA} thick, it would contain only 500 planes, and the diffraction curve would be relatively broad, namely about 4×10^{-3} radian (0.2°).

Nonparallel incident rays, such as B and C in Fig. 3-14, actually exist in any real diffraction experiment, since the "perfectly parallel beam"

assumed in Fig. 3-2 has never been produced in the laboratory. As will be shown in Sec. 5-4, any actual beam of x-rays contains divergent and convergent rays as well as parallel rays, so that the phenomenon of diffraction at angles not exactly satisfying the Bragg law actually takes place.

Neither is any real beam ever strictly monochromatic. The usual "monochromatic" beam is simply one containing the strong $K\alpha$ component superimposed on the continuous spectrum. But the $K\alpha$ line itself has a width of about 0.001\AA and this narrow range of wavelengths in the nominally monochromatic beam is a further cause of line broadening, i.e., of measurable diffraction at angles close, but not equal, to $2\theta_B$, since for each value of λ there is a corresponding value of θ . (Translated into terms of diffraction line width, a range of wavelengths extending over 0.001\AA leads to an increase in line width, for $\lambda = 1.5\text{\AA}$ and $\theta = 45^\circ$, of about 0.08° over the width one would expect if the incident beam were strictly monochromatic.) Line broadening due to this natural "spectral width" is proportional to $\tan \theta$ and becomes quite noticeable as θ approaches 90° .

Finally, there is a kind of crystal imperfection known as *mosaic structure* which is possessed by all real crystals to a greater or lesser degree and which has a decided effect on diffraction phenomena. It is a kind of substructure into which a "single" crystal is broken up and is illustrated in Fig. 3-16 in an enormously exaggerated fashion. A crystal with mosaic structure does not have its atoms arranged on a perfectly regular lattice extending from one side of the crystal to the other; instead, the lattice is broken up into a number of tiny blocks, each slightly disoriented one from another. The size of these blocks is of the order of 1000\AA , while the maximum angle of disorientation between them may vary from a very small value to as much as one degree, depending on the crystal. If this angle is ϵ , then diffraction of a parallel monochromatic beam from a "single" crystal will occur not only at an angle of incidence θ_B but at all angles between θ_B and $\theta_B + \epsilon$. Another effect of mosaic structure is to increase the intensity of the reflected beam relative to that theoretically calculated for an ideally perfect crystal.

These, then, are some examples of diffraction under nonideal conditions, that is, of diffraction as it actually occurs. We should not regard these as "deviations" from the Bragg law, and we will not as long as we remember that this law is derived for certain ideal conditions and that diffraction is

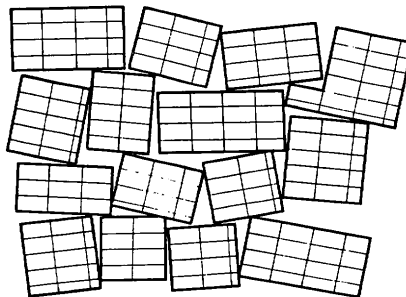


FIG. 3-16. The mosaic structure of a real crystal.

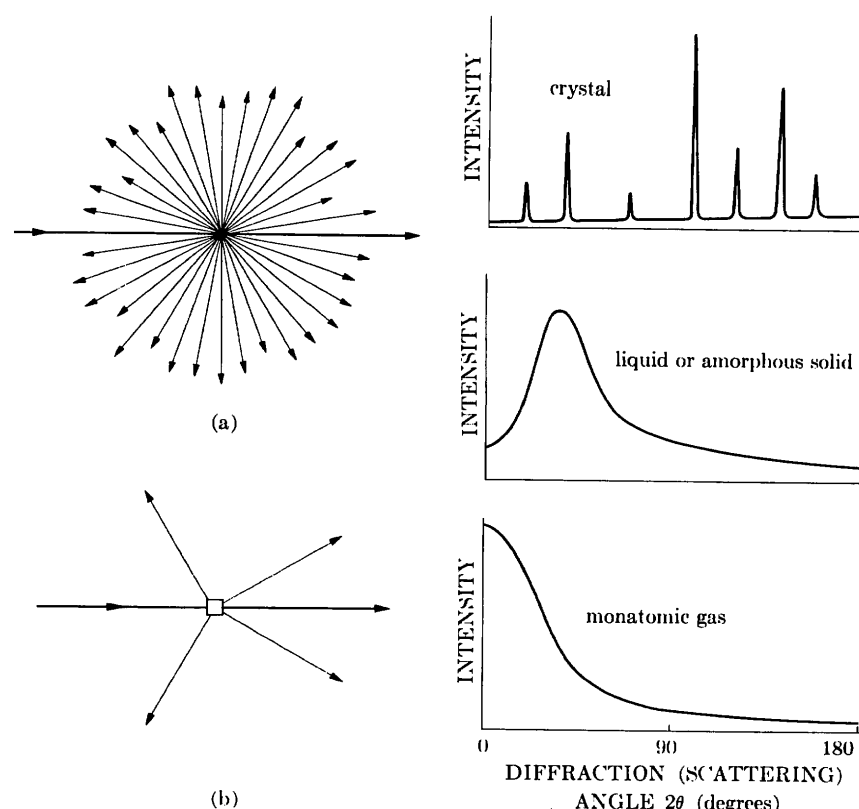


FIG. 3-17. (a) Scattering by an atom. (b) Diffraction by a crystal.

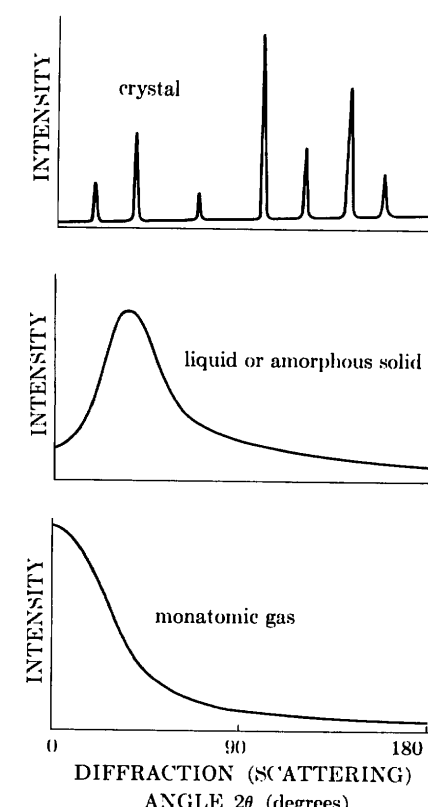


FIG. 3-18. Comparative x-ray scattering by crystalline solids, amorphous solids, liquids, and monatomic gases (schematic).

only a special kind of scattering. This latter point cannot be too strongly emphasized. A single atom scatters an incident beam of x-rays in all directions in space, but a large number of atoms arranged in a perfectly periodic array in three dimensions to form a crystal scatters (diffracts) x-rays in relatively few directions, as illustrated schematically in Fig. 3-17. It does so precisely because the periodic arrangement of atoms causes destructive interference of the scattered rays in all directions *except* those predicted by the Bragg law, and in these directions constructive interference (reinforcement) occurs. It is not surprising, therefore, that measurable diffraction (scattering) occurs at non-Bragg angles whenever any crystal imperfection results in the partial absence of one or more of the necessary conditions for perfect destructive interference at these angles.

These imperfections are generally slight compared to the over-all regularity of the lattice, with the result that diffracted beams are confined to very narrow angular ranges centered on the angles predicted by the Bragg law for ideal conditions.

This relation between destructive interference and structural periodicity can be further illustrated by a comparison of x-ray scattering by solids, liquids, and gases (Fig. 3-18). The curve of scattered intensity *vs.* 2θ for a crystalline solid is almost zero everywhere except at certain angles where high sharp maxima occur: these are the diffracted beams. Both amorphous solids and liquids have structures characterized by an almost complete lack of periodicity and a tendency to "order" only in the sense that the atoms are fairly tightly packed together and show a statistical preference for a particular interatomic distance; the result is an x-ray scattering curve showing nothing more than one or two broad maxima. Finally, there are the monatomic gases, which have no structural periodicity whatever; in such gases, the atoms are arranged perfectly at random and their relative positions change constantly with time. The corresponding scattering curve shows no maxima, merely a regular decrease of intensity with increase in scattering angle.

PROBLEMS

3-1. Calculate the "x-ray density" [the density given by Eq. (3-9)] of copper to four significant figures.

3-2. A transmission Laue pattern is made of a cubic crystal having a lattice parameter of 4.00A. The x-ray beam is horizontal. The [010] axis of the crystal points along the beam towards the x-ray tube, the [100] axis points vertically upward, and the [001] axis is horizontal and parallel to the photographic film. The film is 5.00 cm from the crystal.

(a) What is the wavelength of the radiation diffracted from the $(\bar{3}\bar{1}0)$ planes?

(b) Where will the $\bar{3}\bar{1}0$ reflection strike the film?

3-3. A back-reflection Laue pattern is made of a cubic crystal in the orientation of Prob. 3-2. By means of a stereographic projection similar to Fig. 3-8, show that the beams diffracted by the planes (120) , $(\bar{1}\bar{2}3)$, and (121) , all of which belong to the zone $[210]$, lie on the surface of a cone whose axis is the zone axis. What is the angle ϕ between the zone axis and the transmitted beam?

3-4. Determine the values of 2θ and (hkl) for the first three lines (those of lowest 2θ values) on the powder patterns of substances with the following structures, the incident radiation being Cu $K\alpha$:

- (a) Simple cubic ($a = 3.00\text{A}$)
- (b) Simple tetragonal ($a = 2.00\text{A}$, $c = 3.00\text{A}$)
- (c) Simple tetragonal ($a = 3.00\text{A}$, $c = 2.00\text{A}$)
- (d) Simple rhombohedral ($a = 3.00\text{A}$, $\alpha = 80^\circ$)

PROBLEMS

3-5. Calculate the breadth B (in degrees of 2θ), due to the small crystal effect alone, of the powder pattern lines of particles of diameter 1000, 750, 500, and 250A. Assume $\theta = 45^\circ$ and $\lambda = 1.5\text{A}$. For particles 250A in diameter, calculate the breadth B for $\theta = 10, 45$, and 80° .

3-6. Check the value given in Sec. 3-7 for the increase in breadth of a diffraction line due to the natural width of the $K\alpha$ emission line. (Hint: Differentiate the Bragg law and find an expression for the rate of change of 2θ with λ .)

CHAPTER 4

DIFFRACTION II: THE INTENSITIES OF DIFFRACTED BEAMS

4-1 Introduction. As stated earlier, the positions of the atoms in the unit cell affect the intensities but not the directions of the diffracted beams. That this must be so may be seen by considering the two structures shown in Fig. 4-1. Both are orthorhombic with two atoms of the same kind per unit cell, but the one on the left is base-centered and the one on the right body-centered. Either is derivable from the other by a simple shift of one atom by the vector $\frac{1}{2}c$.

Consider reflections from the (001) planes which are shown in profile in Fig. 4-2. For the base-centered lattice shown in (a), suppose that the Bragg law is satisfied for the particular values of λ and θ employed. This means that the path difference ABC between rays $1'$ and $2'$ is one wavelength, so that rays $1'$ and $2'$ are in phase and diffraction occurs in the direction shown. Similarly, in the body-centered lattice shown in (b), rays $1'$ and $2'$ are in phase, since their path difference ABC is one wavelength. However, in this case, there is another plane of atoms midway between the (001) planes, and the path difference DEF between rays $1'$ and $3'$ is exactly half of ABC , or one half wavelength. Thus rays $1'$ and $3'$ are completely out of phase and annul each other. Similarly, ray $4'$ from the next plane down (not shown) annuls ray $2'$, and so on throughout the crystal. There is no 001 reflection from the body-centered lattice.

This example shows how a simple rearrangement of atoms within the unit cell can eliminate a reflection completely. More generally, the intensity of a diffracted beam is changed, not necessarily to zero, by any change in atomic positions, and, conversely, we can only determine atomic positions by observations of diffracted intensities. To establish an exact relation between atom position and intensity is the main purpose of this chapter. The problem is complex because of the many variables involved, and we will have to proceed step by step: we will consider how x-rays are scattered first by a single electron, then by an atom, and finally by all the

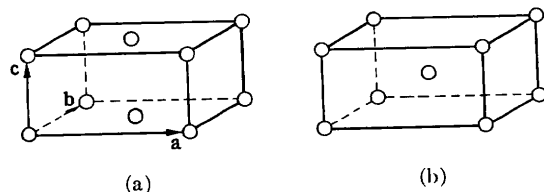


FIG. 4-1. (a) Base-centered and (b) body-centered orthorhombic unit cells.
104

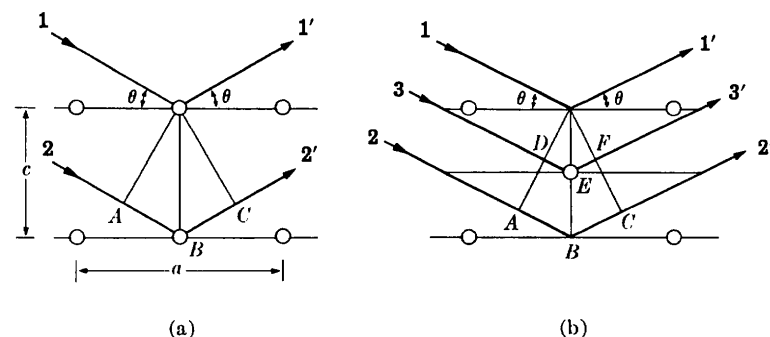


FIG. 4-2. Diffraction from the (001) planes of (a) base-centered and (b) body-centered orthorhombic lattices.

atoms in the unit cell. We will apply these results to the powder method of x-ray diffraction only, and, to obtain an expression for the intensity of a powder pattern line, we will have to consider a number of other factors which affect the way in which a crystalline powder diffracts x-rays.

4-2 Scattering by an electron. We have seen in Chap. 1 that an x-ray beam is an electromagnetic wave characterized by an electric field whose strength varies sinusoidally with time at any one point in the beam. Since an electric field exerts a force on a charged particle such as an electron, the oscillating electric field of an x-ray beam will set any electron it encounters into oscillatory motion about its mean position.

Now an accelerating or decelerating electron emits an electromagnetic wave. We have already seen an example of this phenomenon in the x-ray tube, where x-rays are emitted because of the rapid deceleration of the electrons striking the target. Similarly, an electron which has been set into oscillation by an x-ray beam is continuously accelerating and decelerating during its motion and therefore emits an electromagnetic wave. In this sense, an electron is said to *scatter x-rays*, the scattered beam being simply the beam radiated by the electron under the action of the incident beam. The scattered beam has the same wavelength and frequency as the incident beam and is said to be *coherent* with it, since there is a definite relationship between the phase of the scattered beam and that of the incident beam which produced it.

Although x-rays are scattered in all directions by an electron, the intensity of the scattered beam depends on the angle of scattering, in a way which was first worked out by J. J. Thomson. He found that the intensity I of the beam scattered by a single electron of charge e and mass m , at a distance r from the electron, is given by

$$I = I_0 \frac{e^4}{r^2 m^2 c^4} \sin^2 \alpha, \quad (4-1)$$

where I_0 = intensity of the incident beam, c = velocity of light, and α = angle between the scattering direction and the direction of acceleration of the electron. Suppose the incident beam is traveling in the direction Ox (Fig. 4-3) and encounters an electron at O . We wish to know the scattered intensity at P in the xz plane where OP is inclined at a scattering angle of 2θ to the incident beam. An unpolarized incident beam, such as that issuing from an x-ray tube, has its electric vector \mathbf{E} in a random direction in the yz plane. This beam may be resolved into two plane-polarized components, having electric vectors \mathbf{E}_y and \mathbf{E}_z where

$$\mathbf{E}^2 = \mathbf{E}_y^2 + \mathbf{E}_z^2.$$

On the average, \mathbf{E}_y will be equal to \mathbf{E}_z , since the direction of \mathbf{E} is perfectly random. Therefore

$$\mathbf{E}_y^2 = \mathbf{E}_z^2 = \frac{1}{2}\mathbf{E}^2.$$

The intensity of these two components of the incident beam is proportional to the square of their electric vectors, since \mathbf{E} measures the amplitude of the wave and the intensity of a wave is proportional to the square of its amplitude. Therefore

$$I_{0y} = I_{0z} = \frac{1}{2}I_0.$$

The y component of the incident beam accelerates the electron in the direction Oy . It therefore gives rise to a scattered beam whose intensity at P is found from Eq. (4-1) to be

$$I_{Py} = I_{0y} \frac{e^4}{r^2 m^2 c^4},$$

since $\alpha = \angle yOP = \pi/2$. Similarly, the intensity of the scattered z component is given by

$$I_{Pz} = I_{0z} \frac{e^4}{r^2 m^2 c^4} \cos^2 2\theta,$$

since $\alpha = \pi/2 - 2\theta$. The total scattered intensity at P is obtained by summing the intensities of these two scattered components:

$$\begin{aligned} I_P &= I_{Py} + I_{Pz} \\ &= \frac{e^4}{r^2 m^2 c^4} (I_{0y} + I_{0z} \cos^2 2\theta) \\ &= \frac{e^4}{r^2 m^2 c^4} \left(\frac{I_0}{2} + \frac{I_0}{2} \cos^2 2\theta \right) \\ &= I_0 \frac{e^4}{r^2 m^2 c^4} \left(\frac{1 + \cos^2 2\theta}{2} \right). \end{aligned} \quad (4-2)$$

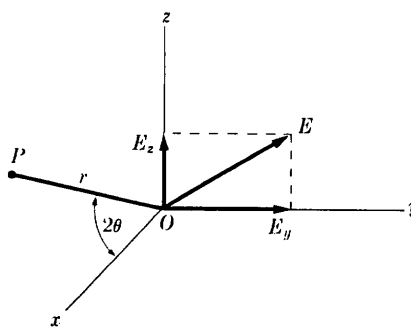


FIG. 4-3. Coherent scattering of x-rays by a single electron.

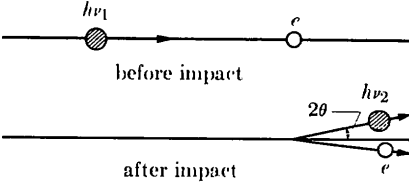


FIG. 4-4. Elastic collision of photon and electron (Compton effect).

This is the Thomson equation for the scattering of an x-ray beam by a single electron. If the values of the constants e , r , m , and c are inserted into this equation, it will be found that the intensity of the scattered beam is only a minute fraction of the intensity of the incident beam. The equation also shows that the scattered intensity decreases as the inverse square of the distance from the scattering electron, as one would expect, and that the scattered beam is stronger in forward or backward directions than in a direction at right angles to the incident beam.

The Thomson equation gives the absolute intensity (in ergs/sq cm/sec) of the scattered beam in terms of the absolute intensity of the incident beam. These absolute intensities are both difficult to measure and difficult to calculate, so it is fortunate that relative values are sufficient for our purposes in practically all diffraction problems. In most cases, all factors in Eq. (4-2) except the last are constant during the experiment and can be omitted. This last factor, $\frac{1}{2}(1 + \cos^2 2\theta)$, is called the *polarization factor*; this is a rather unfortunate term because, as we have just seen, this factor enters the equation simply because the incident beam is unpolarized. The polarization factor is common to all intensity calculations, and we will use it later in our equation for the intensity of a beam diffracted by a crystalline powder.

There is another and quite different way in which an electron can scatter x-rays, and that is manifested in the *Compton effect*. This effect, discovered by A. H. Compton in 1923, occurs whenever x-rays encounter loosely bound or free electrons and can be best understood by considering the incident beam, not as a wave motion, but as a stream of x-ray quanta or photons, each of energy $h\nu_1$. When such a photon strikes a loosely bound electron, the collision is an elastic one like that of two billiard balls (Fig. 4-4). The electron is knocked aside and the photon is deviated through an angle 2θ . Since some of the energy of the incident photon is used in providing kinetic energy for the electron, the energy $h\nu_2$ of the photon

after impact is less than its energy $h\nu_1$ before impact. The wavelength λ_2 of the scattered radiation is thus slightly greater than the wavelength λ_1 of the incident beam, the magnitude of the change being given by the equation

$$\Delta\lambda(A) = \lambda_2 - \lambda_1 = 0.0243 (1 - \cos 2\theta). \quad (4-3)$$

The increase in wavelength depends only on the scattering angle, and it varies from zero in the forward direction ($2\theta = 0$) to 0.05A in the extreme backward direction ($2\theta = 180^\circ$).

Radiation so scattered is called Compton modified radiation, and, besides having its wavelength increased, it has the important characteristic that *its phase has no fixed relation to the phase of the incident beam*. For this reason it is also known as incoherent radiation. It cannot take part in diffraction because its phase is only randomly related to that of the incident beam and cannot therefore produce any interference effects. Compton modified scattering cannot be prevented, however, and it has the undesirable effect of darkening the background of diffraction patterns.

(It should be noted that the quantum theory can account for both the coherent and the incoherent scattering, whereas the wave theory is only applicable to the former. In terms of the quantum theory, coherent scattering occurs when an incident photon bounces off an electron which is so tightly bound that the photon receives no momentum from the impact. The scattered photon therefore has the same energy, and hence wavelength, as it had before.)

4-3 Scattering by an atom. When an x-ray beam encounters an atom, each electron in it scatters part of the radiation coherently in accordance with the Thomson equation. One might also expect the nucleus to take part in the coherent scattering, since it also bears a charge and should be capable of oscillating under the influence of the incident beam. However, the nucleus has an extremely large mass relative to that of the electron and cannot be made to oscillate to any appreciable extent; in fact, the Thomson equation shows that the intensity of coherent scattering is inversely proportional to the square of the mass of the scattering particle. The net effect is that coherent scattering by an atom is due only to the electrons contained in that atom.

The following question then arises: is the wave scattered by an atom simply the sum of the waves scattered by its component electrons? More precisely, does an atom of atomic number Z , i.e., an atom containing Z electrons, scatter a wave whose amplitude is Z times the amplitude of the wave scattered by a single electron? The answer is yes, if the scattering is in the forward direction ($2\theta = 0$), because the waves scattered by all the electrons of the atom are then in phase and the amplitudes of all the scattered waves can be added directly.

This is not true for other directions of scattering. The fact that the electrons of an atom are situated at different points in space introduces differences in phase between the waves scattered by different electrons. Consider Fig. 4-5, in which, for simplicity, the electrons are shown as points arranged around the central nucleus. The waves scattered in the forward direction by electrons A and B are exactly in phase on a wave front such as XX' , because each wave has traveled the same distance before and after scattering. The other scattered waves shown in the figure, however, have a path difference equal to $(CB - AD)$ and are thus somewhat out of phase along a wave front such as YY' , the path difference being less than one wavelength. Partial interference occurs between the waves scattered by A and B , with the result that the net amplitude of the wave scattered in this direction is less than that of the wave scattered by the same electrons in the forward direction.

A quantity f , the *atomic scattering factor*, is used to describe the "efficiency" of scattering of a given atom in a given direction. It is defined as a ratio of amplitudes:

$$f = \frac{\text{amplitude of the wave scattered by an atom}}{\text{amplitude of the wave scattered by one electron}}.$$

From what has been said already, it is clear that $f = Z$ for any atom scattering in the forward direction. As θ increases, however, the waves scattered by individual electrons become more and more out of phase and f decreases. The atomic scattering factor also depends on the wavelength of the incident beam: at a fixed value of θ , f will be smaller the shorter the

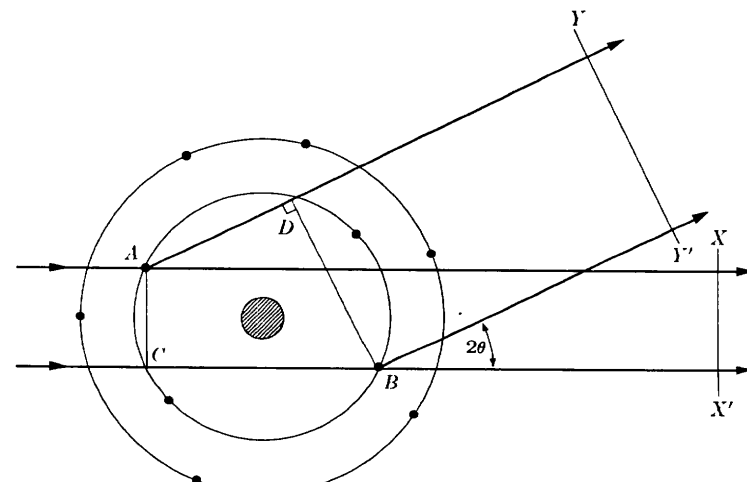


FIG. 4-5. X-ray scattering by an atom.

wavelength, since the path differences will be larger relative to the wavelength, leading to greater interference between the scattered beams. The actual calculation of f involves $\sin \theta$ rather than θ , so that the net effect is that f decreases as the quantity $(\sin \theta)/\lambda$ increases.

Calculated values of f for various atoms and various values of $(\sin \theta)/\lambda$ are tabulated in Appendix 8, and a curve showing the typical variation of f , in this case for copper, is given in Fig. 4-6. Note again that the curve begins at the atomic number of copper, 29, and decreases to very low values for scattering in the backward direction (θ near 90°) or for very short wavelengths. Since the intensity of a wave is proportional to the square of its amplitude, a curve of scattered intensity from an atom can be obtained simply by squaring the ordinates of a curve such as Fig. 4-6. (The resulting curve closely approximates the observed scattered intensity per atom of a monatomic gas, as shown in Fig. 3-18.)

The scattering just discussed, whose amplitude is expressed in terms of the atomic scattering factor, is coherent, or unmodified, scattering, which is the only kind capable of being diffracted. On the other hand, incoherent, or Compton modified, scattering is occurring at the same time. Since the latter is due to collisions of quanta with loosely bound electrons, its intensity relative to that of the unmodified radiation increases as the proportion of loosely bound electrons increases. The intensity of Compton modified radiation thus increases as the atomic number Z decreases. It is for this reason that it is difficult to obtain good diffraction photographs of organic materials, which contain light elements such as carbon, oxygen, and hydrogen, since the strong Compton modified scattering from these substances darkens the background of the photograph and makes it difficult to see the diffraction lines formed by the unmodified radiation. It is also found that the intensity of the modified radiation increases as the quantity $(\sin \theta)/\lambda$ increases. The intensities of modified scattering and of unmodified scattering therefore vary in opposite ways with Z and with $(\sin \theta)/\lambda$.

To summarize, when a monochromatic beam of x-rays strikes an atom, two scattering processes occur. Tightly bound electrons are set into oscillation and radiate x-rays of the same wavelength as that of the incident

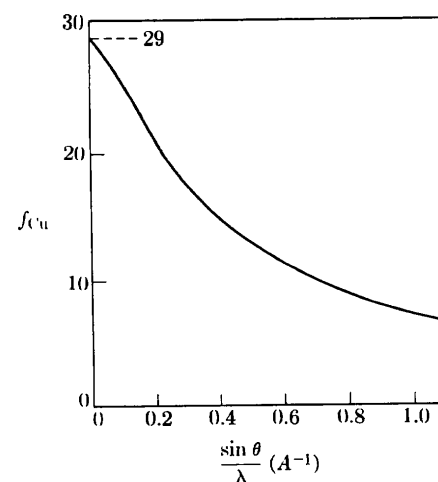


FIG. 4-6. The atomic scattering factor of copper.

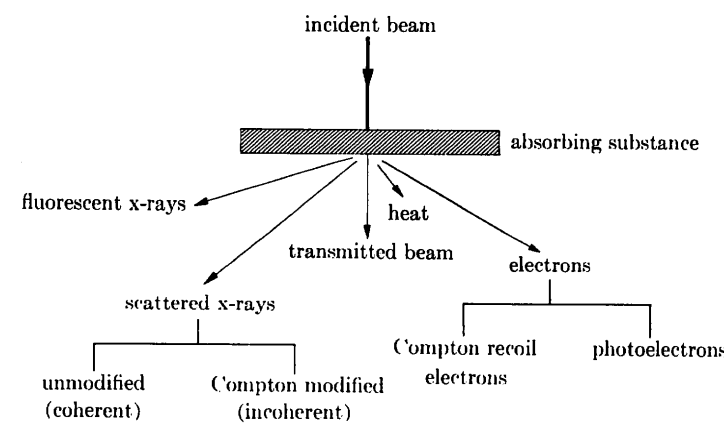


FIG. 4-7. Effects produced by the passage of x-rays through matter. (After N. F. M. Henry, H. Lipson, and W. A. Wooster, *The Interpretation of X-Ray Diffraction Photographs*, Macmillan, London, 1951.)

beam. More loosely bound electrons scatter part of the incident beam and slightly increase its wavelength in the process, the exact amount of increase depending on the scattering angle. The former is called coherent or unmodified scattering and the latter incoherent or modified; both kinds occur simultaneously and in all directions. If the atom is a part of a large group of atoms arranged in space in a regular periodic fashion as in a crystal, then another phenomenon occurs. The coherently scattered radiation from all the atoms undergoes reinforcement in certain directions and cancellation in other directions, thus producing diffracted beams. Diffraction is, essentially, reinforced coherent scattering.

We are now in a position to summarize, from the preceding sections and from Chap. 1, the chief effects associated with the passage of x-rays through matter. This is done schematically in Fig. 4-7. The incident x-rays are assumed to be of high enough energy, i.e., of short enough wavelength, to cause the emission of photoelectrons and characteristic fluorescent radiation. The Compton recoil electrons shown in the diagram are the loosely bound electrons knocked out of the atom by x-ray quanta, the interaction giving rise to Compton modified radiation.

4-4 Scattering by a unit cell. To arrive at an expression for the intensity of a diffracted beam, we must now restrict ourselves to a consideration of the coherent scattering, not from an isolated atom, but from all the atoms making up the crystal. The mere fact that the atoms are arranged in a periodic fashion in space means that the scattered radiation is now severely limited to certain definite directions and is now referred to as a set of diffracted beams. The directions of these beams are fixed by

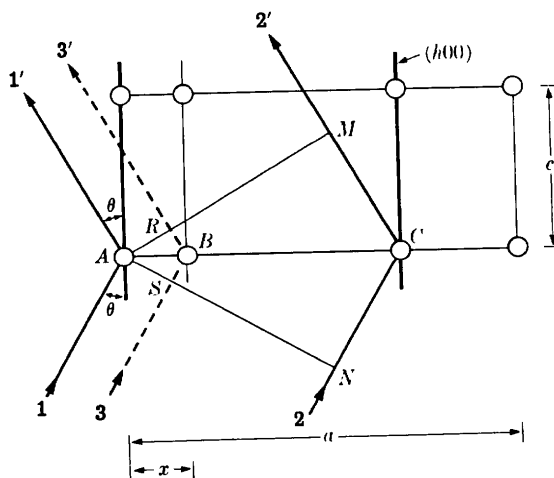


FIG. 4-8. The effect of atom position on the phase difference between diffracted rays.

the Bragg law, which is, in a sense, a negative law. If the Bragg law is not satisfied, no diffracted beam can occur; however, the Bragg law may be satisfied for a certain set of atomic planes and yet no diffraction may occur, as in the example given at the beginning of this chapter, because of a particular arrangement of atoms within the unit cell [Fig. 4-2(b)].

Assuming that the Bragg law is satisfied, we wish to find the intensity of the beam diffracted by a crystal as a function of atom position. Since the crystal is merely a repetition of the fundamental unit cell, it is enough to consider the way in which the arrangement of atoms within a single unit cell affects the diffracted intensity.

Qualitatively, the effect is similar to the scattering from an atom, discussed in the previous section. There we found that phase differences occur in the waves scattered by the individual electrons, for any direction of scattering except the extreme forward direction. Similarly, the waves scattered by the individual atoms of a unit cell are not necessarily in phase except in the forward direction, and we must now determine how the phase difference depends on the arrangement of the atoms.

This problem is most simply approached by finding the phase difference between waves scattered by an atom at the origin and another atom whose position is variable in the x direction only. For convenience, consider an orthogonal unit cell, a section of which is shown in Fig. 4-8. Take atom A as the origin and let diffraction occur from the $(h00)$ planes shown as heavy lines in the drawing. This means that the Bragg law is satisfied for this reflection and that $\delta_{2'1'}$, the path difference between ray $2'$ and ray $1'$, is given by

$$\delta_{2'1'} = MCN = 2d_{h00} \sin \theta = \lambda.$$

From the definition of Miller indices,

$$d_{h00} = AC = \frac{a}{h}.$$

How is this reflection affected by x-rays scattered in the same direction by atom B , located at a distance x from A ? Note that only this direction need be considered since only in this direction is the Bragg law satisfied for the $h00$ reflection. Clearly, the path difference between ray $3'$ and ray $1'$, $\delta_{3'1'}$, will be less than λ ; by simple proportion it is found to be

$$\delta_{3'1'} = RBS = \frac{AB}{AC} (\lambda) = \frac{x}{a/h} (\lambda).$$

Phase differences may be expressed in angular measure as well as in wavelength: two rays, differing in path length by one whole wavelength, are said to differ in phase by 360° , or 2π radians. If the path difference is δ , then the phase difference ϕ in radians is given by

$$\phi = \frac{\delta}{\lambda} (2\pi).$$

The use of angular measure is convenient because it makes the expression of phase differences independent of wavelength, whereas the use of a path difference to describe a phase difference is meaningless unless the wavelength is specified.

The phase difference, then, between the wave scattered by atom B and that scattered by atom A at the origin is given by

$$\phi_{3'1'} = \frac{\delta_{3'1'}}{\lambda} (2\pi) = \frac{2\pi hx}{a}.$$

If the position of atom B is specified by its fractional coordinate $u = \frac{x}{a}$, then the phase difference becomes

$$\phi_{3'1'} = 2\pi hu.$$

This reasoning may be extended to three dimensions, as in Fig. 4-9, in which atom B has actual coordinates $x y z$ or fractional coordinates $\frac{x}{a} \frac{y}{b} \frac{z}{c}$ equal to $u v w$, respectively. We then arrive at the following important relation for the phase difference between the wave scattered by atom B and that scattered by atom A at the origin, for the hkl reflection:

$$\phi = 2\pi(hu + kv + lw). \quad (4-4)$$

This relation is general and applicable to a unit cell of any shape.

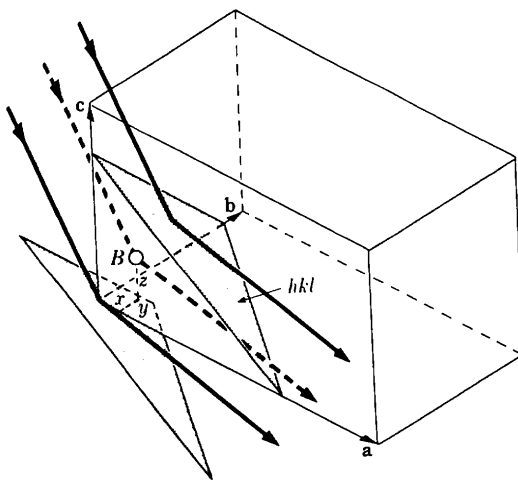


FIG. 4-9. The three-dimensional analogue of Fig. 4-8.

These two waves may differ, not only in phase, but also in amplitude if atom B and the atom at the origin are of different kinds. In that case, the amplitudes of these waves are given, relative to the amplitude of the wave scattered by a single electron, by the appropriate values of f , the atomic scattering factor.

We now see that the problem of scattering from a unit cell resolves itself into one of adding waves of different phase and amplitude in order to find the resultant wave. Waves scattered by all the atoms of the unit cell, including the one at the origin, must be added. The most convenient way of carrying out this summation is by expressing each wave as a complex exponential function.

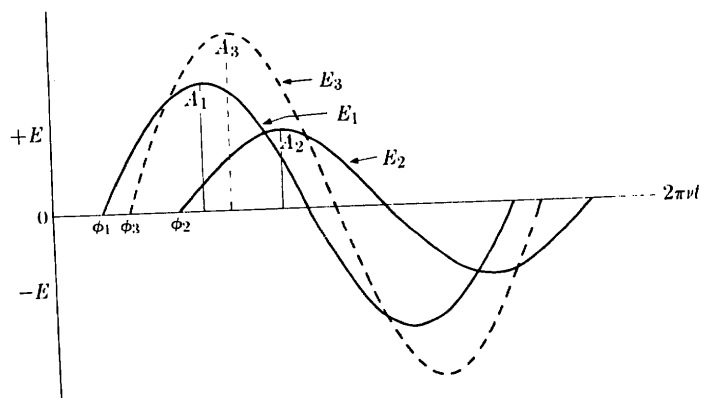


FIG. 4-10. The addition of sine waves of different phase and amplitude.

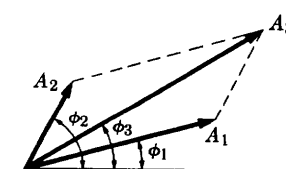


FIG. 4-11. Vector addition of waves.

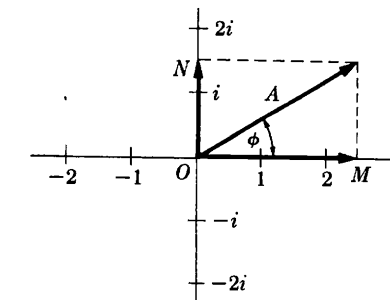


FIG. 4-12. A wave vector in the complex plane.

The two waves shown as full lines in Fig. 4-10 represent the variations in electric field intensity \mathbf{E} with time t of two rays on any given wave front in a diffracted x-ray beam. Their equations may be written

$$\mathbf{E}_1 = A_1 \sin(2\pi\nu t - \phi_1), \quad (4-5)$$

$$\mathbf{E}_2 = A_2 \sin(2\pi\nu t - \phi_2). \quad (4-6)$$

These waves are of the same frequency ν and therefore of the same wavelength λ , but differ in amplitude A and in phase ϕ . The dotted curve shows their sum \mathbf{E}_3 , which is also a sine wave, but of different amplitude and phase.

Waves differing in amplitude and phase may also be added by representing them as vectors. In Fig. 4-11, each component wave is represented by a vector whose length is equal to the amplitude of the wave and which is inclined to the x -axis at an angle equal to the phase angle. The amplitude and phase of the resultant wave is then found simply by adding the vectors by the parallelogram law.

This geometrical construction may be avoided by use of the following analytical treatment, in which complex numbers are used to represent the vectors. A complex number is the sum of a real and an imaginary number, such as $(a + bi)$, where a and b are real and $i = \sqrt{-1}$ is imaginary. Such numbers may be plotted in the "complex plane," in which real numbers are plotted as abscissae and imaginary numbers as ordinates. Any point in this plane or the vector drawn from the origin to this point then represents a particular complex number $(a + bi)$.

To find an analytical expression for a vector representing a wave, we draw the wave vector in the complex plane as in Fig. 4-12. Here again the amplitude and phase of the wave is given by A , the length of the vector, and ϕ , the angle between the vector and the axis of real numbers. The analytical expression for the wave is now the complex number $(A \cos \phi + iA \sin \phi)$, since these two terms are the horizontal and vertical components

This equation may be written more compactly as

$$F_{hkl} = \sum_1^N f_n e^{2\pi i(hu_n + kv_n + lw_n)}, \quad (4-11)$$

the summation extending over all the atoms of the unit cell.

F is, in general, a complex number, and it expresses both the amplitude and phase of the resultant wave. Its absolute value $|F|$ gives the amplitude of the resultant wave in terms of the amplitude of the wave scattered by a single electron. Like the atomic scattering factor f , $|F|$ is defined as a ratio of amplitudes:

$$|F| = \frac{\text{amplitude of the wave scattered by all the atoms of a unit cell}}{\text{amplitude of the wave scattered by one electron}}$$

The intensity of the beam diffracted by all the atoms of the unit cell in a direction predicted by the Bragg law is proportional simply to $|F|^2$, the square of the amplitude of the resultant beam, and $|F|^2$ is obtained by multiplying the expression given for F in Eq. (4-11) by its complex conjugate. Equation (4-11) is therefore a very important relation in x-ray crystallography, since it permits a calculation of the intensity of any hkl reflection from a knowledge of the atomic positions.

We have found the resultant scattered wave by adding together waves, differing in phase, scattered by individual atoms in the unit cell. Note that the phase difference between rays scattered by any two atoms, such as A and B in Fig. 4-8, is *constant* for every unit cell. There is no question here of these rays becoming increasingly out of phase as we go deeper in the crystal as there was when we considered diffraction at angles not exactly equal to the Bragg angle θ_B . In the direction predicted by the Bragg law, the rays scattered by all the atoms A in the crystal are exactly in phase and so are the rays scattered by all the atoms B , but between these two sets of rays there is a definite phase difference which depends on the relative positions of atoms A and B in the unit cell and which is given by Eq. (4-4).

Although it is more unwieldy, the following trigonometric equation may be used instead of Eq. (4-11):

$$F = \sum_1^N f_n [\cos 2\pi(hu_n + kv_n + lw_n) + i \sin 2\pi(hu_n + kv_n + lw_n)].$$

One such term must be written down for each atom in the unit cell. In general, the summation will be a complex number of the form

$$F = a + ib,$$

OM and ON of the vector. Note that multiplication of a vector by i rotates it counterclockwise by 90° ; thus multiplication by i converts the horizontal vector 2 into the vertical vector $2i$. Multiplication twice by i , that is, by $i^2 = -1$, rotates a vector through 180° or reverses its sense; thus multiplication twice by i converts the horizontal vector 2 into the horizontal vector -2 pointing in the opposite direction.

If we write down the power-series expansions of e^{ix} , $\cos x$, and $\sin x$, we find that

$$e^{ix} = \cos x + i \sin x \quad (4-7)$$

or

$$Ae^{i\phi} = A \cos \phi + Ai \sin \phi. \quad (4-8)$$

Thus the wave vector may be expressed analytically by either side of Eq. (4-8). The expression on the left is called a complex exponential function.

Since the intensity of a wave is proportional to the square of its amplitude, we now need an expression for A^2 , the square of the absolute value of the wave vector. When a wave is expressed in complex form, this quantity is obtained by multiplying the complex expression for the wave by its complex conjugate, which is obtained simply by replacing i by $-i$. Thus, the complex conjugate of $Ae^{i\phi}$ is $Ae^{-i\phi}$. We have

$$|Ae^{i\phi}|^2 = Ae^{i\phi}Ae^{-i\phi} = A^2, \quad (4-9)$$

which is the quantity desired. Or, using the other form given by Eq. (4-8), we have

$$A(\cos \phi + i \sin \phi)A(\cos \phi - i \sin \phi) = A^2(\cos^2 \phi + \sin^2 \phi) = A^2.$$

We return now to the problem of adding the scattered waves from each of the atoms in the unit cell. The amplitude of each wave is given by the appropriate value of f for the scattering atom considered and the value of $(\sin \theta)/\lambda$ involved in the reflection. The phase of each wave is given by Eq. (4-4) in terms of the hkl reflection considered and the uvw coordinates of the atom. Using our previous relations, we can then express any scattered wave in the complex exponential form

$$Ae^{i\phi} = fe^{2\pi i(hu + kv + lw)}. \quad (4-10)$$

The resultant wave scattered by all the atoms of the unit cell is called the *structure factor* and is designated by the symbol F . It is obtained by simply adding together all the waves scattered by the individual atoms. If a unit cell contains atoms 1, 2, 3, ..., N , with fractional coordinates $u_1 v_1 w_1$, $u_2 v_2 w_2$, $u_3 v_3 w_3$, ... and atomic scattering factors f_1, f_2, f_3, \dots , then the structure factor for the hkl reflection is given by

$$F = f_1 e^{2\pi i(hu_1 + kv_1 + lw_1)} + f_2 e^{2\pi i(hu_2 + kv_2 + lw_2)} + f_3 e^{2\pi i(hu_3 + kv_3 + lw_3)} + \dots$$

where

$$a = \sum_1^N f_n \cos 2\pi(hu_n + kv_n + lw_n),$$

$$b = \sum_1^N f_n \sin 2\pi(hu_n + kv_n + lw_n),$$

$$|F|^2 = (a + ib)(a - ib) = a^2 + b^2.$$

Substitution for a and b gives the final form of the equation:

$$|F|^2 = [f_1 \cos 2\pi(hu_1 + kv_1 + lw_1) + f_2 \cos 2\pi(hu_2 + kv_2 + lw_2) + \dots]^2 + [f_1 \sin 2\pi(hu_1 + kv_1 + lw_1) + f_2 \sin 2\pi(hu_2 + kv_2 + lw_2) + \dots]^2.$$

Equation (4-11) is much easier to manipulate, compared to this trigonometric form, particularly if the structure is at all complicated, since the exponential form is more compact.

4-5 Some useful relations. In calculating structure factors by complex exponential functions, many particular relations occur often enough to be worthwhile stating here. They may be verified by means of Eq. (4-7).

$$(a) \quad e^{\pi i} = e^{3\pi i} = e^{5\pi i} = -1,$$

$$(b) \quad e^{2\pi i} = e^{4\pi i} = e^{6\pi i} = +1,$$

(c) In general, $e^{n\pi i} = (-1)^n$, where n is any integer,

$$(d) \quad e^{n\pi i} = e^{-n\pi i}, \text{ where } n \text{ is any integer,}$$

$$(e) \quad e^{ix} + e^{-ix} = 2 \cos x.$$

4-6 Structure-factor calculations. Facility in the use of Eq. (4-11) can be gained only by working out some actual examples, and we shall consider a few such problems here and again in Chap. 10.

(a) The simplest case is that of a unit cell containing only one atom at the origin, i.e., having fractional coordinates 0 0 0. Its structure factor is

$$F = fe^{2\pi i(0)} = f$$

and

$$F^2 = f^2.$$

F^2 is thus independent of h , k , and l and is the same for all reflections.

(b) Consider now the base-centered cell discussed at the beginning of this chapter and shown in Fig. 4-1(a). It has two atoms of the same kind per unit cell located at 0 0 0 and $\frac{1}{2} \frac{1}{2} 0$.

$$F = fe^{2\pi i(0)} + fe^{2\pi i(h/2+k/2)}$$

$$= f[1 + e^{\pi i(h+k)}].$$

This expression may be evaluated without multiplication by the complex conjugate, since $(h + k)$ is always integral, and the expression for F is thus real and not complex. If h and k are both even or both odd, i.e., "unmixed," then their sum is always even and $e^{\pi i(h+k)}$ has the value 1. Therefore

$$F = 2f \quad \text{for } h \text{ and } k \text{ unmixed;}$$

$$F^2 = 4f^2.$$

On the other hand, if h and k are one even and one odd, i.e., "mixed," then their sum is odd and $e^{\pi i(h+k)}$ has the value -1 . Therefore

$$F = 0 \quad \text{for } h \text{ and } k \text{ mixed;}$$

$$F^2 = 0.$$

Note that, in either case, the value of the l index has no effect on the structure factor. For example, the reflections 111, 112, 113, and 021, 022, 023 all have the same value of F , namely $2f$. Similarly, the reflections 011, 012, 013, and 101, 102, 103 all have a zero structure factor.

(c) The structure factor of the body-centered cell shown in Fig. 4-1(b) may also be calculated. This cell has two atoms of the same kind located at 0 0 0 and $\frac{1}{2} \frac{1}{2} \frac{1}{2}$.

$$F = fe^{2\pi i(0)} + fe^{2\pi i(h/2+k/2+l/2)}$$

$$= f[1 + e^{\pi i(h+k+l)}].$$

$$F = 2f \quad \text{when } (h+k+l) \text{ is even;}$$

$$F^2 = 4f^2.$$

$$F = 0 \quad \text{when } (h+k+l) \text{ is odd;}$$

$$F^2 = 0.$$

We had previously concluded from geometrical considerations that the base-centered cell would produce a 001 reflection but that the body-centered cell would not. This result is in agreement with the structure-factor equations for these two cells. A detailed examination of the geometry of all possible reflections, however, would be a very laborious process compared to the straightforward calculation of the structure factor, a calculation that yields a set of rules governing the value of F^2 for all possible values of plane indices.

(d) A face-centered cubic cell, such as that shown in Fig. 2-14, may now be considered. Assume it to contain four atoms of the same kind, located at 0 0 0, $\frac{1}{2} \frac{1}{2} 0$, $\frac{1}{2} 0 \frac{1}{2}$, and $0 \frac{1}{2} \frac{1}{2}$.

$$F = fe^{2\pi i(0)} + fe^{2\pi i(h/2+k/2)} + fe^{2\pi i(h/2+l/2)} + fe^{2\pi i(k/2+l/2)}$$

$$= f[1 + e^{\pi i(h+k)} + e^{\pi i(h+l)} + e^{\pi i(k+l)}].$$

If h , k , and l are unmixed, then all three sums $(h+k)$, $(h+l)$, and $(k+l)$ are even integers, and each term in the above equation has the value 1.

$$F = 4f \quad \text{for unmixed indices;}$$

$$F^2 = 16f^2.$$

If h , k , and l are mixed, then the sum of the three exponentials is -1 , whether two of the indices are odd and one even, or two even and one odd. Suppose for example, that h and l are even and k is odd, e.g., 012. Then $F = f(1 - 1 + 1 - 1) = 0$, and no reflection occurs.

$$F = 0 \quad \text{for mixed indices;}$$

$$F^2 = 0$$

Thus, reflections will occur for such planes as (111), (200), and (220) but not for the planes (100), (210), (112), etc.

The reader may have noticed in the previous examples that some of the information given was not used in the calculations. In (a), for example, the cell was said to contain only one atom, but the shape of the cell was not specified; in (b) and (c), the cells were described as orthorhombic and in (d) as cubic, but this information did not enter into the structure-factor calculations. This illustrates the important point that the *structure factor is independent of the shape and size of the unit cell*. For example, *any* body-centered cell will have missing reflections for those planes which have $(h+k+l)$ equal to an odd number, whether the cell is cubic, tetragonal, or orthorhombic. The rules we have derived in the above examples are therefore of wider applicability than would at first appear and demonstrate the close connection between the Bravais lattice of a substance and its diffraction pattern. They are summarized in Table 4-1. These rules are subject to some qualification, since some cells may contain more atoms than the ones given in examples (a) through (d), and these atoms may be in such positions that reflections normally present are now missing. For example, diamond has a face-centered cubic lattice, but it contains eight

TABLE 4-1

Bravais lattice	Reflections present	Reflections absent
Simple Base-centered	all h and k unmixed* $(h+k+l)$ even	none
Body-centered	h and k mixed*	$(h+k+l)$ odd
Face-centered	h , k , and l unmixed	h , k , and l mixed

* These relations apply to a cell centered on the C face. If reflections are present only when h and l are unmixed, or when k and l are unmixed, then the cell is centered on the B or A face, respectively.

carbon atoms per unit cell. All the reflections present have unmixed indices, but reflections such as 200, 222, 420, etc., are missing. The fact that the only reflections *present* have unmixed indices proves that the lattice is face-centered, while the extra missing reflections are a clue to the actual atom arrangement in this crystal.

(e) This point may be further illustrated by the structure of NaCl (Fig. 2-18). This crystal has a cubic lattice with 4 Na and 4 Cl atoms per unit cell, located as follows:

Na	0 0 0	$\frac{1}{2} \frac{1}{2} 0$	$\frac{1}{2} 0 \frac{1}{2}$	$0 \frac{1}{2} \frac{1}{2}$
Cl	$\frac{1}{2} \frac{1}{2} \frac{1}{2}$	0 0 $\frac{1}{2}$	$0 \frac{1}{2} 0$	$\frac{1}{2} 0 0$

In this case, the proper atomic scattering factors for each atom must be inserted in the structure-factor equation:

$$\begin{aligned} F = & f_{\text{Na}}e^{2\pi i(0)} + f_{\text{Na}}e^{2\pi i(h/2+k/2)} + f_{\text{Na}}e^{2\pi i(h/2+l/2)} + f_{\text{Na}}e^{2\pi i(k/2+l/2)} \\ & + f_{\text{Cl}}e^{2\pi i(h/2+k/2+l/2)} + f_{\text{Cl}}e^{2\pi i(l/2)} + f_{\text{Cl}}e^{2\pi i(k/2)} + f_{\text{Cl}}e^{2\pi i(h/2)}, \\ F = & f_{\text{Na}}[1 + e^{\pi i(h+k)} + e^{\pi i(h+l)} + e^{\pi i(k+l)}] \\ & + f_{\text{Cl}}[e^{\pi i(h+k+l)} + e^{\pi il} + e^{\pi ik} + e^{\pi lh}]. \end{aligned}$$

As discussed in Sec. 2-7, the sodium-atom positions are related by the face-centering translations and so are the chlorine-atom positions. Whenever a lattice contains common translations, the corresponding terms in the structure-factor equation can always be factored out, leading to considerable simplification. In this case we proceed as follows:

$$\begin{aligned} F = & f_{\text{Na}}[1 + e^{\pi i(h+k)} + e^{\pi i(h+l)} + e^{\pi i(k+l)}] \\ & + f_{\text{Cl}}e^{\pi i(h+k+l)}[1 + e^{\pi i(-h-k)} + e^{\pi i(-h-l)} + e^{\pi i(-k-l)}]. \end{aligned}$$

The signs of the exponents in the second bracket may be changed, by relation (d) of Sec. 4-5. Therefore

$$F = [1 + e^{\pi i(h+k)} + e^{\pi i(h+l)} + e^{\pi i(k+l)}][f_{\text{Na}} + f_{\text{Cl}}e^{\pi i(h+k+l)}].$$

Here the terms corresponding to the face-centering translations appear in the first factor. These terms have already appeared in example (d), and they were found to have a total value of zero for mixed indices and 4 for unmixed indices. This shows at once that NaCl has a face-centered lattice and that

$$F = 0 \quad \text{for mixed indices;}$$

$$F^2 = 0.$$

For unmixed indices,

$$F = 4[f_{\text{Na}} + f_{\text{Cl}}e^{\pi i(h+k+l)}].$$

$$F = 4(f_{\text{Na}} + f_{\text{Cl}}) \quad \text{if } (h+k+l) \text{ is even;}$$

$$F^2 = 16(f_{\text{Na}} + f_{\text{Cl}})^2.$$

$$F = 4(f_{\text{Na}} - f_{\text{Cl}}) \quad \text{if } (h+k+l) \text{ is odd;}$$

$$F^2 = 16(f_{\text{Na}} - f_{\text{Cl}})^2.$$

In this case, there are more than four atoms per unit cell, but the lattice is still face-centered. The introduction of additional atoms has not eliminated any reflections present in the case of the four-atom cell, but it has decreased some in intensity. For example, the 111 reflection now involves the difference, rather than the sum, of the scattering powers of the two atoms.

(f) One other example of structure factor calculation will be given here. The close-packed hexagonal cell shown in Fig. 2-15 has two atoms of the same kind located at 0 0 0 and $\frac{1}{3} \frac{2}{3} \frac{1}{2}$.

$$\begin{aligned} F &= fe^{2\pi i(0)} + fe^{2\pi i((h/3+2k)/3+l/2)} \\ &= f[1 + e^{2\pi i((h+2k)/3+l/2)}]. \end{aligned}$$

For convenience, put $[(h+2k)/3 + l/2] = g$.

$$F = f(1 + e^{2\pi ig}).$$

Since g may have fractional values, such as $\frac{1}{3}, \frac{2}{3}, \frac{5}{6}$, etc., this expression is still complex. Multiplication by the complex conjugate, however, will give the square of the absolute value of the resultant wave amplitude F .

$$\begin{aligned} |F|^2 &= f^2(1 + e^{2\pi ig})(1 + e^{-2\pi ig}) \\ &= f^2(2 + e^{2\pi ig} + e^{-2\pi ig}). \end{aligned}$$

By relation (e) of Sec. 4-5, this becomes

$$\begin{aligned} |F|^2 &= f^2(2 + 2 \cos 2\pi g) \\ &= f^2[2 + 2(2 \cos^2 \pi g - 1)] \\ &= f^2(4 \cos^2 \pi g) \\ &= 4f^2 \cos^2 \pi \left(\frac{h+2k}{3} + \frac{l}{2} \right) \\ &= 0 \quad \text{when } (h+2k) \text{ is a multiple of 3 and } l \text{ is odd.} \end{aligned}$$

It is by these missing reflections, such as 11·1, 11·3, 22·1, 22·3, that a hexagonal structure is recognized as being close-packed. Not all the reflections present have the same structure factor. For example, if $(h+2k)$ is a multiple of 3 and l is even, then

$$\left(\frac{h+2k}{3} + \frac{l}{2} \right) = n, \quad \text{where } n \text{ is an integer;}$$

$$\cos \pi n = \pm 1,$$

$$\cos^2 \pi n = 1,$$

$$|F|^2 = 4f^2.$$

When all possible values of h , k , and l are considered, the results may be summarized as follows:

$\frac{h+2k}{3}$	$\frac{l}{2}$	$ F ^2$
$3n$	odd	0
$3n$	even	$4f^2$
$3n \pm 1$	odd	$3f^2$
$3n \pm 1$	even	f^2

4-7 Application to powder method. Any calculation of the intensity of a diffracted beam must always begin with the structure factor. The remainder of the calculation, however, varies with the particular diffraction method involved. For the Laue method, intensity calculations are so difficult that they are rarely made, since each diffracted beam has a different wavelength and blackens the film by a variable amount, depending on both the intensity and the film sensitivity for that particular wavelength. The factors governing diffracted intensity in the rotating-crystal and powder methods are somewhat similar, in that monochromatic radiation is used in each, but they differ in detail. The remainder of this chapter will be devoted to the powder method, since it is of most general utility in metallurgical work.

There are six factors affecting the relative intensity of the diffraction lines on a powder pattern:

- (1) polarization factor,
- (2) structure factor,
- (3) multiplicity factor,
- (4) Lorentz factor,
- (5) absorption factor,
- (6) temperature factor.

The first two of these have already been described, and the others will be discussed in the following sections.

4-8 Multiplicity factor. Consider the 100 reflection from a cubic lattice. In the powder specimen, some of the crystals will be so oriented that reflection can occur from their (100) planes. Other crystals of different orientation may be in such a position that reflection can occur from their (010) or (001) planes. Since all these planes have the same spacing, the beams diffracted by them all form part of the same cone. Now consider the 111 reflection. There are four sets of planes of the form {111} which have the same spacing but different orientation, namely, (111), (111), (111), and (111), whereas there are only three sets of the form {100}. Therefore, the probability that {111} planes will be correctly oriented for reflection is $\frac{4}{3}$ the probability that {100} planes will be correctly oriented. It follows that the intensity of the 111 reflection will be $\frac{4}{3}$ that of the 100 reflection, other things being equal.

This relative proportion of planes contributing to the same reflection enters the intensity equation as the quantity p , the *multiplicity factor*, which may be defined as the number of different planes in a form having the same spacing. Parallel planes with different Miller indices, such as (100) and (100), are counted separately as different planes, yielding numbers which are double those given in the preceding paragraph. Thus the multiplicity factor for the {100} planes of a cubic crystal is 6 and for the {111} planes 8.

The value of p depends on the crystal system: in a tetragonal crystal, the (100) and (001) planes do not have the same spacing, so that the value of p for {100} planes is reduced to 4 and the value for {001} planes to 2. Values of the multiplicity factor as a function of hkl and crystal system are given in Appendix 9.

4-9 Lorentz factor. We must now consider certain trigonometrical factors which influence the intensity of the reflected beam. Suppose there is incident on a crystal [Fig. 4-13(a)] a narrow beam of parallel monochromatic rays, and let the crystal be rotated at a uniform angular velocity about an axis through O and normal to the drawing, so that a particular set of reflecting planes, assumed for convenience to be parallel to the crystal surface, passes through the angle θ_B , at which the Bragg law is exactly satisfied. As mentioned in Sec. 3-7, the intensity of reflection is greatest at the exact Bragg angle but still appreciable at angles deviating slightly from the Bragg angle, so that a curve of intensity vs. 2θ is of the form shown in Fig. 4-13(b). If all the diffracted beams sent out by the crystal as it rotates through the Bragg angle are received on a photographic film or in a counter, the total energy of the diffracted beam can be measured. This energy is called the *integrated intensity* of the reflection and is given by the area under the curve of Fig. 4-13(b). The integrated intensity is of much more interest than the maximum intensity, since the former is

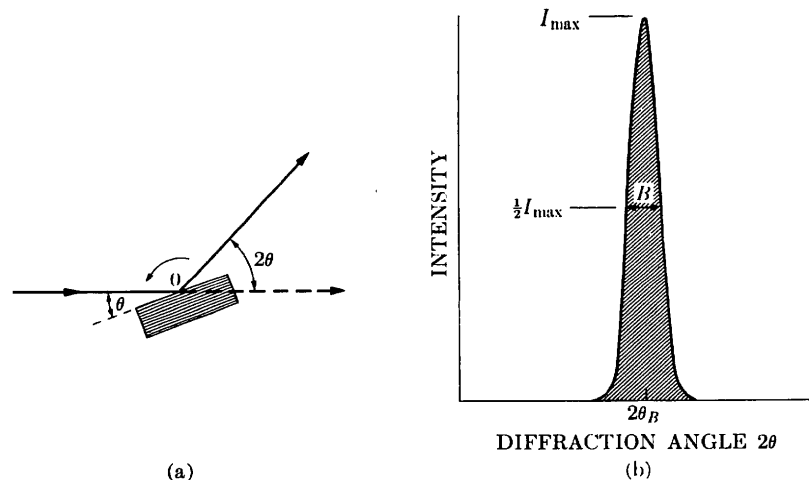


FIG. 4-13. Diffraction by a crystal rotated through the Bragg angle.

characteristic of the specimen while the latter is influenced by slight adjustments of the experimental apparatus. Moreover, in the visual comparison of the intensities of diffraction lines, it is the integrated intensity of the line rather than the maximum intensity which the eye evaluates.

The integrated intensity of a reflection depends on the particular value of θ_B involved, even though all other variables are held constant. We can find this dependence by considering, separately, two aspects of the diffraction curve: the maximum intensity and the breadth. When the reflecting planes make an angle θ_B with the incident beam, the Bragg law is exactly satisfied and the intensity diffracted in the direction $2\theta_B$ is a maximum. But some energy is still diffracted in this direction when the angle of incidence differs slightly from θ_B , and the total energy diffracted in the direction $2\theta_B$ as the crystal is rotated through the Bragg angle is given by the value of I_{\max} of the curve of Fig. 4-13(b). The value of I_{\max} therefore depends on the angular range of crystal rotation over which the energy diffracted in the direction $2\theta_B$ is appreciable. In Fig. 4-14(a), the dashed lines show the position of the crystal after rotation through a small angle

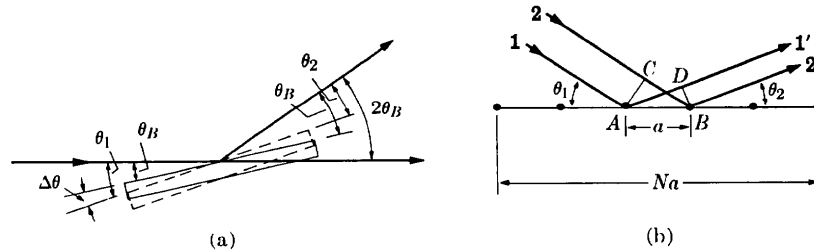


FIG. 4-14. Scattering in a fixed direction during crystal rotation.

$\Delta\theta$ from the Bragg position. The incident beam and the diffracted beam under consideration now make unequal angles with the reflecting planes, the former making an angle $\theta_1 = \theta_B + \Delta\theta$ and the latter an angle $\theta_2 = \theta_B - \Delta\theta$. The situation on an atomic scale is shown in Fig. 4-14(b). Here we need only consider a single plane of atoms, since the rays scattered by all other planes are in phase with the corresponding rays scattered by the first plane. Let a equal the atom spacing in the plane and Na the total length* of the plane. The difference in path length for rays 1' and 2' scattered by adjacent atoms is given by

$$\begin{aligned}\delta_{1'2'} &= AD - CB \\ &= a \cos \theta_2 - a \cos \theta_1 \\ &= a[\cos(\theta_B - \Delta\theta) - \cos(\theta_B + \Delta\theta)].\end{aligned}$$

By expanding the cosine terms and setting $\sin \Delta\theta$ equal to $\Delta\theta$, since the latter is small, we find:

$$\delta_{1'2'} = 2a\Delta\theta \sin \theta_B,$$

and the path difference between the rays scattered by atoms at either end of the plane is simply N times this quantity. When the rays scattered by the two end atoms are one wavelength out of phase, the diffracted intensity will be zero. (The argument here is exactly analogous to that used in Sec. 3-7.) The condition for zero diffracted intensity is therefore

$$2Na\Delta\theta \sin \theta_B = \lambda,$$

or

$$\Delta\theta = \frac{\lambda}{2Na \sin \theta_B}.$$

This equation gives the maximum angular range of crystal rotation over which appreciable energy will be diffracted in the direction $2\theta_B$. Since I_{\max} depends on this range, we can conclude that I_{\max} is proportional to $1/\sin \theta_B$. Other things being equal, I_{\max} is therefore large at low scattering angles and small in the back-reflection region.

The breadth of the diffraction curve varies in the opposite way, being larger at large values of $2\theta_B$, as was shown in Sec. 3-7, where the maximum breadth B was found to be proportional to $1/\cos \theta_B$. The integrated intensity of the reflection is given by the area under the diffraction curve and is therefore proportional to the product $I_{\max}B$, which is in turn proportional to $(1/\sin \theta_B)(1/\cos \theta_B)$ or to $1/\sin 2\theta_B$. Thus, as a crystal is rotated through the Bragg angle, the integrated intensity of a reflection, which is the quantity of most experimental interest, turns out to be greater

* If the crystal is larger than the incident beam, then Na is the irradiated length of the plane; if it is smaller, Na is the actual length of the plane.

for large and small values of $2\theta_B$ than for intermediate values, other things being equal.

The preceding remarks apply just as well to the powder method as they do to the case of a rotating crystal, since the range of orientations available among the powder particles, some satisfying the Bragg law exactly, some not so exactly, are the equivalent of single-crystal rotation.

However, in the powder method, a second geometrical factor arises when we consider that the integrated intensity of a reflection at any particular Bragg angle depends on the number of particles oriented at or near that angle. This number is not constant even though the particles are oriented completely at random. In Fig. 4-15 a reference sphere of radius r is drawn around the powder specimen located at O . For the particular hkl reflection shown, ON is the normal to this set of planes in one particle of the powder. Suppose that the range of angles near the Bragg angle over which reflection is appreciable is $\Delta\theta$. Then, for this particular reflection, only those particles will be in a reflecting position which have the ends of their plane normals lying in a band of width $r\Delta\theta$ on the surface of the sphere. Since the particles are assumed to be oriented at random, the ends of their plane normals will be uniformly distributed over the surface of the sphere; the fraction favorably oriented for a reflection will be given by the ratio of the area of the strip to that of the whole sphere. If ΔN is the number of such particles and N the total number, then

$$\frac{\Delta N}{N} = \frac{r\Delta\theta \cdot 2\pi r \sin(90^\circ - \theta_B)}{4\pi r^2} = \frac{\Delta\theta \cos \theta_B}{2}.$$

The number of particles favorably oriented for reflection is thus proportional to $\cos \theta_B$ and is quite small for reflections in the backward direction.

In assessing relative intensities, we do not compare the total diffracted energy in one cone of rays with that in another but rather the integrated intensity per unit length of one diffraction line with that of another. For example, in the most common arrangement of specimen and film, the Debye-Scherrer method, shown in Fig. 4-16, the film obviously receives a greater proportion of a diffraction cone when the reflection is in the forward or backward direction than it does near $2\theta = 90^\circ$. Inclusion of this effect

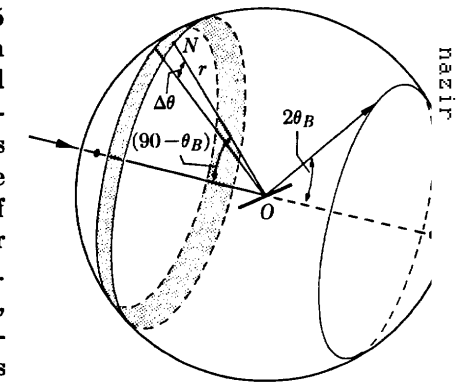


FIG. 4-15. The distribution of plane normals for a particular cone of reflected rays.

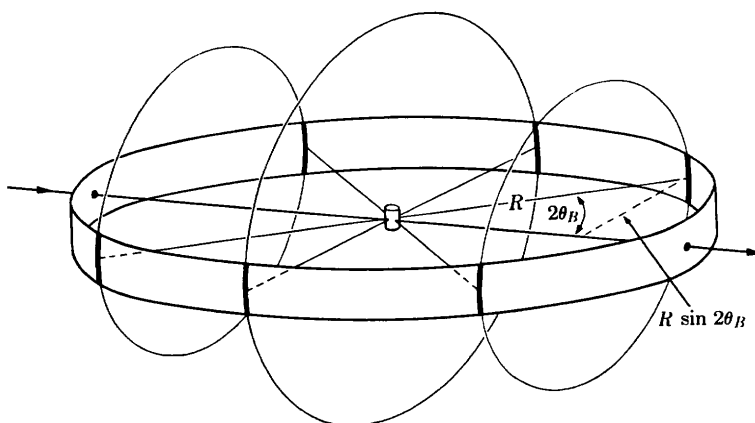


FIG. 4-16. Intersection of cones of diffracted rays with Debye-Scherrer film.

thus leads to a third geometrical factor affecting the intensity of a reflection. The length of any diffraction line being $2\pi R \sin 2\theta_B$, where R is the pro-radius of the camera, the relative intensity per unit length of line is proportional to $1/\sin 2\theta_B$.

In intensity calculations, the three factors just discussed are combined into one and called the Lorentz factor. Dropping the subscript on the Bragg angle, we have:

$$\text{Lorentz factor} = \left(\frac{1}{\sin 2\theta} \right) \left(\cos \theta \right) \left(\frac{1}{\sin 2\theta} \right) = \frac{\cos \theta}{\sin^2 2\theta} = \frac{1}{4 \sin^2 \theta \cos \theta}.$$

This in turn is combined with the polarization factor $\frac{1}{2}(1 + \cos^2 2\theta)$ of Sec. 4-2 to give the combined Lorentz-polarization factor which, with a constant factor of $\frac{1}{8}$ omitted, is given by

Lorentz-polarization factor =

$$\frac{1 + \cos^2 2\theta}{\sin^2 \theta \cos \theta}.$$

Values of this factor are given in Appendix 10 and plotted in Fig. 4-17 as a function of θ . The over-all effect of these geometrical factors is to decrease the intensity of reflections at intermediate angles compared to those in forward or backward directions.

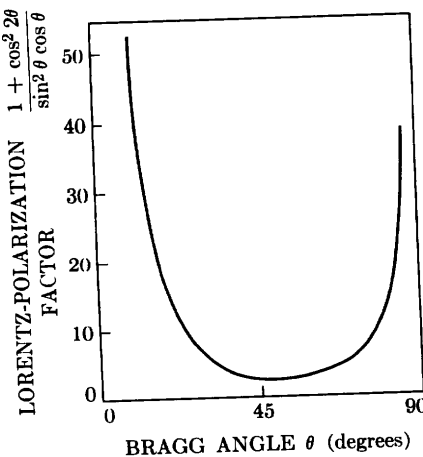


FIG. 4-17. Lorentz-polarization factor.

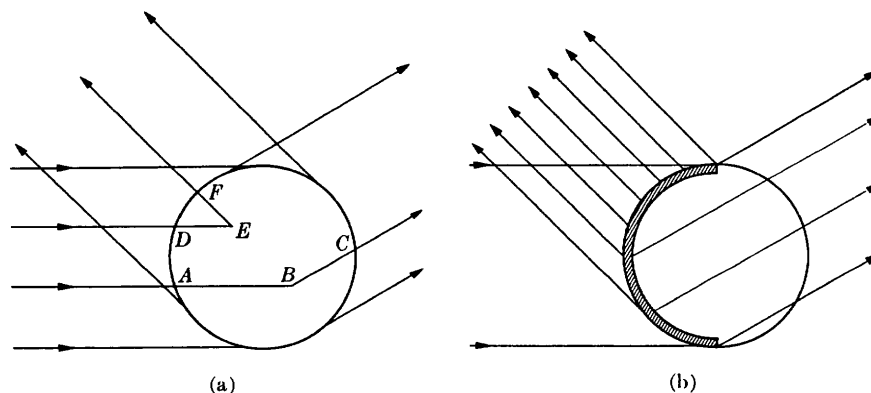


FIG. 4-18. Absorption in Debye-Scherrer specimens: (a) general case, (b) highly absorbing specimen.

4-10 Absorption factor. Still another factor affecting the intensities of the diffracted rays must be considered, and that is the absorption which takes place in the specimen itself. The specimen in the Debye-Scherrer method has the form of a very thin cylinder of powder placed on the camera axis, and Fig. 4-18(a) shows the cross section of such a specimen. For the low-angle reflection shown, absorption of a particular ray in the incident beam occurs along a path such as AB ; at B a small fraction of the incident energy is diffracted by a powder particle, and absorption of this diffracted beam occurs along the path BC . Similarly, for a high-angle reflection, absorption of both the incident and diffracted beams occurs along a path such as $(DE + EF)$. The net result is that the diffracted beam is of lower intensity than one would expect for a specimen of no absorption.

A calculation of this effect shows that the relative absorption increases as θ decreases, for any given cylindrical specimen. That this must be so can be seen from Fig. 4-18(b) which applies to a specimen (for example, tungsten) of very high absorption. The incident beam is very rapidly absorbed, and most of the diffracted beams originate in the thin surface layer on the left side of the specimen; backward-reflected beams then undergo very little absorption, but forward-reflected beams have to pass through the whole specimen and are greatly absorbed. Actually, the forward-reflected beams in this case come almost entirely from the top and bottom edges of the specimen.* This difference in absorption between

* The powder patterns reproduced in Fig. 3-13 show this effect. The lowest-angle line in each pattern is split in two, because the beam diffracted through the center of the specimen is so highly absorbed. It is important to keep the possibility of this phenomenon in mind when examining Debye-Scherrer photographs, or split low-angle lines may be incorrectly interpreted as separate diffraction lines from two different sets of planes.

high- θ and low- θ reflections decreases as the linear absorption coefficient of the specimen decreases, but the absorption is always greater for the low- θ reflections. (These remarks apply only to the cylindrical specimen used in the Debye-Scherrer method. The absorption factor has an entirely different form for the flat-plate specimen used in a diffractometer, as will be shown in Sec. 7-4.)

Exact calculation of the absorption factor for a cylindrical specimen is often difficult, so it is fortunate that this effect can usually be neglected in the calculation of diffracted intensities, when the Debye-Scherrer method is used. Justification of this omission will be found in the next section.

4-11 Temperature factor. So far we have considered a crystal as a collection of atoms located at fixed points in the lattice. Actually, the atoms undergo thermal vibration about their mean positions even at the absolute zero of temperature, and the amplitude of this vibration increases as the temperature increases. In aluminum at room temperature, the average displacement of an atom from its mean position is about 0.17\AA , which is by no means negligible, being about 6 percent of the distance of closest approach of the mean atom positions in this crystal.

Thermal agitation decreases the intensity of a diffracted beam because it has the effect of smearing out the lattice planes; atoms can be regarded as lying no longer on mathematical planes but rather in platelike regions of ill-defined thickness. Thus the reinforcement of waves scattered at the Bragg angle by various parallel planes, the reinforcement which is called a diffracted beam, is not as perfect as it is for a crystal with fixed atoms. This reinforcement requires that the path difference, which is a function of the plane spacing d , between waves scattered by adjacent planes be an integral number of wavelengths. Now the thickness of the platelike "planes" in which the vibrating atoms lie is, on the average, $2u$, where u is the average displacement of an atom from its mean position. Under these conditions reinforcement is no longer perfect, and it becomes more imperfect as the ratio u/d increases, i.e., as the temperature increases, since that increases u , or as θ increases, since high- θ reflections involve planes of low d value. Thus the intensity of a diffracted beam decreases as the temperature is raised, and, for a constant temperature, thermal vibration causes a greater decrease in the reflected intensity at high angles than at low angles.

The temperature effect and the previously discussed absorption effect in cylindrical specimens therefore depend on angle in opposite ways and, to a first approximation, cancel each other. In back reflection, for example, the intensity of a diffracted beam is decreased very little by absorption but very greatly by thermal agitation, while in the forward direction the reverse is true. The two effects do not exactly cancel one other at all

angles; however, if the comparison of line intensities is restricted to lines not differing too greatly in θ values, the absorption and temperature effects can be safely ignored. This is a fortunate circumstance, since both of these effects are rather difficult to calculate exactly.

It should be noted here that thermal vibration of the atoms of a crystal does not cause any broadening of the diffraction lines; they remain sharp right up to the melting point, but their maximum intensity gradually decreases. It is also worth noting that the mean amplitude of atomic vibration is not a function of the temperature alone but depends also on the elastic constants of the crystal. At any given temperature, the less "stiff" the crystal, the greater the vibration amplitude u . This means that u is much greater at any one temperature for a soft, low-melting-point metal like lead than it is for, say, tungsten. Substances with low melting points have quite large values of u even at room temperature and therefore yield rather poor back-reflection photographs.

The thermal vibration of atoms has another effect on diffraction patterns. Besides decreasing the intensity of diffraction lines, it causes some general coherent scattering in all directions. This is called *temperature-diffuse scattering*; it contributes only to the general background of the pattern and its intensity gradually increases with 2θ . Contrast between lines and background naturally suffers, so this effect is a very undesirable one, leading in extreme cases to diffraction lines in the back-reflection region scarcely distinguishable from the background.

In the phenomenon of temperature-diffuse scattering we have another example, beyond those alluded to in Sec. 3-7, of scattering at non-Bragg angles. Here again it is not surprising that such scattering should occur, since the displacement of atoms from their mean positions constitutes a kind of crystal imperfection and leads to a partial breakdown of the conditions necessary for perfect destructive interference between rays scattered at non-Bragg angles.

The effect of thermal vibration also illustrates what has been called "the approximate law of conservation of diffracted energy." This law states that the total energy diffracted by a particular specimen under particular experimental conditions is roughly constant. Therefore, anything done to alter the physical condition of the specimen does not alter the total amount of diffracted energy but only its distribution in space. This "law" is not at all rigorous, but it does prove helpful in considering many diffraction phenomena. For example, at low temperatures there is very little background scattering due to thermal agitation and the diffraction lines are relatively intense; if the specimen is now heated to a high temperature, the lines will become quite weak and the energy which is lost from the lines will appear in a spread-out form as temperature-diffuse scattering.

4-12 Intensities of powder pattern lines. We are now in a position to gather together the factors discussed in preceding sections into an equation for the relative intensity of powder pattern lines:

$$I = |F|^2 p \left(\frac{1 + \cos^2 2\theta}{\sin^2 \theta \cos \theta} \right), \quad (4-12)$$

where I = relative integrated intensity (arbitrary units), F = structure factor, p = multiplicity factor, and θ = Bragg angle. In arriving at this equation, we have omitted factors which are constant for all lines of the pattern. For example, all that is retained of the Thomson equation (Eq. 4-2) is the polarization factor $(1 + \cos^2 2\theta)$, with constant factors, such as the intensity of the incident beam and the charge and mass of the electron, omitted. The intensity of a diffraction line is also directly proportional to the irradiated volume of the specimen and inversely proportional to the camera radius, but these factors are again constant for all diffraction lines and may be neglected. Omission of the temperature and absorption factors means that Eq. (4-12) is valid only for the Debye-Scherrer method and then only for lines fairly close together on the pattern; this latter restriction is not as serious as it may sound. Equation (4-12) is also restricted to the Debye-Scherrer method because of the particular way in which the Lorentz factor was determined; other methods, such as those involving focusing cameras, will require a modification of the Lorentz factor given here. In addition, the individual crystals making up the powder specimen must have completely random orientations if Eq. (4-12) is to apply. Finally, it should be remembered that this equation gives the relative *integrated* intensity, i.e., the relative area under the curve of intensity *vs.* 2θ .

It should be noted that "integrated intensity" is not really *intensity*, since intensity is expressed in terms of energy crossing unit area per unit of time. A beam diffracted by a powder specimen carries a certain amount of energy per unit time and one could quite properly refer to the total *power* of the diffracted beam. If this beam is then incident on a measuring device, such as photographic film, for a certain length of time and if a curve of diffracted intensity *vs.* 2θ is constructed from the measurements, then the area under this curve gives the total *energy* in the diffracted beam. This is the quantity commonly referred to as integrated intensity. A more descriptive term would be "total diffracted energy," but the term "integrated intensity" has been too long entrenched in the vocabulary of x-ray diffraction to be changed now.

4-13 Examples of intensity calculations. The use of Eq. (4-12) will be illustrated by the calculation of the position and relative intensities of

the diffraction lines on a powder pattern of copper, made with $Cu K\alpha$ radiation. The calculations are most readily carried out in tabular form, as in Table 4-2.

TABLE 4-2

Line	hkl	$h^2 + k^2 + l^2$	$\sin^2 \theta$	$\sin \theta$	θ	$\frac{\sin \theta}{\lambda} (A^{-1})$	f_{Cu}
1	111	3	0.1365	0.369	21.7°	0.240	20.0
2	200	4	0.1820	0.426	25.2	0.277	18.7
3	220	8	0.364	0.602	37.0	0.391	15.6
4	311	11	0.500	0.706	44.9	0.459	14.0
5	222	12	0.546	0.738	47.6	0.479	13.7
6	400	16	0.728	0.851	58.3	0.553	12.4
7	331	19	0.865	0.929	68.3	0.604	11.7
8	420	20	0.910	0.951	72.0	0.618	11.4

Line	F^2	p	$\frac{1 + \cos^2 2\theta}{\sin^2 \theta \cos \theta}$	Relative integrated intensity		
				Calc.	Calc.	Obs.
1	6400	8	12.10	6.20×10^5	10.0	s
2	5600	6	8.50	2.86	4.6	m
3	3890	12	3.75	1.75	2.8	m
4	3140	24	2.87	2.16	3.5	s
5	3000	8	2.75	0.66	1.1	w
6	2460	6	3.18	0.47	0.8	w
7	2190	24	4.75	2.50	4.0	vs
8	2080	24	5.92	2.96	4.8	vs

Remarks:

Column 2: Since copper is face-centered cubic, F is equal to $4f_{Cu}$ for lines of unmixed indices and zero for lines of mixed indices. The reflecting plane indices, all unmixed, are written down in this column in order of increasing values of $(h^2 + k^2 + l^2)$, from Appendix 6.

Column 4: For a cubic crystal, values of $\sin^2 \theta$ are given by Eq. (3-10):

$$\sin^2 \theta = \frac{\lambda^2}{4a^2} (h^2 + k^2 + l^2).$$

In this case, $\lambda = 1.542A$ ($Cu K\alpha$) and $a = 3.615A$ (lattice parameter of copper). Therefore, multiplication of the integers in column 3 by $\lambda^2/4a^2 = 0.0455$ gives the values of $\sin^2 \theta$ listed in column 4. In this and similar calculations, slide-rule accuracy is ample.

Column 6: Needed to determine the Lorentz-polarization factor and $(\sin \theta)/\lambda$.

Column 7: Obtained from Appendix 7. Needed to determine f_{Cu} .

Column 8: Read from the curve of Fig. 4-6.

Column 9: Obtained from the relation $F^2 = 16f_{Cu}^2$.

Column 10: Obtained from Appendix 9.

Column 11: Obtained from Appendix 10.

Column 12: These values are the product of the values in columns 9, 10, and 11.

Column 13: Values from column 12 recalculated to give the first line an arbitrary intensity of 10.

Column 14: These entries give the observed intensities, visually estimated according to the following simple scale, from the pattern shown in Fig. 3-13(a) (*vs* = very strong, *s* = strong, *m* = medium, *w* = weak).

The agreement obtained here between observed and calculated intensities is satisfactory. For example, lines 1 and 2 are observed to be of strong and medium intensity, their respective calculated intensities being 10 and 4.6. Similar agreement can be found by comparing the intensities of any pair of neighboring lines in the pattern. Note, however, that the comparison must be made between lines which are not too far apart: for example, the calculated intensity of line 2 is greater than that of line 4, whereas line 4 is observed to be stronger than line 2. Similarly, the strongest lines on the pattern are lines 7 and 8, while calculations show line 1 to be strongest. Errors of this kind arise from the omission of the absorption and temperature factors from the calculation.

A more complicated structure may now be considered, namely that of the zinc-blende form of ZnS, shown in Fig. 2-19(b). This form of ZnS is cubic and has a lattice parameter of 5.41 Å. We will calculate the relative intensities of the first six lines on a pattern made with Cu $K\alpha$ radiation.

As always, the first step is to work out the structure factor. ZnS has four zinc and four sulfur atoms per unit cell, located in the following positions:

Zn: $\frac{1}{4} \frac{1}{4} \frac{1}{4}$ + face-centering translations,

S: 0 0 0 + face-centering translations.

Since the structure is face-centered, we know that the structure factor will be zero for planes of mixed indices. We also know, from example (e) of Sec. 4-6, that the terms in the structure-factor equation corresponding to the face-centering translations can be factored out and the equation for unmixed indices written down at once:

$$F = 4[f_s + f_{Zn}e^{(\pi i/2)(h+k+l)}].$$

$|F|^2$ is obtained by multiplication of the above by its complex conjugate:

$$|F|^2 = 16[f_s + f_{Zn}e^{(\pi i/2)(h+k+l)}][f_s + f_{Zn}e^{-(\pi i/2)(h+k+l)}].$$

This equation reduces to the following form:

$$|F|^2 = 16 \left[f_s^2 + f_{Zn}^2 + 2f_s f_{Zn} \cos \frac{\pi}{2}(h+k+l) \right].$$

Further simplification is possible for various special cases:

$$|F|^2 = 16(f_s^2 + f_{Zn}^2) \text{ when } (h+k+l) \text{ is odd; } \quad (4-13)$$

$$|F|^2 = 16(f_s - f_{Zn})^2 \text{ when } (h+k+l) \text{ is an odd multiple of 2; } \quad (4-14)$$

$$|F|^2 = 16(f_s + f_{Zn})^2 \text{ when } (h+k+l) \text{ is an even multiple of 2. } \quad (4-15)$$

The intensity calculations are carried out in Table 4-3, with some columns omitted for the sake of brevity.

TABLE 4-3

	1	2	3	4	5	6
Line	hkl	θ	$\frac{\sin \theta}{\lambda} (\text{Å}^{-1})$	f_s	f_{Zn}	
1	111	14.3°	0.161	11.5	24.2	
2	200	16.6	0.185	11.0	23.2	
3	220	23.8	0.262	9.5	20.0	
4	311	28.2	0.307	8.9	18.5	
5	222	29.6	0.321	8.6	18.0	
6	400	34.8	0.370	8.1	16.7	

	1	7	8	9	10	11
Line	$ F ^2$	p	$\frac{1 + \cos^2 2\theta}{\sin^2 \theta \cos \theta}$	Relative intensity		
				Calc.	Obs.	
1	11490	8	30.1	10.0	vs	
2	2380	6	21.9	1.1	w	
3	13940	12	9.72	5.9	vs	
4	6750	24	6.65	3.9	vs	
5	1410	8	6.00	0.2	vw	
6	9850	6	4.24	0.9	w	

Remarks:

Columns 5 and 6: These values are read from scattering-factor curves plotted from the data of Appendix 8.

Column 7: $|F|^2$ is obtained by the use of Eq. (4-13), (4-14), or (4-15), depending on the particular values of hkl involved. Thus, Eq. (4-13) is used for the 111 reflection and Eq. (4-15) for the 220 reflection.

Columns 10 and 11: The agreement obtained here between calculated and observed intensities is again satisfactory. In this case, the agreement is good when any pair of lines is compared, because of the limited range of θ values involved.

One further remark on intensity calculations is necessary. In the powder method, two sets of planes with different Miller indices can reflect to the same point on the film: for example, the planes (411) and (330) in the cubic system, since they have the same value of $(h^2 + k^2 + l^2)$ and hence the same spacing, or the planes (501) and (431) of the tetragonal system,

since they have the same values of $(h^2 + k^2)$ and l^2 . In such a case, the intensity of each reflection must be calculated separately, since in general the two will have different multiplicity and structure factors, and then added to find the total intensity of the line.

4-14 Measurement of x-ray intensity. In the examples just given, the observed intensity was estimated simply by visual comparison of one line with another. Although this simple procedure is satisfactory in a surprisingly large number of cases, there are problems in which a more precise measurement of diffracted intensity is necessary. Two methods are in general use today for making such measurements, one dependent on the photographic effect of x-rays and the other on the ability of x-rays to ionize gases and cause fluorescence of light in crystals. These methods have already been mentioned briefly in Sec. 1-8 and will be described more fully in Chaps. 6 and 7, respectively.

PROBLEMS

4-1. By adding Eqs. (4-5) and (4-6) and simplifying the sum, show that \mathbf{E}_3 , the resultant of these two sine waves, is also a sine wave, of amplitude

$$A_3 = [A_1^2 + A_2^2 + 2A_1A_2 \cos(\phi_1 - \phi_2)]^{\frac{1}{2}}$$

and of phase

$$\phi_3 = \tan^{-1} \frac{A_1 \sin \phi_1 + A_2 \sin \phi_2}{A_1 \cos \phi_1 + A_2 \cos \phi_2}.$$

4-2. Obtain the same result by solving the vector diagram of Fig. 4-11 for the right-angle triangle of which A_3 is the hypotenuse.

4-3. Derive simplified expressions for F^2 for diamond, including the rules governing observed reflections. This crystal is cubic and contains 8 carbon atoms per unit cell, located in the following positions:

$$\begin{array}{cccc} 0\ 0\ 0 & \frac{1}{2}\ \frac{1}{2}\ 0 & \frac{1}{2}\ 0\ \frac{1}{2} & 0\ \frac{1}{2}\ \frac{1}{2} \\ \frac{1}{4}\ \frac{1}{4}\ \frac{1}{4} & \frac{3}{4}\ \frac{3}{4}\ \frac{1}{4} & \frac{3}{4}\ \frac{1}{4}\ \frac{3}{4} & \frac{1}{4}\ \frac{3}{4}\ \frac{3}{4} \end{array}$$

4-4. A certain tetragonal crystal has four atoms of the same kind per unit cell, located at $0\ \frac{1}{2}\ \frac{1}{4}$, $\frac{1}{2}\ 0\ \frac{1}{4}$, $\frac{1}{2}\ 0\ \frac{3}{4}$, $0\ \frac{1}{2}\ \frac{3}{4}$.

- (a) Derive simplified expressions for F^2 .
- (b) What is the Bravais lattice of this crystal?
- (c) What are the values of F^2 for the 100, 002, 111, and 011 reflections?

4-5. Derive simplified expressions for F^2 for the wurtzite form of ZnS, including the rules governing observed reflections. This crystal is hexagonal and contains 2 ZnS per unit cell, located in the following positions:

$$\begin{aligned} \text{Zn: } & 0\ 0\ 0, \frac{1}{3}\ \frac{2}{3}\ \frac{1}{2}, \\ \text{S: } & 0\ 0\ \frac{3}{8}, \frac{1}{3}\ \frac{2}{3}\ \frac{7}{8}. \end{aligned}$$

PROBLEMS

Note that these positions involve a common translation, which may be factored out of the structure-factor equation.

4-6. In Sec. 4-9, in the part devoted to scattering when the incident and scattered beams make unequal angles with the reflecting planes, it is stated that "rays scattered by all other planes are in phase with the corresponding rays scattered by the first plane." Prove this.

4-7. Calculate the position (in terms of θ) and the integrated intensity (in relative units) of the first five lines on the Debye pattern of silver made with $\text{Cu K}\alpha$ radiation. Ignore the temperature and absorption factors.

4-8. A Debye-Scherrer pattern of tungsten (BCC) is made with $\text{Cu K}\alpha$ radiation. The first four lines on this pattern were observed to have the following θ values:

Line	θ
1	20.3°
2	29.2
3	36.7
4	43.6

Index these lines (i.e., determine the Miller indices of each reflection by the use of Eq. (3-10) and Appendix 6) and calculate their relative integrated intensities.

4-9. A Debye-Scherrer pattern is made of gray tin, which has the same structure as diamond, with $\text{Cu K}\alpha$ radiation. What are the indices of the first two lines on the pattern, and what is the ratio of the integrated intensity of the first to that of the second?

4-10. A Debye-Scherrer pattern is made of the intermediate phase InSb with $\text{Cu K}\alpha$ radiation. This phase has the zinc-blende structure and a lattice parameter of 6.46 Å. What are the indices of the first two lines on the pattern, and what is the ratio of the integrated intensity of the first to the second?

4-11. Calculate the relative integrated intensities of the first six lines of the Debye-Scherrer pattern of zinc, made with $\text{Cu K}\alpha$ radiation. The indices and observed θ values of these lines are:

Line	hkl	θ
1	00·2	18.8°
2	10·0	20.2
3	10·1	22.3
4	10·2	27.9
5	11·0, 10·3	36.0
6	00·4	39.4

(Line 5 is made up of two unresolved lines from planes of very nearly the same spacing.) Compare your results with the intensities observed in the pattern shown in Fig. 3-13(c).

APPENDIX 15

THE RECIPROCAL LATTICE

A15-1 Introduction. All the diffraction phenomena described in this book have been discussed in terms of the Bragg law. This simple law, admirable for its very simplicity, is in fact applicable to a very wide range of phenomena and is all that is needed for an understanding of a great many applications of x-ray diffraction. Yet there are diffraction effects which the Bragg law is totally unable to explain, notably those involving diffuse scattering at non-Bragg angles, and these effects demand a more general theory of diffraction for their explanation. The reciprocal lattice provides the framework for such a theory. This powerful concept was introduced into the field of diffraction by the German physicist Ewald in 1921 and has since become an indispensable tool in the solution of many problems.

Although the reciprocal lattice may at first appear rather abstract or artificial, the time spent in grasping its essential features is time well spent, because the reciprocal-lattice theory of diffraction, being general, is applicable to all diffraction phenomena from the simplest to the most intricate. Familiarity with the reciprocal lattice will therefore not only provide the student with the necessary key to complex diffraction effects but will deepen his understanding of even the simplest.

A15-2 Vector multiplication. Since the reciprocal lattice is best formulated in terms of vectors, we shall first review a few theorems of vector algebra, namely, those involving the multiplication of vector quantities.

The *scalar product* (or dot product) of two vectors* \mathbf{a} and \mathbf{b} , written $\mathbf{a} \cdot \mathbf{b}$, is a scalar quantity equal in magnitude to the product of the absolute values of the two vectors and the cosine of the angle α between them, or

$$\mathbf{a} \cdot \mathbf{b} = ab \cos \alpha.$$

Geometrically, Fig. A15-1 shows that the scalar product of two vectors may be regarded as the product of the length of one vector and the projection of the other upon the first. If one of the vectors, say \mathbf{a} , is a unit vector (a vector of unit length), then $\mathbf{a} \cdot \mathbf{b}$ gives immediately the length of the projection of \mathbf{b} on \mathbf{a} . The scalar product of sums or differences of vectors is formed simply by term-by-term multiplication:

$$(\mathbf{a} + \mathbf{b}) \cdot (\mathbf{c} - \mathbf{d}) = (\mathbf{a} \cdot \mathbf{c}) - (\mathbf{a} \cdot \mathbf{d}) + (\mathbf{b} \cdot \mathbf{c}) - (\mathbf{b} \cdot \mathbf{d}).$$

* Bold-face symbols stand for vectors. The same symbol in italic stands for the absolute value of the vector.

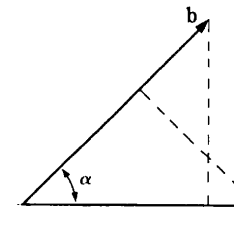


FIG. A15-1. Scalar product of two vectors.

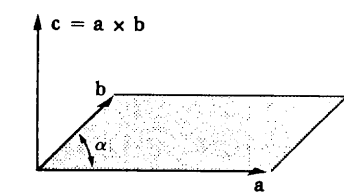


FIG. A15-2. Vector product of two vectors.

The order of multiplication is of no importance; i.e.,

$$\mathbf{a} \cdot \mathbf{b} = \mathbf{b} \cdot \mathbf{a}.$$

The *vector product* (or cross product) of two vectors \mathbf{a} and \mathbf{b} , written $\mathbf{a} \times \mathbf{b}$, is a *vector* \mathbf{c} at right angles to the plane of \mathbf{a} and \mathbf{b} , and equal in magnitude to the product of the absolute values of the two vectors and the sine of the angle α between them, or

$$\mathbf{c} = \mathbf{a} \times \mathbf{b},$$

$$c = ab \sin \alpha.$$

The magnitude of \mathbf{c} is simply the area of the parallelogram constructed on \mathbf{a} and \mathbf{b} , as suggested by Fig. A15-2. The direction of \mathbf{c} is that in which a right-hand screw would move if rotated in such a way as to bring \mathbf{a} into \mathbf{b} . It follows from this that the direction of the vector product \mathbf{c} is reversed if the order of multiplication is reversed, or that

$$\mathbf{a} \times \mathbf{b} = -(\mathbf{b} \times \mathbf{a}).$$

A15-3 The reciprocal lattice. Corresponding to any crystal lattice, we can construct a *reciprocal lattice*, so called because many of its properties are reciprocal to those of the crystal lattice. Let the crystal lattice have a unit cell defined by the vectors \mathbf{a}_1 , \mathbf{a}_2 , and \mathbf{a}_3 . Then the corresponding reciprocal lattice has a unit cell defined by the vectors \mathbf{b}_1 , \mathbf{b}_2 , and \mathbf{b}_3 , where

$$\mathbf{b}_1 = \frac{1}{V} (\mathbf{a}_2 \times \mathbf{a}_3), \quad (1)$$

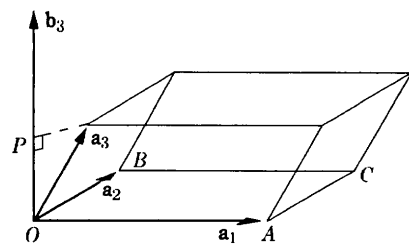
$$\mathbf{b}_2 = \frac{1}{V} (\mathbf{a}_3 \times \mathbf{a}_1), \quad (2)$$

$$\mathbf{b}_3 = \frac{1}{V} (\mathbf{a}_1 \times \mathbf{a}_2), \quad (3)$$

and V is the volume of the crystal unit cell. This way of defining the vectors \mathbf{b}_1 , \mathbf{b}_2 , \mathbf{b}_3 in terms of the vectors \mathbf{a}_1 , \mathbf{a}_2 , \mathbf{a}_3 gives the reciprocal lattice certain useful properties which we will now investigate.

THE RECIPROCAL LATTICE

[APP. 15]

FIG. A15-3. Location of the reciprocal-lattice axis \mathbf{b}_3 .

Consider the general triclinic unit cell shown in Fig. A15-3. The reciprocal-lattice axis \mathbf{b}_3 is, according to Eq. (3), normal to the plane of \mathbf{a}_1 and \mathbf{a}_2 , as shown. Its length is given by

$$\begin{aligned} \mathbf{b}_3 &= \frac{|\mathbf{a}_1 \times \mathbf{a}_2|}{V} \\ &= \frac{(\text{area of parallelogram } OACB)}{(\text{area of parallelogram } OACB)(\text{height of cell})} \\ &= \frac{1}{OP} = \frac{1}{d_{001}}, \end{aligned}$$

since OP , the projection of \mathbf{a}_3 on \mathbf{b}_3 , is equal to the height of the cell, which in turn is simply the spacing d of the (001) planes of the crystal lattice. Similarly, we find that the reciprocal lattice axes \mathbf{b}_1 and \mathbf{b}_2 are normal to the (100) and (010) planes, respectively, of the crystal lattice, and are equal in length to the reciprocals of the spacings of these planes.

By extension, similar relations are found for all the planes of the crystal lattice. The whole reciprocal lattice is built up by repeated translations of the unit cell by the vectors \mathbf{b}_1 , \mathbf{b}_2 , \mathbf{b}_3 . This produces an array of points each of which is labeled with its coordinates in terms of the basic vectors. Thus, the point at the end of the \mathbf{b}_1 vector is labeled 100 , that at the end of the \mathbf{b}_2 vector 010 , etc. This extended reciprocal lattice has the following properties:

(1) A vector \mathbf{H}_{hkl} drawn from the origin of the reciprocal lattice to any point in it having coordinates hkl is perpendicular to the plane in the crystal lattice whose Miller indices are hkl . This vector is given in terms of its coordinates by the expression

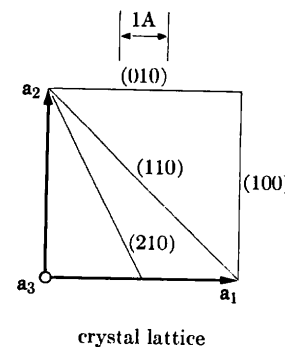
$$\mathbf{H}_{hkl} = h\mathbf{b}_1 + k\mathbf{b}_2 + l\mathbf{b}_3.$$

(2) The length of the vector \mathbf{H}_{hkl} is equal to the reciprocal of the spacing d of the (hkl) planes, or

$$H_{hkl} = \frac{1}{d_{hkl}}.$$

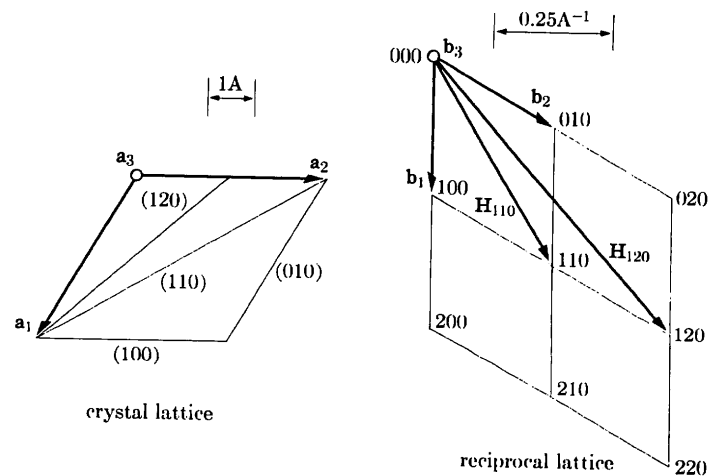
A15-3]

THE RECIPROCAL LATTICE

FIG. A15-4. The reciprocal lattice of a cubic crystal which has $a_1 = 4\text{A}$. The axes \mathbf{a}_3 and \mathbf{b}_3 are normal to the drawing.

The important thing to note about these relations is that the reciprocal-lattice array of points completely describes the crystal, in the sense that each reciprocal-lattice point is related to a set of planes in the crystal and represents the orientation and spacing of that set of planes.

Before proving these general relations, we might consider particular examples of the reciprocal lattice as shown in Figs. A15-4 and A15-5 for cubic and hexagonal crystals. In each case, the reciprocal lattice is drawn from any convenient origin, not necessarily that of the crystal lattice, and to any convenient scale of reciprocal angstroms. Note that Eqs. (1) through (3) take on a very simple form for any crystal whose unit cell is

FIG. A15-5. The reciprocal lattice of a hexagonal crystal which has $a_1 = 4\text{A}$. (Here the three-symbol system of plane indexing is used and \mathbf{a}_3 is the axis usually designated \mathbf{c} .) The axes \mathbf{a}_3 and \mathbf{b}_3 are normal to the drawing.

based on mutually perpendicular vectors, i.e., cubic, tetragonal, or orthorhombic. For such crystals, \mathbf{b}_1 , \mathbf{b}_2 , and \mathbf{b}_3 are parallel, respectively, to \mathbf{a}_1 , \mathbf{a}_2 , and \mathbf{a}_3 , while b_1 , b_2 , and b_3 are simply the reciprocals of a_1 , a_2 , and a_3 . In Figs. A15-4 and A15-5, four cells of the reciprocal lattice are shown, together with two \mathbf{H} vectors in each case. By means of the scales shown, it may be verified that each \mathbf{H} vector is equal in length to the reciprocal of the spacing of the corresponding planes and normal to them. Note that reciprocal lattice points such as nh , nk , nl , where n is an integer, correspond to planes parallel to (hkl) and having $1/n$ their spacing. Thus, \mathbf{H}_{220} is perpendicular to (220) planes and therefore parallel to \mathbf{H}_{110} , since (110) and (220) are parallel, but \mathbf{H}_{220} is twice as long as \mathbf{H}_{110} since the (220) planes have half the spacing of the (110) planes.

Other useful relations between the crystal and reciprocal vectors follow from Eqs. (1) through (3). Since \mathbf{b}_3 , for example, is normal to both \mathbf{a}_1 and \mathbf{a}_2 , its dot product with either one of these vectors is zero, or

$$\mathbf{b}_3 \cdot \mathbf{a}_1 = \mathbf{b}_3 \cdot \mathbf{a}_2 = 0.$$

The dot product of \mathbf{b}_3 and \mathbf{a}_3 , however, is unity, since (see Fig. A15-3)

$$\mathbf{b}_3 \cdot \mathbf{a}_3 = (b_3) \text{ (projection of } \mathbf{a}_3 \text{ on } \mathbf{b}_3)$$

$$= \left(\frac{1}{OP} \right) (OP)$$

$$= 1.$$

In general,

$$\mathbf{a}_m \cdot \mathbf{b}_n = 1, \quad \text{if } m = n, \quad (4)$$

$$= 0, \quad \text{if } m \neq n. \quad (5)$$

The fact that \mathbf{H}_{hkl} is normal to (hkl) and H_{hkl} is the reciprocal of d_{hkl} may be proved as follows. Let ABC of Fig. A15-6 be part of the plane nearest the origin in the set (hkl) . Then, from the definition of Miller indices, the vectors from the origin to the points A , B , and C are \mathbf{a}_1/h , \mathbf{a}_2/k , and \mathbf{a}_3/l , respectively. Consider the vector \mathbf{AB} , that is, a vector drawn from A to B , lying in the plane (hkl) . Since

$$\frac{\mathbf{a}_1}{h} + \mathbf{AB} = \frac{\mathbf{a}_2}{k},$$

then

$$\mathbf{AB} = \frac{\mathbf{a}_2}{k} - \frac{\mathbf{a}_1}{h}.$$

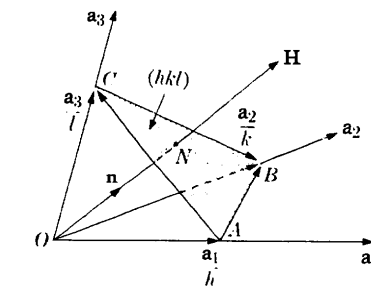


FIG. A15-6. Relation between reciprocal-lattice vector \mathbf{H} and crystal plane (hkl) .

Forming the dot product of \mathbf{H} and \mathbf{AB} , we have

$$\mathbf{H} \cdot \mathbf{AB} = (hb_1 + kb_2 + lb_3) \cdot \left(\frac{\mathbf{a}_2}{k} - \frac{\mathbf{a}_1}{h} \right).$$

Evaluating this with the aid of Eqs. (4) and (5), we find

$$\mathbf{H} \cdot \mathbf{AB} = 1 - 1 = 0.$$

Since this product is zero, \mathbf{H} must be normal to \mathbf{AB} . Similarly, it may be shown that \mathbf{H} is normal to \mathbf{AC} . Since \mathbf{H} is normal to two vectors in the plane (hkl) , it is normal to the plane itself.

To prove the reciprocal relation between H and d , let \mathbf{n} be a unit vector in the direction of \mathbf{H} , i.e., normal to (hkl) . Then

$$d = ON = \frac{\mathbf{a}_1}{h} \cdot \mathbf{n}.$$

But

$$\mathbf{n} = \frac{\mathbf{H}}{H}.$$

Therefore

$$\begin{aligned} d &= \frac{\mathbf{a}_1}{h} \cdot \frac{\mathbf{H}}{H} \\ &= \frac{\mathbf{a}_1}{h} \cdot \frac{(hb_1 + kb_2 + lb_3)}{H} \\ &= \frac{1}{H}. \end{aligned}$$

Used purely as a geometrical tool, the reciprocal lattice is of considerable help in the solution of many problems in crystal geometry. Consider, for example, the relation between the planes of a zone and the axis of that zone. Since the planes of a zone are all parallel to one line, the zone axis, their normals must be coplanar. This means that planes of a zone are represented, in the reciprocal lattice, by a set of points lying on a plane passing through the origin of the reciprocal lattice. If the plane (hkl) belongs to the zone whose axis is $[uvw]$, then the normal to (hkl) , namely, \mathbf{H} , must be perpendicular to $[uvw]$. Express the zone axis as a vector in the crystal lattice and \mathbf{H} as a vector in the reciprocal lattice:

$$\text{Zone axis} = ua_1 + va_2 + wa_3,$$

$$\mathbf{H} = hb_1 + kb_2 + lb_3.$$

If these two vectors are perpendicular, their dot product must be zero:

$$\begin{aligned} (ua_1 + va_2 + wa_3) \cdot (hb_1 + kb_2 + lb_3) &= 0, \\ hu + kv + lw &= 0. \end{aligned}$$

This is the relation given without proof in Sec. 2-6. By similar use of reciprocal-lattice vectors, other problems of crystal geometry, such as the derivation of the plane-spacing equations given in Appendix 1, may be greatly simplified.

A15-4 Diffraction and the reciprocal lattice. The great utility of the reciprocal lattice, however, lies in its connection with diffraction problems. We shall consider how x-rays scattered by the atom O at the origin of the crystal lattice (Fig. A15-7) are affected by those scattered by any other atom A whose coordinates with respect to the origin are $p\mathbf{a}_1$, $q\mathbf{a}_2$ and $r\mathbf{a}_3$, where p , q , and r are integers. Thus,

$$\mathbf{OA} = p\mathbf{a}_1 + q\mathbf{a}_2 + r\mathbf{a}_3.$$

Let the incident x-rays have a wavelength λ , and let the incident and diffracted beams be represented by the unit vectors \mathbf{S}_0 and \mathbf{S} , respectively. \mathbf{S}_0 , \mathbf{S} , and \mathbf{OA} are, in general, not coplanar.

To determine the conditions under which diffraction will occur, we must determine the phase difference between the rays scattered by the atoms O and A . The lines Ou and Ov in Fig. A15-7 are wave fronts perpendicular to the incident beam \mathbf{S}_0 and the diffracted beam \mathbf{S} , respectively. Let δ be the path difference for rays scattered by O and A . Then

$$\begin{aligned}\delta &= uA + Av \\ &= Om + On \\ &= \mathbf{S}_0 \cdot \mathbf{OA} + (-\mathbf{S}) \cdot \mathbf{OA} \\ &= -\mathbf{OA} \cdot (\mathbf{S} - \mathbf{S}_0).\end{aligned}$$

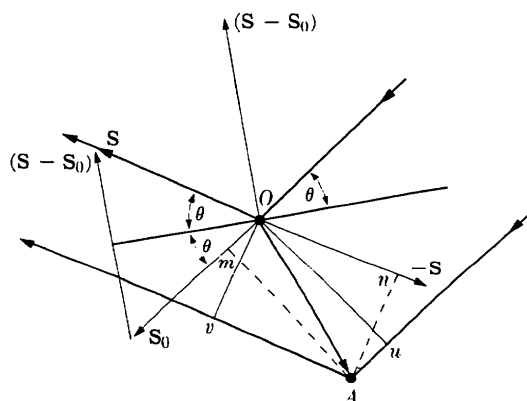


FIG. A15-7. X-ray scattering by atoms at O and A . (After Guinier, *X-Ray Crystallographic Technology*, Hilger & Watts, Ltd., London, 1952.)

The corresponding phase difference is given by

$$\begin{aligned}\phi &= \frac{2\pi\delta}{\lambda} \\ &= -2\pi \left(\frac{\mathbf{S} - \mathbf{S}_0}{\lambda} \right) \cdot \mathbf{OA}. \quad (6)\end{aligned}$$

Diffraction is now related to the reciprocal lattice by expressing the vector $(\mathbf{S} - \mathbf{S}_0)/\lambda$ as a vector in that lattice. Let

$$\frac{\mathbf{S} - \mathbf{S}_0}{\lambda} = h\mathbf{b}_1 + k\mathbf{b}_2 + l\mathbf{b}_3.$$

This is now in the form of a vector in reciprocal space but, at this point, no particular significance is attached to the parameters h , k , and l . They are continuously variable and may assume any values, integral or nonintegral. Equation (6) now becomes

$$\phi = -2\pi(h\mathbf{b}_1 + k\mathbf{b}_2 + l\mathbf{b}_3) \cdot (p\mathbf{a}_1 + q\mathbf{a}_2 + r\mathbf{a}_3) = -2\pi(hp + kq + lr).$$

A diffracted beam will be formed only if reinforcement occurs, and this requires that ϕ be an integral multiple of 2π . This can happen only if h , k and l are integers. Therefore the condition for diffraction is that the vector $(\mathbf{S} - \mathbf{S}_0)/\lambda$ end on a point in the reciprocal lattice, or that

$$\frac{\mathbf{S} - \mathbf{S}_0}{\lambda} = \mathbf{H} = h\mathbf{b}_1 + k\mathbf{b}_2 + l\mathbf{b}_3, \quad (7)$$

where h , k , and l are now restricted to integral values.

Both the Laue equations and the Bragg law can be derived from Eq. (7). The former are obtained by forming the dot product of each side of the equation and the three crystal-lattice vectors \mathbf{a}_1 , \mathbf{a}_2 , \mathbf{a}_3 successively. For example,

$$\begin{aligned}\mathbf{a}_1 \cdot \left(\frac{\mathbf{S} - \mathbf{S}_0}{\lambda} \right) &= \mathbf{a}_1 \cdot (h\mathbf{b}_1 + k\mathbf{b}_2 + l\mathbf{b}_3) \\ &= h,\end{aligned}$$

or

$$\mathbf{a}_1 \cdot (\mathbf{S} - \mathbf{S}_0) = h\lambda. \quad (8)$$

Similarly,

$$\mathbf{a}_2 \cdot (\mathbf{S} - \mathbf{S}_0) = k\lambda, \quad (9)$$

$$\mathbf{a}_3 \cdot (\mathbf{S} - \mathbf{S}_0) = l\lambda. \quad (10)$$

Equations (8) through (10) are the vector form of the equations derived by von Laue in 1912 to express the necessary conditions for diffraction. They must be satisfied simultaneously for diffraction to occur.

As shown in Fig. A15-7, the vector $(\mathbf{S} - \mathbf{S}_0)$ bisects the angle between the incident beam \mathbf{S}_0 and the diffracted beam \mathbf{S} . The diffracted beam \mathbf{S} can therefore be considered as being reflected from a set of planes perpendicular to $(\mathbf{S} - \mathbf{S}_0)$. In fact, Eq. (7) states that $(\mathbf{S} - \mathbf{S}_0)$ is parallel to \mathbf{H} , which is in turn perpendicular to the planes (hkl) . Let θ be the angle between \mathbf{S} (or \mathbf{S}_0) and these planes. Then, since \mathbf{S} and \mathbf{S}_0 are unit vectors,

$$(S - S_0) = 2 \sin \theta.$$

Therefore

$$\frac{2 \sin \theta}{\lambda} = \frac{S - S_0}{\lambda} = H = \frac{1}{d},$$

$$\lambda = 2d \sin \theta.$$

The conditions for diffraction expressed by Eq. (7) may be represented graphically by the "Ewald construction" shown in Fig. A15-8. The vector \mathbf{S}_0/λ is drawn parallel to the incident beam and $1/\lambda$ in length. The terminal point O of this vector is taken as the origin of the reciprocal lattice, drawn to the same scale as the vector \mathbf{S}_0/λ . A sphere of radius $1/\lambda$ is drawn about C , the initial point of the incident-beam vector. Then the condition for diffraction from the (hkl) planes is that the point hkl in the reciprocal lattice (point P in Fig. A15-8) touch the surface of the sphere, and the direction of the diffracted-beam vector \mathbf{S}/λ is found by joining C to P . When this condition is fulfilled, the vector \mathbf{OP} equals both \mathbf{H}_{hkl} and $(\mathbf{S} - \mathbf{S}_0)/\lambda$, thus satisfying Eq. (7). Since diffraction depends on a reciprocal-lattice point's touching the surface of the sphere drawn about C , this sphere is known as the "sphere of reflection."

Our initial assumption that p , q , and r are integers apparently excludes all crystals except those having only one atom per cell, located at the cell corners. For if the unit cell contains more than one atom, then the vector **OA** from the origin to "any atom" in the crystal may have nonintegral coordinates. However, the presence of these additional atoms in the unit cell affects only the intensities of the diffracted beams, not their directions, and it is only the diffraction directions which are predicted by the Ewald construction. Stated in another way, the reciprocal lattice depends only on the shape and size of the unit cell of the crystal lattice and not at all

on the arrangement of atoms within that cell. If we wish to take atom arrangement into consideration, we may weight each reciprocal-lattice point hkl with the appropriate value of the scattering power ($= |F|^2$ where F is the structure factor) of the particular (hkl) planes involved. Some planes may then have zero scattering power, thus eliminating some reciprocal-lattice points from consideration, e.g., all reciprocal-lattice points having odd values of $(h + k + l)$ for body-centered crystals.

The common methods of x-ray diffraction are differentiated by the methods used for bringing reciprocal-lattice points into contact with the surface of the sphere of reflection. The radius of the sphere may be varied by varying the incident wavelength (Laue method), or the position of the reciprocal lattice may be varied by changes in the orientation of the crystal (rotating-crystal and powder methods).

A15-5 The rotating-crystal method. As stated in Sec. 3-6, when monochromatic radiation is incident on a single crystal rotated about one of its axes, the reflected beams lie on the surface of imaginary cones coaxial with the rotation axis. The way in which this reflection occurs may be shown very nicely by the Ewald construction. Suppose a simple cubic crystal is rotated about the axis [001]. This is equivalent to rotation of the reciprocal lattice about the b_3 axis. Figure A15-9 shows a portion of the reciprocal lattice oriented in this manner, together with the adjacent sphere of reflection.

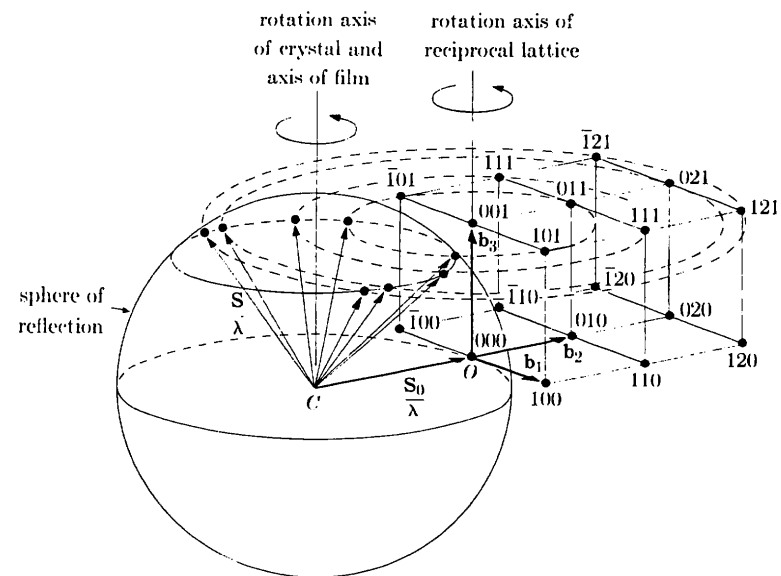


FIG. A15-9. Reciprocal-lattice treatment of rotating-crystal method.

All crystal planes having indices $(hk\bar{l})$ are represented by points lying on a plane (called the " $l = 1$ layer") in the reciprocal lattice, normal to \mathbf{b}_3 . When the reciprocal lattice rotates, this plane cuts the reflection sphere in the small circle shown, and any points on the $l = 1$ layer which touch the sphere surface must touch it on this circle. Therefore all diffracted-beam vectors \mathbf{S}/λ must end on this circle, which is equivalent to saying that the diffracted beams must lie on the surface of a cone. In this particular case, all the $hk\bar{l}$ points shown intersect the surface of the sphere sometime during their rotation about the \mathbf{b}_3 axis, producing the diffracted beams shown in Fig. A15-9. In addition many $hk0$ and $h\bar{k}\bar{l}$ reflections would be produced, but these have been omitted from the drawing for the sake of clarity.

This simple example may suggest how the rotation photograph of a crystal of unknown structure, and therefore having an unknown reciprocal lattice, can yield clues as to the distribution in space of reciprocal-lattice points. By taking a number of photographs with the crystal rotated successively about various axes, the crystallographer gradually discovers the complete distribution of reflecting points. Once the reciprocal lattice is known, the crystal lattice is easily derived, because it is a corollary of Eqs. (1) through (3) that the reciprocal of the reciprocal lattice is the crystal lattice.

A15-6 The powder method. The random orientations of the individual crystals in a powder specimen are equivalent to the rotation of a single crystal about all possible axes during the x-ray exposure. The reciprocal lattice therefore takes on all possible orientations relative to the incident beam, but its origin remains fixed at the end of the \mathbf{S}_0/λ vector.

Consider any point hkl in the reciprocal lattice, initially at P_1 (Fig. A15-10). This point can be brought into a reflecting position on the surface of the reflection sphere by a rotation of the lattice about an axis through O and normal to OC , for example. Such a rotation would move P_1 to P_2 . But the point hkl can still remain on the surface of the sphere [i.e., reflection will still occur from the same set of planes (hkl)] if the reciprocal lattice is then rotated about the axis OC , since the point hkl will then move round the small circle P_2P_3 . During this motion, the \mathbf{H} vector sweeps out a cone whose apex is at O , and the diffracted beams all lie on the surface of another cone whose apex is at C . The axes of both cones coincide with the incident beam.

The number of different hkl reflections obtained on a powder photograph depends, in part, on the relative magnitudes of the wavelength and the crystal-lattice parameters or, in reciprocal-lattice language, on the relative sizes of the sphere of reflection and the reciprocal-lattice unit cell. To find the number of reflections we may regard the reciprocal lattice as fixed and the incident-beam vector \mathbf{S}_0/λ as rotating about its terminal point

A15-6]

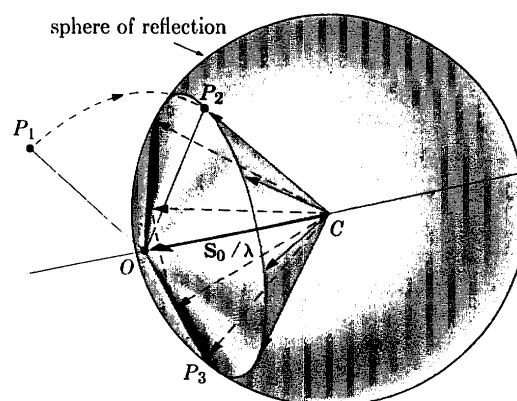


FIG. A15-10. Formation of a cone of diffracted rays in the powder method.

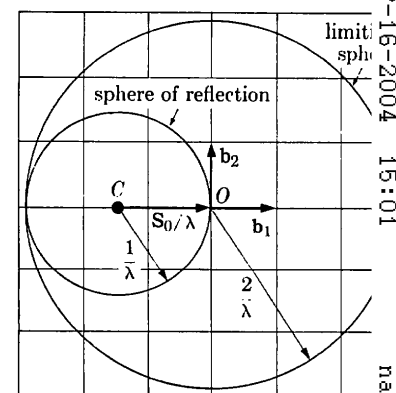


FIG. A15-11. The limiting sphere for the powder method.

through all possible positions. The reflection sphere therefore swings about the origin of the reciprocal lattice and sweeps out a sphere of radius $2/\lambda$ called the "limiting sphere" (Fig. A15-11). All reciprocal-lattice points within the limiting sphere can touch the surface of the reflection sphere and cause reflection to occur.

It is also a corollary of Eqs. (1) through (3) that the volume v of the reciprocal-lattice unit cell is the reciprocal of the volume V of the crystal unit cell. Since there is one reciprocal-lattice point per cell of the reciprocal lattice, the number of reciprocal-lattice points within the limiting sphere is given by

$$n = \frac{(4\pi/3)(2/\lambda)^3}{v} = \frac{32\pi V}{3\lambda^3}. \quad (11)$$

Not all of these n points will cause a separate reflection: some of them may have a zero structure factor, and some may be at equal distances from the reciprocal-lattice origin, i.e., correspond to planes of the same spacing (The latter effect is taken care of by the multiplicity factor, since this gives the number of different planes in a form having the same spacing.) However, Eq. (11) may always be used directly to obtain an upper limit to the number of possible reflections. For example, if $V = 50\text{A}^3$ and $\lambda = 1.54\text{\AA}$ then $n = 460$. If the specimen belongs to the triclinic system, this number will be reduced by a factor of only 2, the multiplicity factor, and the powder photograph will contain 230 separate diffraction lines! As the symmetry of the crystal increases, so does the multiplicity factor and the fraction of reciprocal-lattice points which have zero structure factor, resulting in a decrease in the number of diffraction lines. For example, the powder pattern of a diamond cubic crystal has only 5 lines, for the same values of V and λ assumed above.

A15-7 The Laue method. Diffraction occurs in the Laue method because of the continuous range of wavelengths present in the incident beam. Stated alternatively, contact between a fixed reciprocal-lattice point and the sphere of reflection is produced by continuously varying the radius of the sphere. There is therefore a whole set of reflection spheres, not just one; each has a different center, but all pass through the origin of the reciprocal lattice. The range of wavelengths present in the incident beam is of course not infinite. It has a sharp lower limit at λ_{SWL} , the short-wavelength limit of the continuous spectrum; the upper limit is less definite but is often taken as the wavelength of the K absorption edge of the silver in the emulsion (0.48A), because the effective photographic intensity of the continuous spectrum drops abruptly at that wavelength [see Fig. 1-18(c)].

To these two extreme wavelengths correspond two extreme reflection spheres, as shown in Fig. A15-12, which is a section through these spheres and the $l = 0$ layer of a reciprocal lattice. The incident beam is along the b_1 vector, i.e., perpendicular to the $(h00)$ planes of the crystal. The larger sphere shown is centered at B and has a radius equal to the reciprocal of λ_{SWL} , while the smaller sphere is centered at A and has a radius equal to the reciprocal of the wavelength of the silver K absorption edge.

There is a whole series of spheres lying between these two and centered on the line segment AB . Therefore any reciprocal-lattice point lying in the shaded region of the diagram is on the surface of one of these spheres and corresponds to a set of crystal planes oriented to reflect one of the incident wavelengths. In the forward direction, for example, a 120 reflection will be produced. To find its direction, we locate a point C on AB which is equidistant from the origin O and the reciprocal-lattice point 120; C is therefore the center of the reflection sphere passing through the point 120. Joining C to 120 gives the diffracted-beam vector S/λ for this reflection. The direction of the 410 reflection, one of the many backward-reflected beams, is found in similar fashion; here the reciprocal-lattice point in question is situated on a reflection sphere centered at D .

There is another way of treating the Laue method which is more convenient for many purposes. The basic diffraction equation, Eq. (7), is rewritten in the form

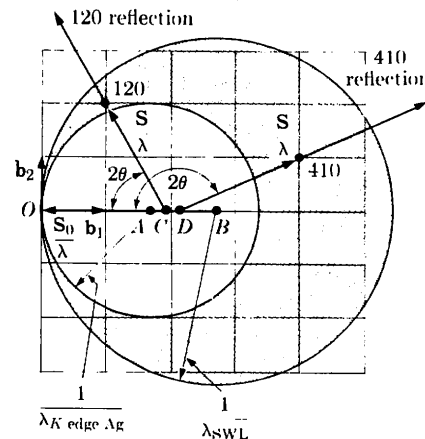


FIG. A15-12. Reciprocal-lattice treatment of the Laue method.
 $(S - S_0)/\lambda = H$.

$$S - S_0 = \lambda H .$$

Both sides of this equation are now dimensionless and the radius of the sphere of reflection is simply unity, since S and S_0 are unit vectors. But the position of the reciprocal-lattice points is now dependent on the wavelength used, since their distance from the origin of the reciprocal lattice is now given by λH .

In the Laue method, each reciprocal-lattice point (except 0 0 0) is drawn out into a line segment directed to the origin, because of the range of wavelengths present in the incident beam. The result is shown in Fig. A15-13, which is drawn to correspond to Fig. A15-12. The point nearest the origin on each line segment has a value of λH corresponding to the shortest wavelength present, while the point on the other end has a value of λH corresponding to the longest effective wavelength. Thus the 100 reciprocal lattice line extends from A to B , where $OA = \lambda_{min}H_{100}$ and $OB = \lambda_{max}H_{100}$. Since the length of any line increases as H increases, for a given range of wavelengths, overlapping occurs for the higher orders, as shown by 200, 300, 400, etc. The reflection sphere is drawn with unit radius, and reflection occurs whenever a reciprocal-lattice line intersects the sphere surface. Graphically, the advantage of this construction over that of Fig. A15-12 is that all diffracted beams are now drawn from the same point C , thus facilitating the comparison of the diffraction angles 2θ for different reflections.

This construction also shows why the diffracted beams from planes of zone are arranged on a cone in the Laue method. All reciprocal-lattice lines representing the planes of one zone lie on a plane passing through

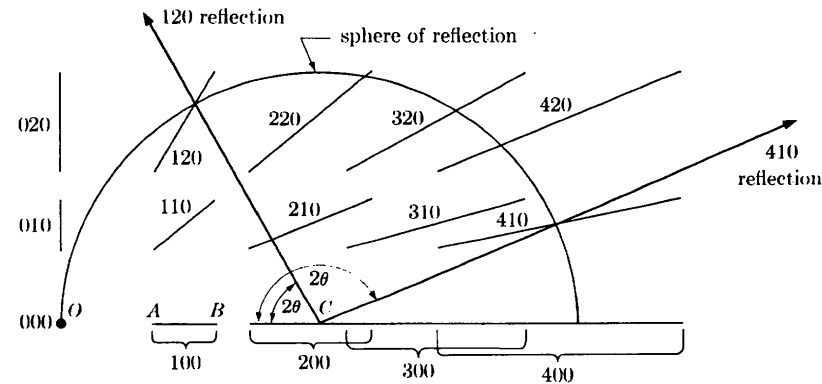


FIG. A15-13. Alternate reciprocal-lattice treatment of the Laue method.
 $S - S_0 = \lambda H$.

* In this figure, as well as in Figs. A15-11 and A15-12, the size of the reciprocal lattice, relative to the size of the reflection sphere, has been exaggerated for clarity.

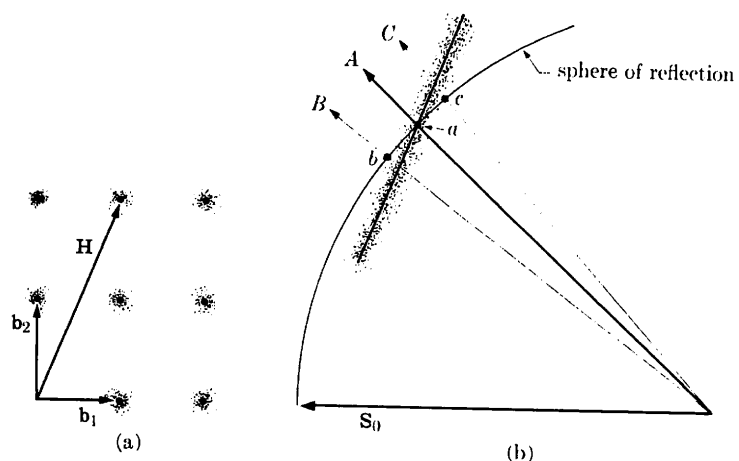


FIG. A15-14. The effect of thermal vibration on the reciprocal lattice.

the origin of the reciprocal lattice. This plane cuts the reflection sphere in a circle, and all the diffracted beam vectors S must end on this circle, thus producing a conical array of diffracted beams, the axis of the cone coinciding with the zone axis.

Another application of this construction, to the problem of temperature-diffuse scattering, will illustrate the general utility of the reciprocal-lattice method in treating diffuse scattering phenomena. The reciprocal lattice of any crystal may be regarded as a distribution of "scattered intensity" in reciprocal space, in the sense that a scattered beam will be produced whenever the sphere of reflection intersects a point in reciprocal space where the "scattered intensity" is not zero. If the crystal is perfect, the scattered intensity is concentrated at points in reciprocal space, the points of the reciprocal lattice, and is zero everywhere else. But if anything occurs to disturb the regularity of the crystal lattice, then these points become smeared out, and appreciable scattered intensity exists in regions of reciprocal space where h , k , and l are nonintegral. For example, if the atoms of the crystal are undergoing thermal vibration, then each point of the reciprocal lattice spreads out into a region which may be considered, to a first approximation, as roughly spherical in shape, as suggested by Fig. A15-14(a). In other words, the thermally produced elastic waves which run through the crystal lattice so disturb the regularity of the atomic planes that the corresponding H vectors end, not on points, but in small spherical regions. The scattered intensity is not distributed uniformly within each region: it remains very high at the central point, where h , k , and l are integral, and is very weak and diffuse in the surrounding volume, as indicated in the drawing.

What then will be the effect of thermal agitation on, for example, a transmission Laue pattern? If we use the construction of Fig. A15-13, i.e., if we make distances in the reciprocal lattice equal to λH , then each spherical volume in the reciprocal lattice will be drawn out into a rod, roughly cylindrical in shape and directed to the origin, as indicated in Fig. A15-14(b), which is a section through the reflection sphere and one such rod. The axis of each rod is a line of high intensity and this is surrounded by a low-intensity region. This line intersects the reflection sphere at a and produces the strong diffracted beam A , the ordinary Laue reflection. But on either side of A there are weak scattered rays, extending from B to C , due to the intersection, extending from b to c , of the diffuse part of the rod with the sphere of reflection.

In a direction normal to the drawing, however, the diffuse rod intersects the sphere in an arc equal only to the rod diameter, which is much shorter than the arc bc . We are thus led to expect, on a film placed in the transmission position, a weak and diffuse streak running *radially* through the usual sharp, intense Laue spot.

Figure A15-15 shows an example of this phenomenon, often called thermal asterism because of the radial direction of the diffuse streaks. This photograph was obtained from aluminum at 280°C in 5 minutes. Actually, thermal agitation is quite pronounced in aluminum even at room temperature, and thermal asterism is usually evident in overexposed room-temperature photographs. Even in Fig. 3-6(a), which was given a normal exposure of about 15 minutes, radial streaks are faintly visible. In this latter photograph, there is a streak near the center which does not pass through any Laue spot: it is due to a reciprocal-lattice rod so nearly tangent to the reflection sphere that the latter intersects only the diffuse part of the rod and not its axis.

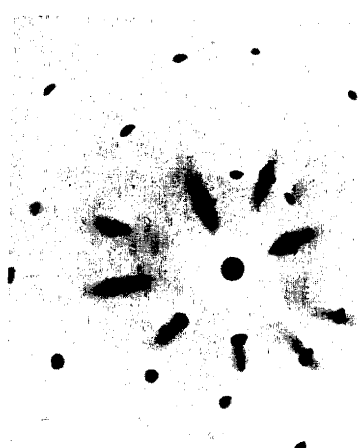


FIG. A15-15. Transmission Laue pattern showing thermal asterism. Aluminum crystal, 280°C, 5 min exposure.